


For Reference

NOT TO BE TAKEN FROM THIS ROOM

Ex LIBRIS
UNIVERSITATIS
ALBERTAENSIS





Digitized by the Internet Archive
in 2022 with funding from
University of Alberta Library

https://archive.org/details/Edwards1978_0

THE UNIVERSITY OF ALBERTA

RADIATIVE DECAYS OF VECTOR
AND PSEUDOSCALAR

MESONS

by



Bonnie Jean Edwards

A THESIS

SUBMITTED TO THE FACULTY OF GRADUATE STUDIES AND RESEARCH
IN PARTIAL FULFILMENT OF THE REQUIREMENTS FOR THE DEGREE
OF DOCTOR OF PHILOSOPHY

IN

THEORETICAL PHYSICS
DEPARTMENT OF PHYSICS

EDMONTON, ALBERTA

FALL, 1978

ABSTRACT

The recent accumulation of radiative decay rates for vector and pseudoscalar mesons has made a test of the theoretical models feasible. Since the standard quark model and nonet symmetry schemes are not in agreement with these data, alternatives must be sought. In this thesis, $VP\gamma$ schemes with symmetry breaking are examined.

A hierarchy of possible symmetry breaking structures is outlined. All conceivable types of $SU(3)$ and nonet symmetry breaking are discussed. Additional considerations, such as the OZI rule and vector meson dominance, are investigated.

Mass splitting, an accepted example of $SU(3)$ symmetry breaking, is used in two models to generate a symmetry breaking structure for the $VP\gamma$ vertex. While the predictions of these models certainly constitute an improvement over the nonet symmetry model predictions, total agreement with experimental measurements is not found.

Several general symmetry breaking schemes are also examined. A number of models can explain most of the measured rates with notable exception of $\Gamma(\rho \rightarrow \pi\gamma)$. There appears to be an inconsistency between the measured value of this rate and vector meson dominance. Problems are also encountered with some processes involving η and η' but the measurements of these rates are recent and unsubstantiated.

Vector meson dominance is used to extend some of the more successful symmetry breaking $VP\gamma$ models to include other decay modes. The measured rates of the type $P\rightarrow\gamma\gamma$, $V\rightarrow PPP$ and $P\rightarrow PP\gamma$ appear most compatible with a model which demonstrates nonet symmetry and $SU(3)$ symmetry breaking.

An $SU(4)$ extension is also performed. No new problems arise in accounting for the measured radiative decay rates of ψ .

Of all the $VP\gamma$ schemes studied, the general $VP\gamma$ model with nonet symmetry and $SU(3)$ symmetry breaking is the most successful. Not only is it phenomenologically justifiable, incorporating the OZI rule and using standard mixing angles, but it accounts for a very wide variety of rates within $SU(3)$ and $SU(4)$.

The real problem is the incompatibility of the measured $\rho\rightarrow\pi\gamma$ rate and vector meson dominance. Given the successes of this last technique, it would be most desirable to repeat the measurement of $\Gamma(\rho\rightarrow\pi\gamma)$.

ACKNOWLEDGEMENTS

I wish to thank Dr. A. N. Kamal for supervising my doctoral research. I have learned much from his broad experience and knowledge in the many areas of particle physics. His interest, patience and availability have made working with him a pleasure.

I thank Drs. D. H. Boal and R. Torgerson who have generously shared both their time and enthusiasm.

I also wish to thank Robert Brooks for his steady hand and, more significantly, steady soul during the preparation of this thesis.

I am grateful to the National Research Council of Canada, the University of Alberta and the Killam Foundation for their financial support during the last three years.

TABLE OF CONTENTS

CHAPTER		PAGE
I	THE RADIATIVE DECAYS OF VECTOR AND PSEUDOSCALAR MESONS	1
	1.1 Introduction to the Problem	1
	1.2 Mesons, Quarks and Radiative Decays	3
	1.3 Implementation of Unitary Symmetry	4
	1.4 The Nonet Symmetry Scheme	9
	1.5 The SU(3) Symmetry Scheme	13
	1.6 SU(3) Symmetry Breaking Models	17
	1.7 Other Decays	18
	1.8 Extensions of SU(4)	19
II	THE HIERARCHY OF SYMMETRY BREAKING SCHEMES	22
	2.1 The Nature of Symmetry Breaking	22
	2.2 The Most General SU(3) Model with λ_8 Symmetry Breaking	23
	2.3 Nonet Symmetry, the OZI Rule and λ_8 Symmetry Breaking	29
	2.4 Vector Meson Dominance	31
	2.5 A Hierarchy of Models with SU(3) Symmetry Breaking	33
III	THE BARYON LOOP MODEL	36
	3.1 The Nature of the Model	36
	3.2 F-type Coupling of the Photon to the Baryon Loop	37
	3.3 The Photon Coupled to the Baryon Loop through VMD	43
	3.4 Conclusions	50

CHAPTER		PAGE
IV	THE CURRENT ALGEBRA MODEL	52
	4.1 Symmetry Breaking through Current Algebra	52
	4.2 The Strong VVP Vertex	54
	4.3 The Radiative Decay Model	58
	4.4 The Predictions of the Model	59
V	THE SU(3) SYMMETRY BREAKING MODELS WITH NONET SYMMETRY	63
	5.1 The Models	63
	5.2 A VVP Model with SU(3) Symmetry Breaking	63
	5.3 The Strong Nonet Model with Boson Symmetry	67
	5.4 The $\rho \rightarrow \pi\gamma$ Width	69
	5.5 Loosening the Symmetry Assumptions	73
	5.6 Conclusions	77
VI	OTHER RADIATIVE AND HADRONIC DECAYS	79
	6.1 The Basic Interactions	79
	6.2 The $P \rightarrow \gamma\gamma$ Width	80
	6.3 The $V \rightarrow PPP$ Width	82
	6.4 The $P \rightarrow PP\gamma$ Width	84
	6.5 The Predictions of the Models	86
VII	RADIATIVE DECAYS IN AN SU(4) SCHEME	90
	7.1 The Advent of SU(4)	90
	7.2 The SU(4) Particle Classifications	91
	7.3 The Radiative Decay Scheme	93
	7.4 The Predictions of the Model	96

CHAPTER	PAGE
7.5 Other Decays	99
7.6 Conclusions	102
VIII CONCLUSIONS	104
8.1 The $SU(3)$ $V \rightarrow P\gamma$ and $P \rightarrow V\gamma$ Decays	104
8.2 The VMD Related Decays	107
8.3 Extensions to $SU(4)$	108
8.4 Experiments	108
8.5 Conclusions	110
FOOTNOTES	111
REFERENCES	112
APPENDIX I	115
APPENDIX II	128

LIST OF TABLES

Table		Page
1	Nonet Predictions of Radiative Decay Widths	12
2	SU(3) Predictions of Radiative Decay Widths	16
3	Contributions to SU(3) Models with λ_8 Symmetry Breaking	35
4	Predictions of the Baryon Loop Model with the Photon Attached to the Loop with F-type Coupling	44
5	Predictions of the Baryon Loop Model with the Photon Attached to the Loop through VMD	49
6	Predictions of the Current Algebra Model	60
7	Predictions of the Strong Nonet Symmetry Model with Boson Symmetry and SU(3) Symmetry Breaking	68
8	Predictions of Other Nonet Symmetry Models with SU(3) Symmetry Breaking	72
9	Predictions of Meson Decay Rates in Two Types of Symmetry Breaking Models	88
10	Predictions of Radiative Decay Widths in the SU(4) Symmetry Breaking Model	97
11	Ratios of $\psi \rightarrow VP$ Widths	100

LIST OF FIGURES

Figure		Page
1	Processes Related by VMD	20
2	Contributions to the Baryon Loop Model with the Photon Attached to the Loop with F-type Coupling	38
3	Contributions to the Baryon Loop Model with the Photon Attached to the Loop through VMD	46
4	Quark Line Diagram for $V \rightarrow P\gamma$	121
5	SU(3) Invariant Contributions to \mathcal{L}	122
6	Totally Connected SU(3) Symmetry Breaking Contributions to \mathcal{L}	123
7	Pairwise Connected SU(3) Symmetry Breaking Contributions to \mathcal{L}	124
8	Disconnected SU(3) Symmetry Breaking Contributions to \mathcal{L}	125

NOTATION

V	vector meson
P	pseudoscalar meson
A	vector potential
γ	photon
B	baryon
q	quark
u	up quark
d	down quark
s	strange quark
c	charmed quark
t	top quark
b	bottom quark
OZI rule	Okubo Zweig Iizuka rule
VMD	vector meson dominance
PCAC	partially conserved axial current

CHAPTER I

THE RADIATIVE DECAYS OF VECTOR AND PSEUDOSCALAR MESONS

1.1 Introduction to the Problem

The radiative decays of vector and pseudoscalar mesons have received much experimental attention in the last few years. Decay widths have now been measured for $\omega \rightarrow \pi\gamma$, $K^{*0} \rightarrow K^0\gamma$, $\phi \rightarrow \eta\gamma$, $\phi \rightarrow \pi\gamma$, and $\rho \rightarrow \pi\gamma$; upper bounds are available for the $\omega \rightarrow \eta\gamma$, $\rho \rightarrow \eta\gamma$, $K^{*+} \rightarrow K^+\gamma$, $\eta' \rightarrow \rho\gamma$ and $\eta' \rightarrow \omega\gamma$ widths. Enough data have now been collected to provide a critical test of the theoretical models for radiative decays.

The best determined rate is $\Gamma(\omega \rightarrow \pi\gamma) = 880 \pm 60 \text{ KeV}$ [1] which has been measured five times since 1967. The $K^{*} \rightarrow K\gamma$ rates have been studied in two Primakoff effect experiments: $\Gamma(K^{*0} \rightarrow K^0\gamma) = 75 \pm 35 \text{ KeV}$ [2], $\Gamma(K^{*+} \rightarrow K^+\gamma) < 80 \text{ KeV}$ [3]. In a similar experiment, Gobbi et al. [4] have found $\Gamma(\rho \rightarrow \pi\gamma) = 35 \pm 10 \text{ KeV}$. The Orsay group [5] obtained $\Gamma(\phi \rightarrow \pi\gamma) = 5.9 \pm 2.1 \text{ KeV}$ and $\Gamma(\phi \rightarrow \eta\gamma) = 62 \pm 15 \text{ KeV}$ in an e^+e^- experiment. This last rate is much lower than two previous measurements [6] and consistent with a recent one by Andrews et al. [7]. Andrews et al. also made the first measurements on the $\rho \rightarrow \eta\gamma$ and $\omega \rightarrow \eta\gamma$ widths; depending on the relative phases of the ρ and ω amplitudes, they found $\Gamma(\rho \rightarrow \eta\gamma) = 50 \pm 13 \text{ KeV}$ and $\Gamma(\omega \rightarrow \eta\gamma) = 3.0^{+2.5}_{-1.8} \text{ KeV}$ or $\Gamma(\rho \rightarrow \eta\gamma) = 76 \pm 15 \text{ KeV}$ and

$\Gamma(\omega \rightarrow \eta \gamma) = 29 \pm 7 \text{ KeV}$. These fall well within the old bounds [1] of $\Gamma(\rho \rightarrow \eta \gamma) < 150 \text{ KeV}$ and $\Gamma(\omega \rightarrow \eta \gamma) < 50 \text{ KeV}$. Zangwill et al. [8] have measured the $\eta' \rightarrow \omega \gamma$ partial width which together with the available $\eta' \rightarrow \rho \gamma$ partial width [1] gives $\Gamma(\eta' \rightarrow \rho \gamma) / \Gamma(\eta' \rightarrow \omega \gamma) = 9.9 \pm 2.0$; only upper bounds are available for the absolute widths [1] of these decays: $\Gamma(\eta' \rightarrow \rho \gamma) < 300 \text{ KeV}$ and $\Gamma(\eta' \rightarrow \omega \gamma) < 50 \text{ KeV}$.

Until the appearance of the recent data, no theoretical problems existed. The quark model [9], some strong anomaly calculations [10] and a vector meson dominance (VMD) scheme [11] were all in reasonable agreement. The only measured rate, $\Gamma(\omega \rightarrow \pi \gamma) \sim 1 \text{ MeV}$, could be explained *ab initio*. Assuming ideal mixing of vector mesons, it was anticipated that $\Gamma(\omega \rightarrow \pi \gamma) / \Gamma(\rho \rightarrow \pi \gamma) \sim 9$. Not only did $\Gamma(\rho \rightarrow \pi \gamma)$ turn out a factor of three too low, but $\Gamma(K^{*0} \rightarrow K^0 \gamma)$ and $(\phi \rightarrow \eta \gamma)$ were also measured to be considerably lower than any of the models predicted. With $\Gamma(\omega \rightarrow \pi \gamma) = 880 \pm 60 \text{ KeV}$ firmly established, the radiative decays of vector and pseudoscalar mesons clearly required further theoretical attention.

Which assumptions of the traditional models could, if altered, lead to improved predictions for meson radiative decay widths? Could these assumptions be so altered without undoing previous successes in particle theory? The explanation of the radiative decays of vector and pseudoscalar mesons might involve a reassessment of the following unitary symmetry aspects of the traditional approaches: the multiplet assignment of the mesons and the electromagnetic current,

the choice of mixing angles, the use of the Okubo Zweig Iizuka (OZI) rule [12] and the nature of the symmetry structure of the $VP\gamma$ amplitude. In this thesis, it is this last possibility which is explored.

1.2 Mesons, Quarks and Radiative Decays

The J^{PC} and unitary symmetry properties of the mesons can be explained by a simple quark model. Given quarks with $J^P = \frac{1}{2}^+$, the lowest mass $q\bar{q}$ bound states are expected to be the 1S_0 ; $C = +1$ (pseudoscalar) and 3S_1 ; $C = -1$ (vector) states in quark terms, the $V \rightarrow P\gamma$ decay is an M1 transition from the 3S_1 to the 1S_0 $q\bar{q}$ bound state. While the quark model provides a picturesque description of the $V \rightarrow P\gamma$ and $P \rightarrow V\gamma$ processes, it is questionable whether it is the most useful computational model.

In a quark model calculation of the $VP\gamma$ amplitude, several assumptions regarding the quark potentials or the quark wavefunctions must be made. While the general Lorentz structure of the M1 decay amplitude is fixed, some energy dependence awaits the specification of the meson overlap integrals. The usual long wavelength assumption suggests that these overlaps are unity and a $VP\gamma$ decay amplitude results which has the same form as that which results from treating the mesons as structureless particles. The quark model seems to complicate rather than clarify the kinematical aspects of the radiative decay calculation.

The unitary symmetry part of the calculation may

also be discussed more easily on the meson level. Since the mesons themselves are assigned to unitary representations, it is much less cumbersome to work with two meson representations rather than four quark representations. Once the mesons have been built from $q\bar{q}$ states, all the unitary symmetry information has been transferred to meson representatives.

For these reasons, throughout most of this thesis computations are ventured on the meson level. Occasionally mention is made of the quark content of the mesons when the quark picture provides a vivid illustration of a physical principle. Some sample quark model calculations appear in Appendix I--these serve to indicate the correspondence between the two approaches.

1.3 Implementation of Unitary Symmetry

Unitary symmetry enters the radiative decay rate calculation in two ways. First of all, the vector mesons (V) and the pseudoscalar mesons (P) are assigned to SU(3) multiplets and the SU(3) content of the photon (γ) is specified. Then a Lagrangian is constructed which demonstrates certain transformation properties under SU(3) rotations. In this connection, the terms SU(3) symmetry and nonet symmetry must be defined.

The vector mesons are assigned to an SU(3) octet (indices 1-8) and an SU(3) singlet (index 0). The SU(3) content of ρ and K^* is:

$$\begin{aligned}
|\rho^+\rangle &= |\rho^-\rangle^\dagger = \frac{1}{\sqrt{2}} (|1\rangle - i|2\rangle) \\
|\rho^0\rangle &= |3\rangle \\
|K^{*+}\rangle &= |K^{*-}\rangle^\dagger = \frac{1}{\sqrt{2}} (|4\rangle - i|5\rangle) \\
|K^{*0}\rangle &= |\bar{K}^{*0}\rangle^\dagger = \frac{1}{\sqrt{2}} (|6\rangle - i|7\rangle).
\end{aligned} \tag{1.1}$$

The ω and ϕ mesons are mixtures of the SU(3) singlet and the eighth member of the SU(3) octet:

$$\begin{aligned}
|\omega\rangle &= \sin \theta_V |8\rangle + \cos \theta_V |0\rangle \\
|\phi\rangle &= \cos \theta_V |8\rangle - \sin \theta_V |0\rangle.
\end{aligned} \tag{1.2}$$

The vector mixing angle θ_V is usually taken to be that of ideal mixing (and close to that determined by the quadratic mass formula), $\theta_V = \tan^{-1}(1/\sqrt{2}) \sim 35^\circ$. This ideal value of θ_V gives ω pure $u\bar{u}$ and $d\bar{d}$ quark content while ϕ has pure $s\bar{s}$ quark content.

The pseudoscalar mesons are similarly assigned to an SU(3) octet and an SU(3) singlet. The SU(3) content of π and K is:

$$\begin{aligned}
|\pi^+\rangle &= |\pi^-\rangle^\dagger = \frac{1}{\sqrt{2}} (|1\rangle - i|2\rangle) \\
|\pi^0\rangle &= |3\rangle \\
|K^+\rangle &= |K^-\rangle^\dagger = \frac{1}{\sqrt{2}} (|4\rangle - i|5\rangle) \\
|K^0\rangle &= |\bar{K}^0\rangle^\dagger = \frac{1}{\sqrt{2}} (|6\rangle - i|7\rangle).
\end{aligned} \tag{1.3}$$

The η and η' mesons are the following mixtures of the singlet and octet:

$$\begin{aligned}
|\eta'\rangle &= \sin \theta_P |8\rangle + \cos \theta_P |0\rangle \\
|\eta\rangle &= \cos \theta_P |8\rangle - \sin \theta_P |0\rangle.
\end{aligned} \tag{1.4}$$

where θ_p is the pseudoscalar mixing angle. θ_p is usually taken to be -10° , the magnitude being deduced from the quadratic mass formula and the sign from $\Gamma(\eta \rightarrow \gamma\gamma)/\Gamma(\pi \rightarrow \gamma\gamma)$ experiments.

The usual electromagnetic current is constructed from the third and eighth members of an SU(3) octet of currents:

$$J_\mu^{\text{em}} = J_\mu^3 + \frac{1}{\sqrt{3}} J_\mu^8.$$

The SU(3) content of the photon is seen to be

$$|\gamma\rangle = |3\rangle + \frac{1}{\sqrt{3}} |8\rangle. \quad (1.5)$$

Other forms of J_μ^{em} have been suggested [13] leading to more complicated versions of (1.5). This point is discussed in Appendix II.

In the SU(3) symmetry scheme, an SU(3) rotationally invariant structure is given to the simplest minimally coupled, Lorentz and charge conjugation invariant Lagrangian which may be constructed from the vector (V_μ^i) and the pseudoscalar (P_μ^i) wavefunctions and the vector potentials (A_μ^i):

$$\begin{aligned} \mathcal{L} = \frac{1}{\sqrt{2}} \epsilon^{\mu\nu\rho\sigma} [& g_0 \text{Tr} (\{ \partial_\mu V_\nu^{(8)}, \partial_\rho A_\sigma^{(8)} \} P^{(8)}) \\ & + g_1 \text{Tr} (\{ \partial_\mu V_\nu^{(0)}, \partial_\rho A_\sigma^{(8)} \} P^{(8)}) \\ & + g_2 \text{Tr} (\{ \partial_\mu V_\nu^{(8)}, \partial_\rho A_\sigma^{(8)} \} P^{(0)})] \quad (1.6) \end{aligned}$$

where

$$V_{\mu}^{(8)} = \frac{1}{\sqrt{2}} \sum_{i=1}^8 \lambda_i V_{\mu}^i$$

$$V_{\mu}^{(0)} = \frac{1}{\sqrt{2}} \lambda_0 V_{\mu}^0$$

$$P^{(8)} = \frac{1}{\sqrt{2}} \sum_{i=1}^8 \lambda_i P^i$$

$$P^{(0)} = \frac{1}{\sqrt{2}} \lambda_0 P^0$$

$$A_{\mu}^{(8)} = \frac{1}{\sqrt{2}} \sum_{i=1}^8 \lambda_i A_{\mu}^i,$$

λ_i ($i=1, \dots, 8$) are the SU(3) generating matrices and $\lambda_0 = \sqrt{\frac{2}{3}} I$. Other SU(3) invariant structures could be considered in (1.6) but they either vanish (eg. $\text{Tr} (\{\partial_{\mu} V_{\nu}^{(8)}, \partial_{\rho} A_{\sigma}^{(8)}\}) \text{Tr} (P^{(8)})$) or depend linearly on those already used (eg. $\text{Tr} (\{\partial_{\mu} V_{\nu}^{(8)}, \partial_{\rho} A_{\sigma}^{(8)}\}) \text{Tr} (P^{(0)})$).

Nonet symmetry is the special case of SU(3) symmetry in which the SU(3) octets and singlets couple with the same strength ($g_0 = g_1 = g_2$). In a model with nonet symmetry, only those processes which obey the OZI rule [12] are allowed--any process for which the quark line diagram contains an individual disconnected initial or final state particle is forbidden. Since the OZI rule seems to hold in other areas of hadron physics, nonet symmetry is a likely ingredient for a meson radiative decay model.

To more easily implement nonet symmetry, it is convenient to work directly with nonets of particles. The SU(3) Lagrangian (1.6) may be rewritten:

$$\begin{aligned}
 \mathcal{L} = & \frac{1}{\sqrt{2}} \epsilon^{\mu\nu\rho\sigma} [g_0 \text{Tr} (\{\partial_\mu V_\nu, \partial_\rho A_\sigma\} P) \\
 & + \frac{1}{3} (g_1 - g_0) \text{Tr} (\{\partial_\mu V_\nu, \partial_\rho A_\sigma\}) \text{Tr} (P) \\
 & + \frac{1}{3} (g_2 - g_0) \text{Tr} (\partial_\mu V_\nu) \text{Tr} (\{\partial_\rho A_\sigma, P\})]
 \end{aligned} \tag{1.7}$$

where

$$\begin{aligned}
 V_\mu &= \frac{1}{\sqrt{2}} \sum_{i=0}^8 \lambda_i V_\mu^i \\
 P &= \frac{1}{\sqrt{2}} \sum_{i=0}^8 \lambda_i P^i \\
 A_\mu &= \frac{1}{\sqrt{2}} \sum_{i=0}^8 \lambda_i A_\mu^i .
 \end{aligned}$$

Terms involving A_μ^0 that do not appear in (1.6) are included in (1.7); these are of no consequence for radiative decays. The last two terms of (1.7) include traces over the internal degrees of freedom of individual particles. Since these terms can not be reexpressed to avoid such traces, these terms constitute OZI violations. It is clear that the $(g_1 - g_0)$ term involves only the singlet part of P and that the $(g_2 - g_0)$ term uses only the singlet part of V ; these terms break nonet symmetry by giving singlets special rôles. Nonet symmetry and, equivalently, adherence to the OZI rule are

achieved when $g_0 = g_1 = g_2$.

In the next sections the predictions of the nonet model and the general SU(3) model are discussed.

1.4 The Nonet Symmetry Scheme

The Lagrangian with nonet symmetry which describes the radiative decay of vector and pseudoscalar mesons has only one coupling constant. The $V \rightarrow P\gamma$ decay widths computed from such a Lagrangian are related simply by ratios of phase space factors and SU(3) Clebsch Gordan coefficients.

The Lagrangian with nonet symmetry which describes the VPA interaction is:

$$\mathcal{L} = \frac{g_0}{\sqrt{2}} \epsilon^{\mu\nu\rho\sigma} \text{Tr} (\{\partial_\mu V_\nu, \partial_\rho A_\sigma\} P) \quad (1.8)$$

where

$$V_\mu = \frac{1}{\sqrt{2}} \sum_{i=0}^8 \lambda_i V_\mu^i$$

$$P = \frac{1}{\sqrt{2}} \sum_{i=0}^8 \lambda_i P^i$$

$$A_\mu = \frac{1}{\sqrt{2}} \sum_{i=0}^8 \lambda_i A_\mu^i.$$

The part of the Lagrangian (1.8) which describes the interaction of the vector V^m (momentum p_m , polarization ϵ_m) with the pseudoscalar P^i (momentum p_i) and a photon (momentum p_n , polarization ϵ_n) is

$$\mathcal{L}_{V P \gamma} = g_0 d_{\min} \epsilon_{\mu\nu\rho\sigma} (p_m)^\mu (\epsilon_m)^\nu (p_n)^\rho (\epsilon_n)^\sigma \quad (1.9)$$

where the photon index is

$$|n\rangle = |3\rangle + \frac{1}{\sqrt{3}} |8\rangle.$$

and d_{\min} is the SU(3) structure constant. The corresponding T matrix is

$$T_{V^m P^i \gamma} = \frac{1}{(2\pi)^9/2} \frac{1}{(8E_m E_i E_n)^{1/2}} g_0 d_{\min} \epsilon_{\mu\nu\rho\sigma} (p_m)^\mu (\epsilon_m)^\nu (p_n)^\rho (\epsilon_n)^\sigma$$

where E_m , E_i and E_n are the V^m , P^i and γ energies respectively.

The $V^m \rightarrow P^i \gamma$ decay rate is

$$\Gamma(V^m \rightarrow P^i \gamma) = \frac{1}{3} \sum_{\text{pol}} \frac{(2\pi)^4}{\eta} \int |T|^2 \delta^4(p_m - p_i - p_n) d^3 p_i d^3 p_n$$

where η is the density of final states, $(\frac{1}{2\pi})^3$. After simplification, the $V^m \rightarrow P^i \gamma$ decay rate is

$$\Gamma(V^m \rightarrow P^i \gamma) = \frac{1}{96\pi} (g_0 d_{\min})^2 \left(\frac{M_m^2 - M_i^2}{M_m} \right)^3 \quad (1.10)$$

where M_m and M_i are the V^m and P^i masses respectively. When the pseudoscalar is more massive than the vector, a $P^i \rightarrow V^m \gamma$ decay occurs:

$$\Gamma(P^i \rightarrow V^m \gamma) = \frac{1}{32\pi} (g_0 d_{\min})^2 \left(\frac{M_i^2 - M_m^2}{M_i} \right)^3. \quad (1.11)$$

The nonet predictions of radiative decay rates are obtained from (1.10) and (1.11). The $\omega \rightarrow \pi\gamma$ and $\rho \rightarrow \pi\gamma$ widths are simply related by a ratio of Clebsch Gordan coefficients

since they have almost identical phase space factors. Assuming ideal vector mixing ($\theta_V \sim 35^\circ$), it is predicted that

$$\Gamma(\omega \rightarrow \pi\gamma) / \Gamma(\rho \rightarrow \pi\gamma) \sim 9 \quad (1.12)$$

and furthermore that

$$\Gamma(\phi \rightarrow \pi\gamma) / \Gamma(\rho \rightarrow \pi\gamma) = 0. \quad (1.13)$$

That $\phi \rightarrow \pi\gamma$ should be forbidden is anticipated--under the OZI rule, an $s\bar{s}$ state does not decay into a $u\bar{u}$ and $d\bar{d}$ state.

Another ratio predicted by this nonet model is

$$\Gamma(K^{*0} \rightarrow K^0\gamma) / \Gamma(K^{*+} \rightarrow K^+\gamma) \sim 4. \quad (1.14)$$

This ratio will be seen to be quite model dependent.

In Table 1 are displayed the nonet predictions for several values of g_0 . Solution 1 uses $g_0 = 0.656 \text{ GeV}^{-1}$; this value is obtained by fitting (1.10) and (1.11) to the five measured rates: $\Gamma(\omega \rightarrow \pi\gamma)$, $\Gamma(K^{*0} \rightarrow K^0\gamma)$, $\Gamma(\rho \rightarrow \pi\gamma)$, $\Gamma(\phi \rightarrow \eta\gamma)$ and $\Gamma(\phi \rightarrow \pi\gamma)$. Solution 2 shows the predictions for $g_0 = 0.483 \text{ GeV}^{-1}$, this value arising from a fit which omits $\Gamma(\omega \rightarrow \pi\gamma)$. Solution 3 uses $g_0 = 0.778 \text{ GeV}^{-1}$, thus fixing $\Gamma(\omega \rightarrow \pi\gamma) = 880 \text{ KeV}$. All fits, in this and other chapters, are linear least squares fits to $\pm \Gamma^{1/2}(V^m \rightarrow P^i \gamma)$. The phase ambiguity is resolved by selecting the phases which yield the smallest χ^2 ; these phases are always those of the amplitudes $T_{VP}^m i_\gamma$.

The problems with this model are evident in Table 1. No value of g_0 gives rates consistent with all the experimental

TABLE 1

Nonet Predictions of Radiative Decay Widths[†]

Decay Mode	Solution 1	Solution 2	Solution 3	Experiment
$\omega \rightarrow \pi\gamma$	(630)*	340	(880)	880 ± 60 [1]
$K^{*0} \rightarrow K^0 \gamma$	(150)	(80)	210	75 ± 35 [1]
$\rho \rightarrow \pi\gamma$	(65)	(35)	92	35 ± 10 [1]
$\phi \rightarrow \pi\gamma$	(0.03)	(0.02)	0.04	5.7 ± 2.1 [1]
$\phi \rightarrow \eta\gamma$	(120)	(64)	170	64 ± 10 [1,7]
$\omega \rightarrow \eta\gamma$	5.1	2.8	7.2	$3.0^{+2.5}_{-1.8}$ or 29 ± 7 [7]
$K^{*+} \rightarrow K^+ \gamma$	36	20	51	< 80 [3]
$\rho \rightarrow \eta\gamma$	39	21	55	50 ± 13 or 76 ± 15 [7]
$\eta' \rightarrow \omega\gamma$	7.4	4.0	10	< 50 [1]
$\eta' \rightarrow \rho\gamma$	82	44	120	< 300 [1]
$\phi \rightarrow \eta' \gamma$	0.56	0.31	0.79	--
$\Gamma(\eta' \rightarrow \rho\gamma) / \Gamma(\eta' \rightarrow \omega\gamma)$	11	11	11	9.9 ± 2.0 [8]

[†] All widths in KeV.

* In all tables, those widths whose experimental values are used as input to the fit are indicated by parentheses.

data. The rate $\Gamma(\phi \rightarrow \pi\gamma) \sim 6 \text{ KeV}$ might possibly be explained with a small deviation from ideal vector mixing; with a small $u\bar{u}/d\bar{d}$ content, $\phi \rightarrow \pi\gamma$ may proceed by an OZI allowed transition. However, the other rates remain mutually inconsistent. Solution 2 suggests that the rates for $K^{*0} \rightarrow K^0\gamma$, $\rho \rightarrow \pi\gamma$ and $\phi \rightarrow \eta\gamma$ demonstrate the proper nonet ratios but that $\Gamma(\omega \rightarrow \pi\gamma)$ should be about 340 KeV. Unfortunately for the nonet model, $\Gamma(\omega \rightarrow \pi\gamma)$ is well established at about 880 KeV. Solution 3, which fixes $\Gamma(\omega \rightarrow \pi\gamma) = 880 \text{ KeV}$, indicates that the $K^{*0} \rightarrow K^0\gamma$, $\rho \rightarrow \pi\gamma$ and $\phi \rightarrow \eta\gamma$ rates are actually a factor of 2.6 lower than the nonet predictions. Contrary to the belief of O'Donnell [14], the present data for radiative decays are not consistent with the nonet model.

1.5 The SU(3) Symmetry Scheme

Boal, Graham and Moffat [15] suggest that the nonet symmetry of section 1.4 may be too restrictive and that by simply demanding SU(3) symmetry, it may be possible to understand the radiative decays of vector and pseudoscalar mesons.

The SU(3) Lagrangian (1.6) is used, with $g_0=g$, $g_1=f'$ and $g_2=f$. The kinematics are the same as in the nonet calculation. The $V^m \rightarrow P^i \gamma$ rate takes a form similar to (1.10):

$$\Gamma(V^m \rightarrow P^i \gamma) = \frac{1}{96\pi} (g_{\min})^2 \left(\frac{M_m^2 - M_i^2}{M_m} \right)^3 \quad (1.15)$$

where

$$\begin{aligned}
g_{\min} &= g \, d_{\min} & m, i &= 1, \dots, 8 \\
g_{\text{mon}} &= f \, d_{\text{mon}} & m &= 1, \dots, 8 \\
g_{\text{oin}} &= f' \, d_{\text{oin}} & i &= 1, \dots, 8
\end{aligned} \tag{1.16}$$

The photon index is, as before,

$$|n\rangle = |3\rangle + \frac{1}{\sqrt{3}} |8\rangle .$$

The coupling constants g , f and f' are $SU(3)$ invariants. If they should all be equal, nonet symmetry is restored; if they should be different, violations of the OZI rule occur.

Independent of the choice of θ_V and θ_P , a number of observations may be made. The ratio $\Gamma(K^{*0} \rightarrow K^0 \gamma) / \Gamma(\rho \rightarrow \pi \gamma)$ maintains its experimentally substantiated nonet value-- since all the involved particles are members of $SU(3)$ octets, nonet breaking does not affect this ratio. Of the five measured rates, $\Gamma(\phi \rightarrow \eta \gamma)$ is the only one to use f and may thus be adjusted independently from the other four rates. This adjustment may, however, not be consistent with the measured $\Gamma(\eta' \rightarrow \rho \gamma) / \Gamma(\eta' \rightarrow \omega \gamma)$ ratio.

Assuming the usual ideal mixing of vector mesons, an inconsistency arises. Even though the OZI forbidden decay $\phi \rightarrow \pi \gamma$ is seen to proceed, it does so very slowly considering the available phase space. This means that $g \sim f'$. If $g \sim f'$, there is not sufficient nonet breaking to account for $\Gamma(\omega \rightarrow \pi \gamma) / \Gamma(\rho \rightarrow \pi \gamma) \sim 25$. Choosing $g = 0.480 \text{ GeV}^{-1}$ and $f' = 0.926 \text{ GeV}^{-1}$ to obtain $\Gamma(\omega \rightarrow \pi \gamma) = 880 \text{ KeV}$ and

and $\Gamma(\rho \rightarrow \pi\gamma) = 35 \text{ KeV}$, a rate $\Gamma(\phi \rightarrow \pi\gamma) = 140 \text{ KeV}$ is predicted. If $SU(3)$ symmetry is to succeed in explaining the radiative decays, it is necessary to adopt a nonideal value of θ_V .

Boal, Graham and Moffat [15] present two fits, each corresponding to different combinations of mixing angles. These fits are displayed in Table 2; note that the experimental rates are those current to publication. In the fit for solution 1, θ_P is fixed at its quadratic mass formula value (-10°) and g , f , f' and θ_V are treated as free parameters. The resulting values ($g=0.476 \text{ GeV}^{-1}$, $f=0.769 \text{ GeV}^{-1}$, $f'=0.889 \text{ GeV}^{-1}$, $\theta_V=24^\circ$) indicate substantial¹ nonet breaking and large deviation from ideal mixing. All experimental rates are predicted and all experimental bounds satisfied; only $\Gamma(\eta' \rightarrow \rho\gamma)/\Gamma(\eta' \rightarrow \omega\gamma)$ deviates from experiment. Solution 2 uses mixing angles from the linear mass formula ($\theta_V=37^\circ$, $\theta_P=-24^\circ$). The resulting coupling constants display less nonet breaking than solution 1 ($g=0.746 \text{ GeV}^{-1}$, $f=0.876 \text{ GeV}^{-1}$, $f'=0.790 \text{ GeV}^{-1}$) but the predicted rates don't agree with experiment. In particular, $\Gamma(\rho \rightarrow \pi\gamma)$ and $\Gamma(K^{*0} \rightarrow K^0\gamma)$ are about a factor of 2.5 too large; this is the result of θ_V being nearly ideal. The $SU(3)$ scheme is reasonably successful only when large nonet breaking and an artificial θ_V are used. The further implications of these unusual features are investigated later when other $SU(3)$ decays are considered.

The $SU(3)$ scheme does offer an explanation of the observed radiative decay rates. The necessary nonet breaking

TABLE 2

SU(3) Predictions of Radiative Decay Widths[†]

Decay Mode	Solution 1	Solution 2	Experiment ^{††}
$\omega \rightarrow \pi\gamma$	(870)	(870)	870 ± 61
$K^{*0} \rightarrow K^0\gamma$	(78)	(190)	75 ± 35
$\rho \rightarrow \pi\gamma$	(35)	(85)	35 ± 10
$\phi \rightarrow \pi\gamma$	(6.5)	(6.5)	6.5 ± 1.9
$\phi \rightarrow \eta\gamma$	(81)	(80)	81 ± 32
$\omega \rightarrow \eta\gamma$	24	12	<50
$K^{*+} \rightarrow K^+\gamma$	20	48	<80
$\rho \rightarrow \eta\gamma$	26	84	<160
$\eta' \rightarrow \omega\gamma$	2.6	8.9	<80
$\eta' \rightarrow \rho\gamma$	130	89	<270
$\phi \rightarrow \eta'\gamma$	0.84	1.3	--
$\Gamma(\eta' \rightarrow \rho\gamma) / \Gamma(\eta' \rightarrow \omega\gamma)$	50	10	--

[†] All widths in KeV.

^{††} References as in [15]. These are 1975 data.

requires large violations of the OZI rule. Furthermore, the traditional connection between mixing angles and mass formulae is lost--the mass formula which yields $\theta_V \sim 24^\circ$, the inverse mass squared formula, cannot be applied to pseudoscalars because the resulting θ_P is complex. Although the $V \rightarrow P\gamma$ predictions of this SU(3) model are reasonably good, it would be desirable to retain mass formula mixing angles and some remnant of the OZI rule.

1.6 SU(3) Symmetry Breaking Models

The approach to $V \rightarrow P\gamma$ decays investigated in this thesis is one of SU(3) breaking. It is hoped that a physically reasonable SU(3) breaking scheme may permit the use of quadratic mass formula mixing angles and, to some extent, the preservation of the OZI rule.

The SU(3) symmetry observed in particle physics is only approximate. The most familiar example of SU(3) breaking concerns the mass splittings within the octet of baryons. The Gell-Mann--Okubo mass formula prediction

$$\frac{M_{\Xi} + M_N}{2} = \frac{3M_{\Lambda} + M_{\Sigma}}{4}$$

is obtained by assuming a Lagrangian of the form

$$\mathcal{L} = m_0 \text{Tr} (B\bar{B}) + m_1 \text{Tr} (B\bar{B}\lambda_8) + m_2 \text{Tr} (B\lambda_8\bar{B}).$$

Symmetry breaking by one λ_8 accounts for the observed regularities of the baryon mass splittings. This type of SU(3) breaking is the only one consistent with charge,

isospin and strangeness conservation.

In Chapter II, a hierarchy of SU(3) symmetry breaking models for the meson radiative decay vertex is discussed. The relationship between symmetry breaking and the OZI rule is studied. The implications of vector meson dominance are noted.

In the next chapters, specific SU(3) breaking models are examined in detail. In each case, the available coupling constants are fit using the experimental $V \rightarrow P\gamma$ rate, and the success of the model evaluated.

Various forms of SU(3) breaking for radiative decays of vector mesons have been discussed previously. References [16] present schemes analagous to the weak and strong nonet models of Chapter II, omitting one or more of the SU(3) singlet sectors. Reference [17] takes a slightly different approach, generating apparent SU(3) breaking with the meson masses. These discussions were all published prior to the recent experiments. The experimental $V \rightarrow P\gamma$ rates now available make a comprehensive treatment of the SU(3) breaking models feasible.

1.7 Other Decays

Vector meson dominance (VMD) in its original form related the nucleon electromagnetic form factors (essentially the $N\bar{N}\gamma$ vertex) to the $N\bar{N}V$ interaction. In a more general form, it relates processes involving photons to those involving vector mesons--a process involving a photon may be

considered to proceed through a $C=-1$ vector meson, the photon being attached to the vector meson according to

$$\chi_{V\gamma}^m = \frac{e}{g_\rho} M_m^2 \delta_{mn} \quad (1.17)$$

where n is the photon index and g_ρ is the $\rho\pi\pi$ coupling constant [18]:

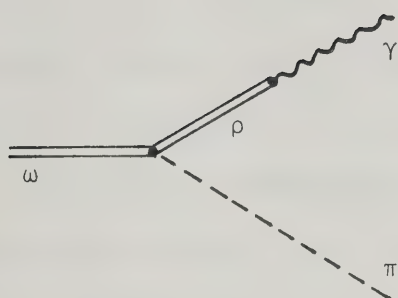
$$\frac{g_\rho^2}{4\pi} = 2.93 \pm 0.02 .$$

Most models for radiative decays of vector mesons may be used, with VMD, to deduce a model for the VVP vertex. A VVP and a VPP vertex, together with VMD, may be used to predict a variety of radiative and hadronic rates. Examples of some describable processes are illustrated in Figure 1.

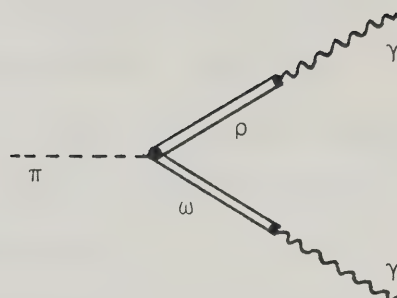
In Chapter VI, these further decays are discussed in detail. Predictions for the $\pi \rightarrow \gamma\gamma$, $\eta \rightarrow \gamma\gamma$, $\eta' \rightarrow \gamma\gamma$, $\omega \rightarrow 3\pi$, $\phi \rightarrow 3\pi$, $\eta \rightarrow \pi\pi\gamma$ and $\eta' \rightarrow \pi\pi\gamma$ rates are made on the basis of the SU(3) model [15] and one SU(3) breaking model discussed in Chapter V. The ability of these models to predict such rates may provide an indication of their validity. It must be remembered, however, that the additional assumption of VMD is incorporated in these predictions.

1.8 Extensions to SU(4)

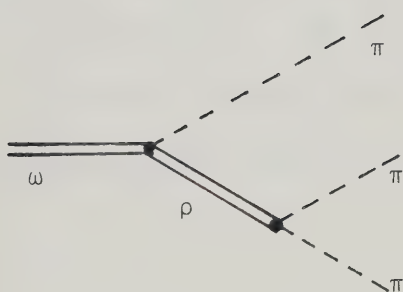
Recent experiments [19,20] on the radiative decays of the ψ meson suggest that an SU(4) description of the radiative decays of mesons is now needed. If ψ is in fact



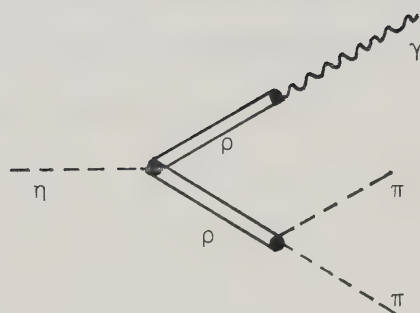
(a)



(b)



(c)



(d)

Figure 1. Processes Related by VMD. Examples of (a) $V \rightarrow P\gamma$, (b) $P \rightarrow \gamma\gamma$, (c) $V \rightarrow PPP$ and (d) $P \rightarrow PP\gamma$.

a pure $c\bar{c}$ state, the $SU(4)$ radiative decays are to prove as recalcitrant as the $SU(3)$ ones. Already the OZI forbidden decays $\psi \rightarrow \pi\gamma$, $\psi \rightarrow \eta\gamma$ and $\psi \rightarrow \eta'\gamma$ are observed to proceed while the decay $\psi \rightarrow \eta_c (2.83 \text{ GeV})\gamma$, which is OZI allowed and which has ample phase space, is quite suppressed. An $SU(4)$ symmetry or symmetry breaking scheme for radiative decays must incorporate a solution to the $SU(3)$ radiative decay problem and explain the ψ rates as well.

In Chapter VII, a model for $SU(4)$ breaking is discussed. This is a natural extension of one of the $SU(3)$ breaking schemes of Chapter V--all mesons and the photon have standard $SU(4)$ content, reasonable mixing angles are used, the OZI rule is, to some extent, incorporated and the symmetry breaking occurs in a fashion similar to mass splitting, by λ_8 and λ_{15} . No new difficulties are encountered in treating the ψ rates; some previously unresolved $SU(3)$ inconsistencies do however persist.

CHAPTER II

THE HIERARCHY OF SYMMETRY BREAKING SCHEMES

2.1 The Nature of Symmetry Breaking

Just as an $SU(3)$ symmetric $VP\gamma$ amplitude is derived from an $SU(3)$ invariant Lagrangian, so does a $VP\gamma$ amplitude which has the unitary symmetry broken by λ_j come from a Lagrangian which transforms as λ_j under unitary rotations. Such a Lagrangian is constructed from different trace combinations of V , P , A and λ_j . While not invariant under arbitrary unitary rotations of V , P and A , it is invariant under those rotations whose generators commute with λ_j ; furthermore, the quantum numbers corresponding to these operators are conserved even under the broken symmetry.

It is convenient to picture symmetry breaking by λ_j in terms of a scalar spurion [21], an imaginary particle which carries only an internal symmetry label. If the radiative decay $V \rightarrow P\gamma$ were to proceed with an additional scalar particle in the final state which was massless, momentumless and bore the unitary index j , the corresponding Lagrangian would have exactly the same form as the Lagrangian with λ_j symmetry breaking. The radiative decay $V \rightarrow P\gamma$ with symmetry breaking is equivalent to the decay $V \rightarrow P\gamma U_j$. The concept of a scalar spurion will prove most useful in Appendix I when symmetry breaking is discussed on the quark level.

Charge and hypercharge are conserved in electromagnetic

interactions. Total isospin is also conserved if the photon is assigned the isospin content dictated by its SU(3) content. In order that these quantum numbers be conserved, all terms in the Lagrangian must be invariant under $\lambda_1, \lambda_2, \lambda_3$, and λ_8 rotations of the V, P and A multiplets--the only possible symmetry breaking is by λ_8 and λ_0 . In the spurion picture, any spurion which carries off no charge, isospin or strangeness must have T=0 and Y=0--only U_8 and U_0 are possible.

In the next section, a general SU(3) scheme with λ_8 symmetry breaking is discussed. The OZI rule is then enforced and the connection between λ_0 breaking and OZI violations elucidated. The implications of VMD are also studied. In the last section, a hierarchy of symmetry breaking schemes is presented.

2.2 The Most General SU(3) Model With λ_8 Symmetry Breaking

In this section, the SU(3) model of section 1.3 is expanded to include λ_8 symmetry breaking. The SU(3) invariant contributions to the VPA Lagrangian are, as before, various trace combinations of the V, P and A multiplets; the λ_8 symmetry breaking terms arise from various trace combinations of the V, P and A multiplets with one λ_8 matrix. The kinematics remain unchanged from the previous calculations.

The Lagrangians that describe the radiative decays are

$$\mathcal{L}_{V(8)P(8)A(8)} = \epsilon^{\mu\nu\rho\sigma} \left[\frac{g_0}{\sqrt{2}} \text{Tr} (\{ \partial_\mu V_\nu^{(8)}, \partial_\rho A_\sigma^{(8)} \} P^{(8)}) \right] \text{ (cont.)}$$

$$\begin{aligned}
& + \frac{g_1}{\sqrt{2}} (\text{Tr } (\partial_\mu V_\nu^{(8)} \partial_\rho A_\sigma^{(8)} P^{(8)} \lambda_8) \\
& \quad + \text{Tr } (\partial_\mu V_\nu^{(8)} \lambda_8 P^{(8)} \partial_\rho A_\sigma^{(8)})) \\
& + \frac{g_2}{\sqrt{2}} (\text{Tr } (\partial_\mu V_\nu^{(8)} P^{(8)} \partial_\rho A_\sigma^{(8)} \lambda_8) \\
& \quad + \text{Tr } (\partial_\mu V_\nu^{(8)} \lambda_8 \partial_\rho A_\sigma^{(8)} P^{(8)})) \\
& + \frac{g_3}{\sqrt{2}} (\text{Tr } (\partial_\mu V_\nu^{(8)} \partial_\rho A_\sigma^{(8)} \lambda_8 P^{(8)}) \\
& \quad + \text{Tr } (\partial_\mu V_\nu^{(8)} P^{(8)} \lambda_8 \partial_\rho A_\sigma^{(8)})) \\
& + \frac{g_4}{\sqrt{2}} \text{Tr } (\partial_\mu V_\nu^{(8)} \partial_\rho A_\sigma^{(8)}) \text{Tr } (P^{(8)} \lambda_8) \\
& + \frac{g_5}{\sqrt{2}} \text{Tr } (\partial_\mu V_\nu^{(8)} P^{(8)}) \text{Tr } (\partial_\rho A_\sigma^{(8)} \lambda_8) \\
& + \frac{g_6}{\sqrt{2}} \text{Tr } (\partial_\mu V_\nu^{(8)} \lambda_8) \text{Tr } (\partial_\rho A_\sigma^{(8)} P^{(8)})], \tag{2.1}
\end{aligned}$$

$$\begin{aligned}
\mathcal{L}_{V^{(8)} P^{(0)} A^{(8)}} &= \varepsilon^{\mu\nu\rho\sigma} \left[\frac{g_7}{\sqrt{2}} \text{Tr } (\{\partial_\mu V_\nu^{(8)}, \partial_\rho A_\sigma^{(8)}\} P^{(0)}) \right. \\
& \quad \left. + \frac{\sqrt{3}g_8}{2} \text{Tr } (\{\partial_\mu V_\nu^{(8)}, \partial_\rho A_\sigma^{(8)}\} P^{(0)} \lambda_8) \right], \tag{2.2}
\end{aligned}$$

$$\begin{aligned}
\mathcal{L}_{V^{(0)} P^{(8)} A^{(8)}} &= \varepsilon^{\mu\nu\rho\sigma} \left[\frac{g_9}{\sqrt{2}} \text{Tr } (\partial_\mu V_\nu^{(0)} \{\partial_\rho A_\sigma^{(8)}, P^{(8)}\}) \right. \\
& \quad \left. + \frac{\sqrt{3}g_{10}}{2} \text{Tr } (\partial_\mu V_\nu^{(0)} \{\partial_\rho A_\sigma^{(8)}, P^{(8)}\} \lambda_8) \right], \tag{2.3}
\end{aligned}$$

$$\mathcal{L}_{V^{(0)} P^{(0)} A^{(8)}} = \varepsilon^{\mu\nu\rho\sigma} \left[\frac{3g_{11}}{\sqrt{2}} \text{Tr } (\partial_\mu V_\nu^{(0)} \partial_\rho A_\sigma^{(8)} P^{(0)} \lambda_8) \right], \tag{2.4}$$

where

$$V_\mu^{(8)} = \frac{1}{\sqrt{2}} \sum_{i=1}^8 \lambda_i V_\mu^i,$$

$$V_{\mu}^{(0)} = \frac{1}{\sqrt{2}} \lambda_0 V_{\mu}^0,$$

$$P^{(8)} = \frac{1}{\sqrt{2}} \sum_{i=1}^8 \lambda_i P^i,$$

$$P^{(0)} = \frac{1}{\sqrt{2}} \lambda_0 P^0,$$

$$A_{\mu}^{(8)} = \frac{1}{\sqrt{2}} \sum_{i=1}^8 \lambda_i A_{\mu}^i.$$

Other terms could be included in the above, notably terms involving $\text{Tr} (V_{\mu}^{(0)})$ or $\text{Tr} (P^{(0)})$, but these depend linearly on the terms already considered.

The decay rate takes the form:

$$\Gamma(V^m \rightarrow P^i \gamma) = \frac{1}{96\pi} (g_{\min})^2 \left(\frac{M_m^2 - M_i^2}{M_m} \right)^3 \quad (2.5)$$

where g_{\min} is different for octets and singlets. For $V^{(8)} \rightarrow P^{(8)} \gamma$,

$$\begin{aligned} g_{\min} = & g_0 d_{\min} + (g_1 - g_2 + g_3) d_{8ik} d_{kmn} \\ & + (-g_1 + g_2 + g_3) d_{8nk} d_{kim} + (g_1 + g_2 - g_3) d_{8mk} d_{kin} \\ & + (g_4 + \frac{2}{3} (g_1 - g_2 + g_3)) \delta_{8i} \delta_{mn} \\ & + (g_5 + \frac{2}{3} (-g_1 + g_2 + g_3)) \delta_{8n} \delta_{im} \\ & + (g_6 + \frac{2}{3} (g_1 + g_2 - g_3)) \delta_{8m} \delta_{in}. \end{aligned} \quad (2.6)$$

For $V^{(8)} \rightarrow P^{(0)} \gamma$,

$$g_{\min} = (g_7 d_{\min} + g_8 d_{8mn}) \delta_{i0}. \quad (2.7)$$

For $V^{(0)} \rightarrow P^{(8)} \gamma$,

$$g_{\min} = (g_9 d_{oin} + g_{10} d_{8in}) \delta_{m0}. \quad (2.8)$$

For $V^{(0)} \rightarrow P^{(0)}_\gamma$,

$$g_{\min} = g_{11} \delta_{8n} \delta_{m0} \delta_{i0} . \quad (2.9)$$

The repeated symmetry index k is summed from 1 to 8 and n is the photon index.

Not all the above terms are independent as may be seen from the application of these identities:

$$d_{8ik} d_{kmn} + \frac{2}{3} \delta_{8i} \delta_{mn} = d_{8mk} d_{kin} + \frac{2}{3} \delta_{8m} \delta_{in}, \quad (2.10)$$

$$d_{8ik} d_{kmn} + d_{8nk} d_{kim} + d_{8mk} d_{kin} = \frac{1}{3} (\delta_{8i} \delta_{mn} + \delta_{8n} \delta_{im} + \delta_{8m} \delta_{in}), \quad (2.11)$$

where $i, m, k=1, \dots, 8$ and n is the photon index. The last identity is a special case of the well known SU(3) identity:

$$d_{ijk} d_{kmn} + d_{imk} d_{kjn} + d_{ink} d_{knj} = \frac{1}{3} (\delta_{ij} \delta_{mn} + \delta_{im} \delta_{jn} + \delta_{in} \delta_{jm}). \quad (i, j, k, m, n=1, \dots, 8) \quad (2.12)$$

Using (2.10) and (2.11) in (2.6), two of the $V^{(8)} \rightarrow P^{(8)}_\gamma$ symmetry breaking terms may be eliminated--only four coupling constants characterize the SU(3) symmetry breaking for $V^{(8)} \rightarrow P^{(8)}_\gamma$.

The most general SU(3) model for the radiative decays of vector and pseudoscalar mesons which uses λ_8 symmetry breaking has three SU(3) invariant and seven symmetry breaking terms. Ten SU(3) invariant coupling constants are needed in such a model.

This SU(3) scheme with λ_8 symmetry breaking may be

reformulated using nonets. The appropriate Lagrangian is:

$$\begin{aligned}
 \mathcal{L}_{\varepsilon}^{\mu\nu\rho\sigma} &= \frac{f_0}{\sqrt{2}} \text{Tr} (\{\partial^\mu V^\nu, \partial^\rho A^\sigma\} P) \\
 &+ \frac{f_1}{\sqrt{3}} \text{Tr} (\partial^\mu V^\nu \partial^\rho A^\sigma) \text{Tr} (P) \\
 &+ \frac{f_2}{\sqrt{3}} \text{Tr} (\partial^\mu V^\nu) \text{Tr} (\partial^\rho A^\sigma P) \\
 &+ \frac{f_3}{\sqrt{2}} (\text{Tr} (\partial^\mu V^\nu \partial^\rho A^\sigma P \lambda_8) + \text{Tr} (\partial^\mu V^\nu \lambda_8 P \partial^\rho A^\sigma)) \\
 &+ \frac{f_4}{\sqrt{2}} (\text{Tr} (\partial^\mu V^\nu P \partial^\rho A^\sigma \lambda_8) + \text{Tr} (\partial^\mu V^\nu \lambda_8 \partial^\rho A^\sigma P)) \\
 &+ \frac{f_5}{\sqrt{2}} (\text{Tr} (\partial^\mu V^\nu \partial^\rho A^\sigma \lambda_8 P) + \text{Tr} (\partial^\mu V^\nu P \lambda_8 \partial^\rho A^\sigma)) \\
 &+ \frac{f_6}{\sqrt{2}} \text{Tr} (\partial^\mu V^\nu \partial^\rho A^\sigma) \text{Tr} (P \lambda_8) \\
 &+ \frac{f_7}{\sqrt{2}} \text{Tr} (\partial^\mu V^\nu P) \text{Tr} (\partial^\rho A^\sigma \lambda_8) \\
 &+ \frac{f_8}{\sqrt{2}} \text{Tr} (\partial^\mu V^\nu \lambda_8) \text{Tr} (\partial^\rho A^\sigma P) \\
 &+ \frac{f_9}{2\sqrt{3}} \text{Tr} (\{\partial^\mu V^\nu, \partial^\rho A^\sigma\} \lambda_8) \text{Tr} (P) \\
 &+ \frac{f_{10}}{2\sqrt{3}} \text{Tr} (\partial^\mu V^\nu) \text{Tr} (\{\partial^\rho A^\sigma, P\} \lambda_8) \\
 &+ \frac{f_{11}}{3\sqrt{2}} \text{Tr} (\partial^\mu V^\nu) \text{Tr} (P) \text{Tr} (\partial^\rho A^\sigma \lambda_8)] \tag{2.13}
 \end{aligned}$$

where

$$\begin{aligned}
 V_\mu &= \frac{1}{\sqrt{2}} \sum_{i=0}^8 \lambda_i V_\mu^i \\
 P &= \frac{1}{\sqrt{2}} \sum_{i=0}^8 \lambda_i P^i \\
 A_\mu &= \frac{1}{\sqrt{2}} \sum_{i=0}^8 \lambda_i A_\mu^i .
 \end{aligned}$$

The $V^m \rightarrow P^i \gamma$ rate predicted by this Lagrangian is

$$\Gamma(V^m \rightarrow P^i \gamma) = \frac{1}{96\pi} |g_{\min}|^2 \left(\frac{M_m^2 - M_i^2}{M_m} \right)^3 \quad (2.14)$$

where

$$\begin{aligned} g_{\min} = & f_0 d_{\min} + f_1 \delta_{mn} \delta_{io} + f_2 \delta_{mo} \delta_{ni} \\ & + (f_3 - f_4 + f_5) d_{8ik} d_{kmn} \\ & + (-f_3 + f_4 + f_5) d_{8nk} d_{kim} \\ & + (f_3 + f_4 - f_5) d_{8mk} d_{kin} \\ & + f_6 \delta_{8i} \delta_{mn} + f_7 \delta_{8n} \delta_{im} + f_8 \delta_{8m} \delta_{in} \\ & + f_9 d_{mn8} \delta_{io} + f_{10} d_{ni8} \delta_{mo} \\ & + f_{11} \delta_{mo} \delta_{io} \delta_{n8} . \end{aligned} \quad (2.15)$$

The repeated symmetry index k is summed from 0 to 8 and n is the photon index.

Of the nine symmetry breaking terms, only seven are independent. This follows from two identities which are analogous to (2.10) and (2.11):

$$d_{8ik} d_{kmn} = d_{8mk} d_{kin}, \quad (2.16)$$

$$d_{8ik} d_{kmn} + d_{8nk} d_{kim} + d_{8mk} d_{kin}$$

$$= \delta_{8i} \delta_{mn} + \delta_{8n} \delta_{im} + \delta_{8m} \delta_{in} \quad (\text{cont.})$$

$$\begin{aligned}
& + \sqrt{6}(d_{mn8}\delta_{io} + d_{ni8}\delta_{mo}) \\
& - 3 \delta_{mo}\delta_{io}\delta_{n8}
\end{aligned} \tag{2.17}$$

where $i, m, k=0, \dots, 8$ and n is the photon index. The last identity is a special case of the identity:

$$\begin{aligned}
& d_{ijk}d_{kmn} + d_{imk}d_{kjn} + d_{ink}d_{kmj} \\
& = \delta_{ij}\delta_{mn} + \delta_{im}\delta_{jn} + \delta_{in}\delta_{mj} \\
& + \sqrt{6}(d_{jmn}\delta_{io} + d_{imn}\delta_{jo} + d_{ijn}\delta_{mo} + d_{ijm}\delta_{no}) \\
& - 3 (\delta_{ij}\delta_{mo}\delta_{no} + \delta_{mn}\delta_{io}\delta_{jo} + \delta_{im}\delta_{jo}\delta_{no} \\
& \quad + \delta_{jn}\delta_{io}\delta_{mo} + \delta_{in}\delta_{mo}\delta_{jo} + \delta_{mj}\delta_{io}\delta_{no}) \\
& + 9 \delta_{io}\delta_{jo}\delta_{mo}\delta_{no} . \quad (i, j, k, m, n=0, \dots, 8) \tag{2.18}
\end{aligned}$$

Using (2.16) and (2.17), two symmetry breaking terms may be eliminated from (2.15). The most general SU(3) radiative decay model with λ_8 symmetry breaking is seen to have three SU(3) invariant and seven SU(3) symmetry breaking terms. Ten SU(3) invariant coupling constants characterize this model.

2.3 Nonet Symmetry, the OZI Rule And λ_0 Symmetry Breaking

Nonet Symmetry may be imposed separately on the invariant and the symmetry breaking terms of the SU(3) Lagrangian. When demanding that the singlets and octets couple with equal strength, it is convenient to examine the

first form of the Lagrangian and decay amplitude, (2.1) - (2.9). Imposing nonet symmetry on just the invariant terms, the condition $g_0=g_7=g_9$ is obtained; this type of nonet symmetry is referred to as weak nonet symmetry. If nonet symmetry is imposed on the λ_8 symmetry breaking terms as well (i.e., $g_0=g_7=g_9$, $g_8=g_{10}=\sqrt{\frac{2}{3}}(g_1+g_2+g_3)$ and $g_{11}=g_5+\frac{2}{3}(g_1+g_2+g_3)$), another type of nonet symmetry is achieved--this is referred to as strong nonet symmetry.

It is more transparent to use the second form of the Lagrangian and decay amplitude, (2.13)-(2.15), when discussing OZI violations. None of the terms in (2.13) which involve traces over the internal degrees of freedom of individual particles may be rewritten so as not to involve traces over the internal degrees of freedom of individual particles; all these terms, therefore, constitute violations to the OZI rule. Setting $f_1=f_2=0$, OZI violations among the SU(3) invariant terms are eliminated--this is the same as weak nonet symmetry. Strong nonet symmetry is obtained by further demanding that $f_9=f_{10}=f_{11}=0$. There are no OZI violations among the remaining symmetry breaking terms in that the corresponding quark line diagrams, with the scalar spurion U_8 included, are properly connected. If the presence of the scalar spurion is ignored, apparent OZI violations are generated by these terms.

Imposition of nonet symmetry, or equivalently the OZI rule, on the general SU(3) scheme with λ_8 symmetry breaking has the effect of reducing the number of SU(3) invariant coupling constants required in the model. The

most general SU(3) scheme has ten terms in the Lagrangian (3 SU(3) invariant, 7 symmetry breaking); the weak nonet symmetry model has eight terms (1 SU(3) invariant, 7 symmetry breaking); and the scheme with strong nonet symmetry has six terms (1 SU(3) invariant, 5 symmetry breaking). Further symmetry assumptions are necessary to further reduce the number of coupling constants.

Symmetry breaking by λ_0 is equivalent to nonet symmetry breaking. Beginning with a decay model which demonstrates strong nonet symmetry, the inclusion of λ_0 symmetry breaking terms regenerates the terms which break nonet symmetry. For instance, from V, P, A and λ_0 , the term $\text{Tr} (VA) \text{Tr} (P\lambda_0)$ may be constructed; this is equivalent to the f_1 term in (2.13). Similarly, from V, P, A, λ_8 and λ_0 , $\text{Tr} (\{V, A\}\lambda_8) \text{Tr} (P\lambda_0)$ may be built; this is equivalent to the f_9 term in (2.13). Symmetry breaking by λ_0 is seen to destroy nonet symmetry. Furthermore, in a scheme which has no nonet symmetry, λ_0 symmetry breaking terms are redundant. Since λ_0 symmetry breaking yields no new structure for the desired radiative decay amplitude, it is not considered further.

2.4 Vector Meson Dominance

Many $V \rightarrow P\gamma$ models have their origins in models for the hadronic process $V \rightarrow VP$. If the assumed VVP vertex demonstrates symmetry breaking, so does the $VP\gamma$ vertex which is derived from the VVP vertex by latching a photon onto one of the

vectors using the VMD Lagrangian (1.17). The $V \rightarrow P\gamma$ models so obtained form a restricted class of all $V \rightarrow P\gamma$ models described so far.

A model for $V \rightarrow VP$ with symmetry breaking is obtained by taking various charge conjugation invariant trace combinations of two vector multiplets, a pseudoscalar multiplet, a λ_8 and a λ_0 . Boson symmetry further requires that when the two vector multiplets are identical (i.e., both octets or singlets) that the resulting amplitude be symmetric in the two vector indices. When the photon is attached, the $V \rightarrow P\gamma$ amplitude is necessarily symmetric in the vector and photon indices.

This Boson symmetry is compatible with the general $SU(3)$ model with λ_8 symmetry breaking only when certain coupling constant restrictions are met. For the amplitude (2.6) to be symmetric in m and n , it is necessary that $g_1 = g_3$ and $g_5 = g_6$. Equivalently, it is necessary that $f_3 = f_5$ and $f_7 = f_8$ in (2.15). Fewer coupling constants are permitted in a $V \rightarrow P\gamma$ model which is derived from a $V \rightarrow VP$ model through VMD.

VMD may sometimes be used to deduce a VVP vertex from a $VP\gamma$ vertex. If the radiative decay model satisfies the coupling constant constraints outlined above, then this is possible. In Chapter VI, some $V \rightarrow P\gamma$ models are used in this way.

2.5 A Hierarchy of Models With SU(3) Symmetry Breaking

A wide variety of models which describe the radiative decay of SU(3) multiplets of vector and pseudoscalar mesons has been presented. The interaction Lagrangian may be invariant under all SU(3) rotations or may have a part which transforms as λ_8 . SU(3) octets and singlets may couple with the same strength or may be totally independent. The resulting $V P \gamma$ model may or may not be compatible with VMD.

The two schemes which display the simplest symmetry structure use SU(3) invariant Lagrangians. The nonet symmetry model is the most simple--no OZI violations are allowed. The general SU(3) model does permit OZI violations.

Among the models with λ_8 symmetry breaking, the strong nonet symmetry model has the fewest coupling constants. OZI violations, in a strict sense, do not occur; the symmetry breaking terms do, however, simulate OZI violations. The weak nonet symmetry scheme forbids OZI violations in the SU(3) invariant terms but permits them in the symmetry breaking terms. The most general SU(3) model with λ_8 symmetry breaking allows OZI violations in both the invariant and the symmetry breaking terms.

A $V \rightarrow P \gamma$ model which may be related to a $V \rightarrow V P$ model through VMD must satisfy Boson symmetry in the vector meson and photon indices. As a result, fewer independent symmetry breaking terms appear in such a model.

The numbers of couplings available under the different

symmetry assumptions are summarized in Table 3.

The nonet and $SU(3)$ models having proved unsatisfactory in predicting the observed decay rates, some of the λ_8 symmetry breaking schemes are now explored. It is hoped that a λ_8 symmetry breaking scheme exists that demonstrates some sort of nonet symmetry and that, when used with standard mixing angles, offers an explanation for the experimentally observed rates. All of the schemes to be examined demonstrate either weak or strong nonet symmetry. Only on two occasions are nonstandard mixing angles mentioned. In addition, most of the models to be discussed are compatible with VMD. With only five measured absolute rates, two preliminary absolute rates and two relative rates, it is impossible to fully explore all the symmetry breaking schemes presented in this chapter. It is, however, possible to thoroughly test some of the schemes and sample particular cases of others. In the next chapters such a wide variety of symmetry breaking structures is explored that many conclusions may be drawn regarding the success of λ_8 symmetry breaking in explaining the radiative decay rates of mesons.

TABLE 3

Contributions to SU(3) Models with λ_8 Symmetry Breaking

Symmetry	Number of SU(3) Invariant Terms	Number of λ_8 Symmetry Breaking Terms	
		Boson Symmetry	No Boson Symmetry
No λ_8 breaking, nonet symmetry	1	0	0
No λ_8 breaking, no nonet symmetry	3	0	0
λ_8 breaking, strong nonet symmetry	1	4	5
λ_8 breaking, weak nonet symmetry	1	6	7
λ_8 breaking, no nonet symmetry	3	6	7

CHAPTER III

THE BARYON LOOP MODEL

3.1 The Nature of the Model

The baryon loop model was first used by Steinberger [22] to describe the $\pi^0 \rightarrow \gamma\gamma$ decay. A modified version has been used by Rockmore and collaborators [23] to study the nonleptonic decays of K mesons. It has been further suggested by Rockmore [24] that a baryon loop model might lend itself quite naturally to a description of symmetry breaking in strong and radiative decays of mesons. In this chapter two baryon loop models are used to produce λ_8 symmetry breaking in the radiative decays of vector and pseudoscalar mesons.

In a baryon loop model, the decay $V \rightarrow P\gamma$ is imagined to proceed via a baryon-antibaryon loop. As indicated in Figures 2 and 3, the photon may be attached directly to the baryon loop or VMD may be assumed and the photon attached to a vector meson which in turn is attached to the baryon loop. Assuming that the intermediate baryons form an SU(3) octet bearing a single octet mass and adopting SU(3) invariant couplings at all vertices, a $V \rightarrow P\gamma$ model results which has SU(3) symmetry.

SU(3) symmetry breaking is introduced very naturally through the baryon masses. Taking the baryon masses as prescribed by the octet mass formula,

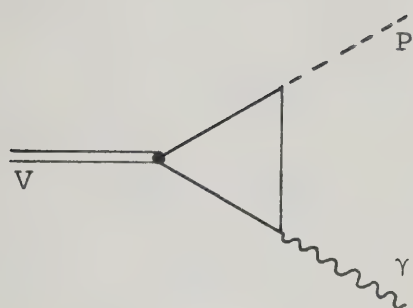
$$M_{ij} = m_0 \delta_{ij} + \delta m_D d_{8ij} + i \delta m_F f_{8ij}, \quad (3.1)$$

a $V \rightarrow P\gamma$ model which demonstrates λ_8 symmetry breaking is obtained. The three baryon masses, m_0 , δm_D and δm_F may be obtained from the observed baryon mass spectrum and (3.1). Alternately, just the symmetry breaking structure of the $V \rightarrow P\gamma$ amplitude may be taken seriously and the baryon masses may be taken as symmetry breaking parameters to be fitted. Both these approaches are tried.

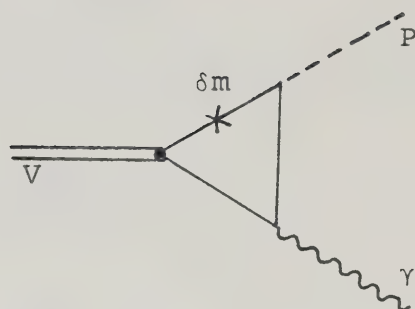
In this chapter, the mesons are assumed to have the standard SU(3) content, mixing angles and masses. The usual forms of the $V\bar{B}\bar{B}$, $P\bar{B}\bar{B}$, $\gamma\bar{B}\bar{B}$ and $V\gamma$ interactions are used with accepted coupling constants and f/d ratios. Only for the $V^0\bar{B}\bar{B}$ and $P^0\bar{B}\bar{B}$ interactions are coupling constants not available; these may, however, be fixed if weak nonet symmetry is assumed.

3.2 F-type Coupling of the Photon to the Baryon Loop

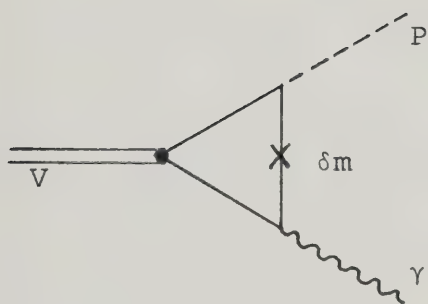
The baryon loop model in which the photon is attached directly to the baryon loop using standard $\gamma\bar{B}\bar{B}$ coupling is now discussed. The Feynman diagrams of interest to this model are presented in Figure 2. Figure 2 a illustrates the SU(3) invariant contribution to the $VP\gamma$ amplitude. Figures 2 b , c and d give the symmetry breaking contributions to first order in $\delta m_D/m_0$ and $\delta m_F/m_0$; these terms demonstrate symmetry breaking by one λ_8 . Higher order terms are expected to be negligible since, according to the baryon mass spectrum,



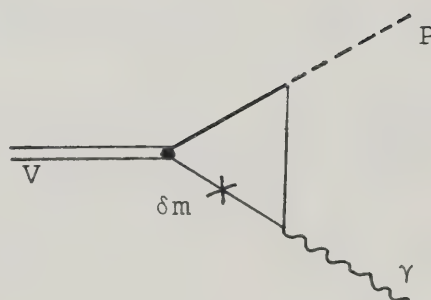
(a)



(b)



(c)



(d)

Figure 2. Contributions to the Baryon Loop Model with the Photon Attached to the Loop with F-type Coupling. (a) SU(3) invariant contribution; (b), (c) and (d) SU(3) symmetry breaking contributions.

$\delta m_D/m_0$ and $\delta m_F/m_0$ are of the order of 5-10% [24]. Such a first order calculation is seen to be justifiable even when the masses are treated as free parameters--the symmetry breaking is always found to be less than 25%.

The Lagrangian used to describe the various interactions is:

$$\begin{aligned}
 \mathcal{L} = & 2g_1 (-if_i + d d_i)_{mn} \bar{B}^m i\gamma_5 B^n p^i \\
 & + 2g_2 d_{omn} \bar{B}^m i\gamma_5 B^n p^o \\
 & + 2g_3 (-i\phi f_i + \delta d_i)_{mn} \bar{B}^m \gamma^\mu B^n V_\mu^i \\
 & + 2g_4 d_{omn} \bar{B}^m \gamma^\mu B^n V_\mu^o \\
 & - (-i \delta m_F f_8 + \delta m_D d_8)_{mn} \bar{B}^m B^n \\
 & - ie (f_3 + \frac{1}{\sqrt{3}} f_8)_{mn} \bar{B}^m \gamma^\mu B^n A_\mu. \quad (m, n, i = 1, \dots, 8) \quad (3.2)
 \end{aligned}$$

The g_i are SU(3) invariant coupling constants. The relative amounts of f-type and d-type coupling are given by f and d ($f + d = 1$) for the $P\bar{B}B$ interaction and by ϕ and δ ($\phi + \delta = 1$) for the $V\bar{B}B$ interaction.

The computation of the $V_{P\gamma}^{m_i}$ amplitude is a straight forward but tedious exercise in Feynman integrals. Only two details are of particular note. Firstly, it is assumed that the average baryon octet mass, m_0 , is large compared to the meson masses--this permits the loop integration to be simply approximated. Secondly, SU(3) traces of three and four f and d matrices are needed--these are available in [24].

The resulting T-matrix for $V^m P^i_\gamma$ is

$$T_{V^m P^i_\gamma} = \frac{1}{(2\pi)^{9/2}} \frac{1}{(8E_m E_i E_n)^{1/2}} g_{\min} \varepsilon_{\mu\nu\rho\sigma} (p_m)^\mu (\varepsilon_m)^\nu (p_n)^\rho (\varepsilon_n)^\sigma \quad (3.3)$$

where the momentum and polarization assignments are as in section 1.4. For V^m and P^i both members of octets,

$$\begin{aligned} g_{\min} = & \frac{(2g_1)(2g_3)e}{(2\pi)^2 m_o} \left[-\frac{3}{2} (\delta f + \phi d) d_{\min} \right. \\ & + d_{8mk} d_{kni} \left[\left(\frac{29}{36} \phi d + \frac{5}{36} \delta f \right) \frac{\delta m_D}{m_o} + \left(\frac{9}{12} \phi f + \frac{29}{36} \delta d \right) \frac{\delta m_F}{m_o} \right] \\ & + d_{8nk} d_{kmi} \left[\left(\frac{29}{36} \phi d + \frac{29}{36} \delta f \right) \frac{\delta m_D}{m_o} + \left(\frac{9}{12} \phi f + \frac{5}{36} \delta d \right) \frac{\delta m_F}{m_o} \right] \\ & + d_{8ik} d_{kmn} \left[\left(\frac{5}{36} \phi d + \frac{29}{36} \delta f \right) \frac{\delta m_D}{m_o} + \left(\frac{9}{12} \phi f + \frac{5}{36} \delta d \right) \frac{\delta m_F}{m_o} \right] \\ & + \delta_{8m} \delta_{ni} \left[\left(-\frac{8}{27} \phi d + \frac{7}{27} \delta f \right) \frac{\delta m_D}{m_o} + \left(\frac{1}{2} \phi f - \frac{8}{27} \delta d \right) \frac{\delta m_F}{m_o} \right] \\ & + \delta_{8n} \delta_{mi} \left[\left(-\frac{8}{27} \phi d - \frac{8}{27} \delta f \right) \frac{\delta m_D}{m_o} + \left(\frac{1}{2} \phi f + \frac{7}{27} \delta d \right) \frac{\delta m_F}{m_o} \right] \\ & \left. + \delta_{8i} \delta_{mn} \left[\left(\frac{7}{27} \phi d - \frac{8}{27} \delta f \right) \frac{\delta m_D}{m_o} + \left(\frac{1}{2} \phi f - \frac{8}{27} \delta d \right) \frac{\delta m_F}{m_o} \right] \right] \\ & (k = 1, \dots, 8). \quad (3.4) \end{aligned}$$

For V^m a singlet and P^i a member of an octet,

$$g_{\min} = \frac{(2g_1)(2g_4)e}{(2\pi)^2 m_o} \left[-3\sqrt{\frac{2}{3}} f \delta_{in} + \frac{3}{2}\sqrt{\frac{2}{3}} \left(f \frac{\delta m_D}{m_o} + d \frac{\delta m_F}{m_o} \right) d_{8in} \right]. \quad (3.5)$$

For V^m a member of an octet and P^i a singlet,

$$g_{\min} = \frac{(2g_2)(2g_3)e}{(2\pi)^2 m_o} \left[-3\sqrt{\frac{2}{3}} \phi \delta_{mn} + \frac{3}{2}\sqrt{\frac{2}{3}} \left(\phi \frac{\delta m_D}{m_o} + \delta \frac{\delta m_F}{m_o} \right) d_{8mn} \right]. \quad (3.6)$$

For V^m and P^i both singlets,

$$g_{\min} = \frac{(2g_2)(2g_4)e}{(2\pi)^2 m_o} \left[2 \frac{\delta m_F}{m_o} \delta_{8n} \right]. \quad (3.7)$$

As before, n is the photon index. The $V^m \rightarrow P^i \gamma$ decay width which is obtained from (3.3) is

$$\Gamma(V^m \rightarrow P^i \gamma) = \frac{1}{96\pi} (g_{\min})^2 \left(\frac{M_m^2 - M_i^2}{M_m} \right)^3, \quad (3.8)$$

and the $P^i \rightarrow V^m \gamma$ decay width is

$$\Gamma(P^i \rightarrow V^m \gamma) = \frac{1}{32\pi} (g_{\min})^2 \left(\frac{M_i^2 - M_m^2}{M_i} \right)^3. \quad (3.9)$$

The symmetry structure of this model is that of a general $SU(3)$ model with λ_8 symmetry breaking. The twelve coupling constants of (2.5) - (2.9) are built from the following parameters of the baryon loop model: $g_1, g_2, g_3, g_4, d, f, \delta, \phi, m_o, \delta m_D$ and δm_F . Because the photon is coupled to the baryon loop with pure f -type coupling, the amplitude (3.3) is not symmetric in m and n . This lack of symmetry in m and n means that this $VP\gamma$ model is not compatible with VMD--a VVP model, which must necessarily demonstrate Boson symmetry, can not be derived from this radiative decay model. This model displays weak nonet

symmetry if

$$g_2 = g_1 \frac{\delta f + \phi d}{2\phi}, \quad (3.10)$$

$$g_4 = g_3 \frac{\delta f + \phi d}{2f}. \quad (3.11)$$

If (3.8) and (3.9) do not hold, OZI violations are permitted in the SU(3) invariant terms. No relationship exists among the baryon loop parameters (except $\delta m_D = \delta m_F = 0$) which would produce strong nonet symmetry.

The coupling constants and d/f ratios are assigned accepted values if available: $g_1^2/4\pi = 14.6$ [25], $g_3 = 0.303 g_\rho$ [26] so that $g_3^2/4\pi = 0.27$, $d/f = 1.8$ [25] and $\delta/\phi = -0.5$ [25]. Lacking any information on g_2 and g_4 , the weak nonet relations (3.10) and (3.11) are used. The $VP\gamma$ amplitude is now a linear combination of $1/m_\phi$, $\delta m_D/m_\phi^2$ and $\delta m_F/m_\phi^2$; equivalently, it is a linear combination of K, D and F:

$$K = \frac{(2g_1)(2g_3)e}{(2\pi)^2 m_\phi} \frac{3}{2} (\delta f + \phi d),$$

$$D = K \delta m_D/m_\phi,$$

$$F = K \delta m_F/m_\phi. \quad (3.12)$$

Once K, D and F have been specified, the radiative decay rates may be predicted.

At this point, one of two approaches may be adopted. The baryon masses m_ϕ , δm_D and δm_F may be determined from the observed baryon mass spectrum ($m_\phi = 1155$ MeV, $\delta m_D = 67$ MeV,

$\delta m_F = -55 \text{ MeV}$ [24]). The $V \rightarrow P\gamma$ and $P \rightarrow V\gamma$ decays widths are then predicted by (3.8) and (3.9) with no free parameters. These predictions are tabulated as solution 1 Table 4 ($K = 0.923 \text{ GeV}^{-1}$, $D = 0.054 \text{ GeV}^{-1}$, $F = -0.044 \text{ GeV}^{-1}$). Adjusting the overall scale to bring these predictions into better agreement with experiment, solution 2 is obtained ($K = 0.735 \text{ GeV}^{-1}$, $D = 0.043 \text{ GeV}^{-1}$, $F = -0.035 \text{ GeV}^{-1}$). It is remarkable that this model should come so close to the proper scale. The predictions of solution 2 are only somewhat of an improvement over the nonet predictions of Table 1.

Another approach is to take the symmetry breaking structure of (3.4) - (3.7) seriously but to treat m_0 , δm_D and δm_F or, equivalently K , D and F , as free parameters. Three fits of K , D and F to the available rates are given in Table 4. Solution 3 ($K = 0.749 \text{ GeV}^{-1}$, $D = -0.140 \text{ GeV}^{-1}$, $F = -0.113 \text{ GeV}^{-1}$) shows the results of a fit to the five available data; solution 4 ($K = 0.491 \text{ GeV}^{-1}$, $D = -0.086 \text{ GeV}^{-1}$, $F = 0.012 \text{ GeV}^{-1}$) omits $\Gamma(\omega \rightarrow \pi\gamma)$ from the fit; in solution 5 ($K = 0.871 \text{ GeV}^{-1}$, $D = -0.175 \text{ GeV}^{-1}$, $F = -0.231 \text{ GeV}^{-1}$), $\Gamma(\rho \rightarrow \pi\gamma)$ is omitted. Whenever $\Gamma(\omega \rightarrow \pi\gamma)$ is predicted to be consistent with experiment, $\Gamma(\rho \rightarrow \pi\gamma)$ and $\Gamma(K^0 \rightarrow K^*\gamma)$ are too high; when the latter are reasonable, $\Gamma(\omega \rightarrow \pi\gamma)$ is too low. This model can account for the observed $\phi \rightarrow \pi\gamma$ and $\phi \rightarrow \eta\gamma$ rates.

3.3 The Photon Coupled to the Baryon Loop Through VMD

The diagrams appropriate to coupling the photon to the baryon-antibaryon loop through a vector meson are given in

TABLE 4

Predictions[†] of the Baryon Loop Model with the Photon
Attached to the Loop with F-type Coupling

Decay Mode	Soln 1	Soln 2	Soln 3	Soln 4	Soln 5	Experiment
$\omega \rightarrow \pi\gamma$	1200	(630)	(680)	370	(780)	880 ± 60 [1]
$K^{*0} \rightarrow K^0 \gamma$	280	(150)	(200)	(87)	(270)	75 ± 35 [1]
$\rho \rightarrow \pi\gamma$	130	(73)	(78)	(33)	110	35 ± 10 [1]
$\phi \rightarrow \pi\gamma$	4.6	(2.5)	(6.9)	(5.7)	(5.9)	5.7 ± 2.1 [1]
$\phi \rightarrow \eta\gamma$	210	(120)	(88)	(64)	(75)	64 ± 10 [1,7]
$\omega \rightarrow \eta\gamma$	11	61	7.6	2.5	12	$3.0^{+2.5}_{-1.8}$ or 29 ± 7 [7]
$K^{*+} \rightarrow K^+ \gamma$	75	40	58	20	88	< 80 [3]
$\rho \rightarrow \eta\gamma$	73	39	87	30	140	50 ± 13 or 76 ± 15 [7]
$\eta' \rightarrow \omega\gamma$	16	8.9	11	3.6	18	< 50 [1]
$\eta' \rightarrow \rho\gamma$	160	84	100	49	130	< 300 [1]
$\phi \rightarrow \eta' \gamma$	1.2	0.60	0.58	0.29	0.69	--
$\Gamma(\eta' \rightarrow \rho\gamma) / \Gamma(\eta' \rightarrow \omega\gamma)$	9.4	9.4	9.1	14	7.1	9.9 ± 2.0 [8]

[†] All rates in KeV.

Figure 3. As in the other baryon loop model, a first order calculation is executed.

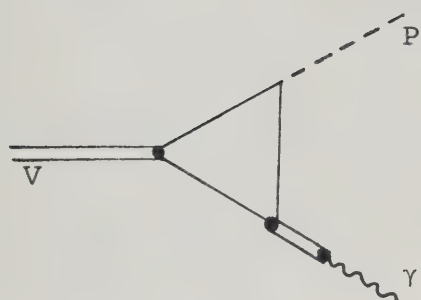
The Lagrangian (3.2), without the $\gamma B\bar{B}$ term, is used. The VMD Lagrangian is also needed,

$$\mathcal{L} = e \frac{M_n^2}{g_\rho} (\delta_{n3} + \frac{1}{\sqrt{3}} \delta_{n8}) A^\mu V_\mu^n. \quad (3.13)$$

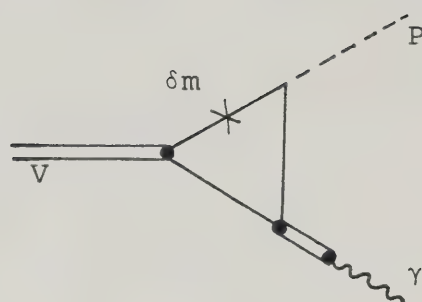
The resulting $V^m P^i_\gamma$ T-matrix is the same as (3.3) where g_{\min} now has the following form. For V^m and P^i both members of octets,

$$\begin{aligned} g_{\min} = & \frac{(2g_1)(2g_3)^2 e}{(2\pi)^2 m_o g_\rho} \left[(-3d\phi^2 + d\delta^2 - 6f\delta\phi) d_{\min} \right. \\ & + (d_{8mk} d_{kni} + d_{8nk} d_{kmi}) \left(\frac{-5d\delta^2 + 29d\phi^2 + 34f\delta\phi}{36} \frac{\delta m_D}{m_o} + \right. \\ & \left. \left. \frac{29f\delta^2 + 27f\phi^2 + 34d\delta\phi}{36} \frac{\delta m_F}{m_o} \right) \right. \\ & + (d_{8ik} d_{kmn}) \left(\frac{-5d\delta^2 + 5d\phi^2 + 58f\delta\phi}{36} \frac{\delta m_D}{m_o} + \frac{13f\delta^2 + 27f\phi^2 + 58d\delta\phi}{36} \frac{\delta m_F}{m_o} \right) \\ & + (\delta_{8m} \delta_{ni} + \delta_{8n} \delta_{mi}) \left(\frac{11d\delta^2 - 16d\phi^2 - 2f\delta\phi}{54} \frac{\delta m_D}{m_o} + \right. \\ & \left. \left. \frac{-16f\delta^2 + 27f\phi^2 - 2d\delta\phi}{54} \frac{\delta m_F}{m_o} \right) \right. \\ & \left. + (\delta_{8i} \delta_{mn}) \left[\frac{11d\delta^2 + 14d\phi^2 - 32f\delta\phi}{54} \frac{\delta m_D}{m_o} + \frac{14f\delta^2 + 27f\phi^2 - 32d\delta\phi}{54} \frac{\delta m_F}{m_o} \right] \right]. \quad (3.14) \end{aligned}$$

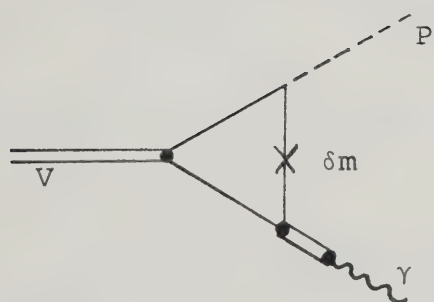
For V^m a singlet and P^i a member of an octet,



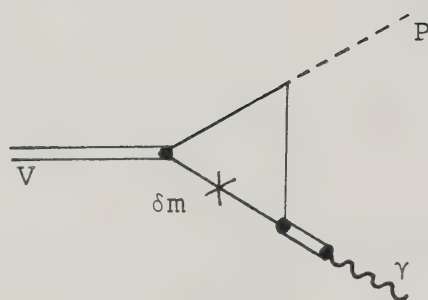
(a)



(b)



(c)



(d)

Figure 3. Contributions to the Baryon Loop Model with the Photon Attached to the Loop through VMD. (a) $SU(3)$ invariant contribution; (b), (c) and (d) $SU(3)$ symmetry breaking contributions.

$$g_{\min} = \frac{(2g_1)(2g_3)(2g_4)e}{(2\pi)^2 m_o g_\rho} \left[-\sqrt{\frac{2}{3}} \frac{5d\delta+9f\phi}{3} \delta_{in} + \sqrt{\frac{2}{3}} \left(\frac{-d\delta+3f\phi}{2} \frac{\delta m_D}{m_o} + \frac{3f\delta+3d\phi}{2} \frac{\delta m_F}{m_o} \right) d_{8in} \right]. \quad (3.15)$$

For V^m a member of an octet and P^i a singlet,

$$g_{\min} = \frac{(2g_2)(2g_3)^2 e}{(2\pi)^2 m_o g_\rho} \left[-\sqrt{\frac{2}{3}} \frac{5\delta^2+9\phi^2}{3} \delta_{mn} + \sqrt{\frac{2}{3}} \left(\frac{-\delta^2+3\phi^2}{2} \frac{\delta m_D}{m_o} + 3\delta\phi \frac{\delta m_F}{m_o} \right) d_{8mn} \right]. \quad (3.16)$$

For V^m and P^i both singlets,

$$g_{\min} = \frac{(2g_2)(2g_3)(2g_4)e}{(2\pi)^2 m_o g_\rho} \left[\frac{2}{3} \left(\frac{5\delta}{3} \frac{\delta m_D}{m_o} + 3\phi \frac{\delta m_F}{m_o} \right) \delta_{8n} \right]. \quad (3.17)$$

As before, n is the photon index. The decay widths are as in (3.8) and (3.9).

This model is an $SU(3)$ model with λ_8 symmetry breaking which demonstrates Boson symmetry. Since the photon is attached to the baryon loop through a vector meson, it is attached with the same d/f ratio as the initial (or final) state vector meson--the $VP\gamma$ amplitude is automatically symmetric in m and n . Weak nonet symmetry may be imposed by requiring

$$g_2 = g_1 \frac{3(3d\phi^2 - d\delta^2 + 6f\delta\phi)}{(5\delta^2 + 9\phi^2)}, \quad (3.18)$$

$$g_4 = g_3 \frac{3(3d\phi^2 - d\delta^2 + 6f\delta\phi)}{(5\delta d + 9f\phi)}. \quad (3.19)$$

No relationship exists among the baryon loop parameters (except $\delta m_D = \delta m_F = 0$) which produces strong nonet symmetry.

The previously quoted values for g_1 , g_3 , d/f and δ/ϕ are used and g_2 and g_4 are determined by the weak nonet relations (3.18) and (3.19). The $VP\gamma$ amplitude is now a linear combination of $1/m_0$, $\delta m_D/m_0^2$ and $\delta m_F/m_0^2$ or, equivalently of K , D and F :

$$K = \frac{(2g_1)(2g_3)^2 e}{(2\pi)^2 m_0 g_\rho} (3d\phi^2 - d\delta^2 + 6fd\phi),$$

$$D = K \delta m_D / m_0,$$

$$F = K \delta m_F / m_0. \quad (3.20)$$

Taking the baryon masses from the baryon mass spectrum, solution 1 Table 5 ($K = 1.120 \text{ GeV}^{-1}$, $D = 0.065 \text{ GeV}^{-1}$, $F = -0.053 \text{ GeV}^{-1}$) is obtained. Scaling this solution down to better agree with experiment, solution 2 ($K = 0.715 \text{ GeV}^{-1}$, $D = 0.041 \text{ GeV}^{-1}$, $F = -0.034 \text{ GeV}^{-1}$) is obtained. Again, this is not remarkably different from the nonet model.

When the baryon masses are treated as free parameters, the model is more flexible. Solution 3 ($K = 0.660 \text{ GeV}^{-1}$, $D = -0.025 \text{ GeV}^{-1}$, $F = -0.130 \text{ GeV}^{-1}$) uses the five available rates; solution 4 ($K = 0.510 \text{ GeV}^{-1}$, $D = -0.075 \text{ GeV}^{-1}$, $F = 0.011 \text{ GeV}^{-1}$) omits $\Gamma(\omega \rightarrow \pi\gamma)$ from the fit; solution 5 ($K = 0.673 \text{ GeV}^{-1}$, $D = -0.193 \text{ GeV}^{-1}$, $F = -0.060 \text{ GeV}^{-1}$) omits

TABLE 5

Predictions[†] of the Baryon Loop Model with the Photon
Attached to the Loop Through VMD

Decay Mode	Soln 1	Soln 2	Soln 3	Soln 4	Soln 5	Experiment
$\omega \rightarrow \pi\gamma$	1900	640	(800)	400	(860)	880 ± 60 [1]
$K^{*0} \rightarrow K^0 \gamma$	410	140	(150)	(97)	(180)	75 ± 35 [1]
$\rho \rightarrow \pi\gamma$	210	72	(69)	(33)	51	35 ± 10 [1]
$\phi \rightarrow \pi\gamma$	3.5	1.2	(6.5)	(5.6)	(5.3)	5.7 ± 2.1 [1]
$\phi \rightarrow \eta\gamma$	330	110	(61)	(63)	(62)	64 ± 10 [1,7]
$\omega \rightarrow \eta\gamma$	17	6.1	5.7	2.2	3.0	$3.0^{+2.5}_{-1.8}$ or 29 ± 7 [7]
$K^{*+} \rightarrow K^+ \gamma$	110	38	45	22	44	< 80 [3]
$\rho \rightarrow \eta\gamma$	110	38	60	32	85	50 ± 13 or 76 ± 15 [7]
$\eta' \rightarrow \omega\gamma$	27	9.3	13	3.5	7.9	< 50 [1]
$\eta' \rightarrow \rho\gamma$	230	79	69	51	82	< 300 [1]
$\phi \rightarrow \eta\gamma$	1.6	0.55	0.45	0.33	0.49	--
$\Gamma(\eta' \rightarrow \rho\gamma) / \Gamma(\eta' \rightarrow \omega\gamma)$	8.5	8.5	5.2	15	10	9.9 ± 2.0 [8]

[†]All rates in KeV.

$\Gamma(\rho \rightarrow \pi\gamma)$. With this SU(3) breaking structure, it is still difficult to make both $\Gamma(\omega \rightarrow \pi\gamma)$ and $\Gamma(\rho \rightarrow \pi\gamma)$ consistent with experiment; $\Gamma(K^{*0} \rightarrow K^0\gamma)$ is lower in this model than in the other baryon loop model but still much above the observed value; $\Gamma(\phi \rightarrow \pi\gamma)$ and $\Gamma(\phi \rightarrow \eta\gamma)$ are well predicted.

3.4 Conclusions

In these two $V \rightarrow P\gamma$ decay models, symmetry breaking is induced by nondegenerate baryon masses. The first of these models does not display Boson symmetry, while the second, being derived with VMD, does. Weak nonet symmetry is used in both cases.

When the baryon mass splittings are taken as determined by the baryon mass spectrum, these models predict meson radiative decay rates very similar to the unsatisfactory nonet predictions.

When the baryon masses are treated as free parameters, the models demonstrate marginal success. The symmetry breaking structure is compatible with the measured ϕ rates, $\Gamma(\phi \rightarrow \pi\gamma)$ and $\Gamma(\phi \rightarrow \eta\gamma)$. In particular, the first decay proceeds entirely through the symmetry breaking terms. The nonet problem of the inconsistency of $\Gamma(\rho \rightarrow \pi\gamma)$ and $\Gamma(K^{*0} \rightarrow K^0\gamma)$ with $\Gamma(\omega \rightarrow \pi\gamma)$ persists. In the second model, the problem with $\Gamma(K^{*0} \rightarrow K^0\gamma)$ is not quite so severe as in the first model and the nonet model; this is reflected by $\Gamma(K^{*0} \rightarrow K^0\gamma)/\Gamma(K^{*+} \rightarrow K^+\gamma)$ deviating somewhat from its SU(3) value of 4.

The symmetry breaking structures of the baryon loop

models are only somewhat successful in predicting the vector and pseudoscalar meson decay rates. Problems still occur in the mutual consistency of $\Gamma(\rho \rightarrow \pi\gamma)$, $\Gamma(K^{*0} \rightarrow K^0\gamma)$ and $\Gamma(\omega \rightarrow \pi\gamma)$.

CHAPTER IV

THE CURRENT ALGEBRA MODEL

4.1 Symmetry Breaking Through Current Algebra

Current algebra techniques may be applied to a quark model Hamiltonian with symmetry breaking to generate a variety of strong interaction vertices, all of which demonstrate symmetry breaking. The further assumption of VMD produces a variety of radiative decay vertices with symmetry breaking. This programme is carried out by Aubrecht and Razmi [27] in the context of SU(4). They investigate the VPP and VVP strong vertices and several associated radiative processes. In this chapter, the SU(3) VVP interaction is studied and a symmetry breaking model for the radiative decay of vector and pseudoscalar mesons is developed.

The free quark model Hamiltonian density is

$$\mathcal{H}(x) = \sum_{k=1}^3 \bar{q}_k(x) (-i\gamma \cdot \partial + m_k) q_k(x) \quad (4.1)$$

where the k th quark, q_k , has mass m_k ($m_1 = m_2 \neq m_3$). Writing the quarks as an SU(3) triplet q ,

$$\mathcal{H}(x) = \bar{q}(x) (-i\gamma \cdot \partial + m + \delta m \lambda_8) q(x) \quad (4.2)$$

where

$$m = (2m_1 + m_3)/3 ,$$

$$\delta m = (m_1 - m_3)/\sqrt{3} .$$

The Hamiltonian corresponding to the mass terms is:

$$H(x_0) = \int d^3x \bar{q}(x) \left(\sqrt{\frac{3}{2}} m\lambda_0 + \delta m\lambda_8 \right) q(x) . \quad (4.3)$$

This may be written

$$H(x_0) = \int d^3x \left(a_0 U_0(x) + a_8 U_8(x) \right) \quad (4.4)$$

using the scalar densities:

$$U_i = \frac{1}{2} \bar{q}(x) \lambda_i q(x) .$$

This standard quark model Hamiltonian [28] has an SU(3) invariant part whose strength is related to the average quark mass

$$a_0 = \sqrt{6} m .$$

A λ_8 symmetry breaking term is also present; its strength is related to the quark mass difference

$$a_8 = 2\delta m .$$

As in the baryon loop calculations, these masses may be taken literally; alternately these masses may be considered merely as a parametrization of the symmetry breaking. It is this last attitude that is taken.

4.2 The Strong VVP Vertex

The matrix element $\langle V^n P^i | H(0) | V^m \rangle$ is to be computed. This constitutes the first order calculation of the VVP strong vertex. The following quark content is assumed for the vector and axial vector current densities and for the pseudoscalar density:

$$\begin{aligned} V_\mu^i(x) &= \frac{1}{2} \bar{q}(x) \gamma_\mu \lambda_i q(x), \\ A_\mu^i(x) &= \frac{i}{2} \bar{q}(x) \gamma_\mu \gamma_5 \lambda_i q(x), \\ P^i(x) &= \frac{i}{2} \bar{q}(x) \gamma_5 \lambda_i q(x). \end{aligned} \quad (4.5)$$

The calculation proceeds in several stages with special assumptions to be enunciated as required.

First, an LSZ reduction [29] is performed on the matrix element, the result being a matrix element between the two vector states of a time ordered product of the pseudoscalar field and the Hamiltonian.

$$\begin{aligned} \langle V^n P^i | H(0) | V^m \rangle &= \langle V^n | \phi_i^{\text{out}} H(0) | V^m \rangle \\ &= \lim_{t \rightarrow \infty} \langle V^n | \phi_i(t) H(0) | V^m \rangle \\ &= \lim_{t \rightarrow \infty} i \int d^3 x f_i^*(x) \overleftrightarrow{\partial}_0 \langle V^n | \phi_i(x) H(0) | V^m \rangle \\ &= i \int d^4 x \frac{\partial}{\partial x^0} (f_i^*(x) \overleftrightarrow{\partial}_0 \langle V^n | T(\phi_i(x) H(0)) | V^m \rangle) \\ &= i \int d^4 x f_i^*(x) (\square + m_i^2) \langle V^n | T(\phi_i(x) H(0)) | V^m \rangle \end{aligned} \quad (4.6)$$

where ϕ_i is the pseudoscalar field and f_i is a c-number plane wave solution to the Klein-Gordon equation:

$$\phi_i(t) = i \int d^3(x) f_i^*(x) \phi_i(x) ,$$

$$f_i(x) = \frac{1}{(2\pi)^{3/2}} \frac{e^{-i p \cdot x}}{\sqrt{2E_i}} .$$

In the second last line of (4.6), a term which reduces to $\langle V^n | H(0) \phi_i^{\text{in}} | V^m \rangle$ is omitted; this term is zero because there is no pseudoscalar in the initial state.

Now the partially conserved axial current (PCAC) [30] assumption is used. This states that the pseudoscalar density is, apart from a constant, the divergence of the axial current density:

$$\partial^\mu A_\mu^i(x) = C_i m_i^2 \phi_i(x) . \quad (4.7)$$

The PCAC coupling constants, C_i , are specified later. Using (4.7),

$$\begin{aligned} & \langle V_P^{n,i} | H(0) | V^m \rangle \\ &= \frac{i}{C_i m_i} \int d^4 x f_i^*(x) (\square + m_i^2) \langle V^n | T(\partial^\mu A_\mu^i(x) H(0)) | V^m \rangle \\ &= \frac{i}{C_i m_i} \int d^4 x f_i^*(x) (\square + m_i^2) \partial^\mu \langle V^n | T(A_\mu^i(x) H(0)) | V^m \rangle \\ &- \frac{i}{C_i m_i} \int d^4 x f_i^*(x) (\square + m_i^2) \delta(x_0) \langle V^n | [A_0^i(x), H(0)] | V^m \rangle \end{aligned}$$

$$\begin{aligned}
&= \frac{1}{(2\pi)^{3/2}} \frac{1}{\sqrt{2E_i}} \frac{p^\mu}{C_i m_i^2} (-p^2 + m_i^2) \int d^4 x e^{ip \cdot x} \\
&\quad \langle V^n | T(A_\mu^i(x) H(0)) | V^m \rangle \\
&+ \frac{1}{(2\pi)^{3/2}} \frac{1}{\sqrt{2E_i}} \frac{1}{C_i m_i^2} (-p^2 + m_i^2) \int d^4 x e^{ip \cdot x} \delta(x_0) \\
&\quad \langle V^n | [A_\mu^i(x), H(0)] | V^m \rangle. \tag{4.8}
\end{aligned}$$

This last step is valid as long as the pseudoscalar is off mass shell.

When the pseudoscalar masses are small, $p_\mu=0$ is a reasonable approximation to the real pseudoscalar momentum. This soft pseudoscalar limit [31] yields a simple form for the desired matrix element. With $p_\mu=0$,

$$\begin{aligned}
&(2E_i (2\pi)^3)^{1/2} \langle V^n P^i | H(0) | V^m \rangle \\
&= \frac{-i}{C_i} \langle V^n | [A_\mu^i(x_0), H(0)] | V^m \rangle \Big|_{x_0=0} \tag{4.9}
\end{aligned}$$

where the axial vector current is defined

$$A_\mu^i(x_0) = \int d^3 x A_\mu^i(x).$$

The quark commutation rules are now used to compute the equal time commutator. From

$$\begin{aligned}
&\{(q_i^\dagger)_\alpha(x), (q_j)_\beta(y)\} \Big|_{x_0=y_0} = \delta_{ij} \delta_{\alpha\beta} \delta^3(\vec{x}-\vec{y}) \\
&\{(q_i)_\alpha(x), (q_j)_\beta(y)\} \Big|_{x_0=y_0} = 0 \tag{4.10}
\end{aligned}$$

it may be shown [32] that:

$$\begin{aligned}
 & [q^\dagger(x) \Gamma_\alpha \lambda_a q(x), q^\dagger(y) \Gamma_\beta \lambda_b q(y)] \Big|_{x_0=y_0} \\
 &= q^\dagger(x) [\Gamma_\alpha \lambda_a, \Gamma_\beta \lambda_b] q(y) \delta^3_{\sim \sim}(x-y) \Big|_{x_0=y_0}. \quad (4.11)
 \end{aligned}$$

The commutator

$$[\Gamma_\alpha \lambda_a, \Gamma_\beta \lambda_b] = \frac{1}{2} \{\Gamma_\alpha, \Gamma_\beta\} [\lambda_a, \lambda_b] + \frac{1}{2} [\Gamma_\alpha, \Gamma_\beta] \{\lambda_a, \lambda_b\}$$

is easily computed from the SU(3) and Dirac algebras. The commutators of interest are

$$\begin{aligned}
 [A_0^i(x), a_0 U_0(y)] \Big|_{x_0=y_0} &= -a_0 d_{i0k} A_0^k(x) \delta^3_{\sim \sim}(x-y) \Big|_{x_0=y_0} / \\
 [A_0^i(x), a_8 U_8(y)] \Big|_{x_0=y_0} &= -a_8 d_{i8k} A_0^k(x) \delta^3_{\sim \sim}(x-y) \Big|_{x_0=y_0} . \\
 & (i, k=0, \dots, 8) \quad (4.12)
 \end{aligned}$$

The standard current algebra form of the desired matrix element is

$$\begin{aligned}
 & (2E_i (2\pi)^3)^{1/2} \langle V^m_P | H(0) | V^m \rangle \\
 &= \frac{i}{C_i} \{a_0 d_{i0k} + a_8 d_{i8k}\} \langle V^n | A_0^k(0) | V^m \rangle. \quad (i, m, n, k=0, \dots, 8) \\
 & \quad (4.13)
 \end{aligned}$$

Further symmetry assumptions are needed to simplify this expression. If $\langle V^n | A_0^k(0) | V^m \rangle$ exhibits nonet symmetry, thereby introducing no new symmetry breaking into the model, a simple VVP vertex results. Using

$$\langle V^n | A_0^k(0) | V^m \rangle \sim g d_{nkm} \quad (n, k, m=0, \dots, 8) \quad (4.14)$$

in (4.13), a VVP model is obtained whose effective Lagrangian is

$$\begin{aligned} \mathcal{L}_{V^m V^i P^i} = & \frac{g}{C_i} \left(\sqrt{\frac{2}{3}} a_0 d_{\min} + a_8 d_{8ik} d_{kmn} \right) \\ & \epsilon_{\mu\nu\rho\sigma} (p_m)^\mu (\epsilon_m)^\nu (p_n)^\rho (\epsilon_n)^\sigma. \end{aligned} \quad (4.15)$$

A more complicated symmetry structure for $\langle V^m | A_0^k(0) | V^m \rangle$ would result in a more complicated version of (4.15).

4.3 The Radiative Decay Model

VMD is now used to derive an effective $VP\gamma$ Lagrangian.

The result

$$\begin{aligned} \mathcal{L}_{V^m P^i \gamma} = & \frac{2ge}{C_i g_\rho} \left(\sqrt{\frac{2}{3}} a_0 d_{\min} + a_8 d_{8ik} d_{kmn} \right) \\ & \left(\delta_{n3} + \frac{1}{\sqrt{3}} \delta_{n8} \right) \epsilon_{\mu\nu\rho\sigma} (p_m)^\mu (\epsilon_m)^\nu (p_n)^\rho (\epsilon_n)^\sigma \end{aligned} \quad (4.16)$$

leads to the following $V^m \rightarrow P^i \gamma$ decay width

$$\Gamma(V^m \rightarrow P^i \gamma) = \frac{1}{96\pi} \frac{C_\pi^2}{C_i^2} (A_0 d_{\min} + A_8 d_{8ik} d_{kmn})^2 \left(\frac{M_m^2 - M_i^2}{M_m} \right)^3, \quad (4.17)$$

where n is the photon index and

$$A_0 = \frac{2ge}{C_\pi g_\rho} \sqrt{\frac{2}{3}} a_0,$$

$$A_8 = \frac{2ge}{C_\pi g_\rho} a_8.$$

Symmetry breaking enters this model in two ways, either through the A_8 term or through the PCAC coupling

constants. If $C_\pi = C_K = C_8 = C_0$ and if $A_8 = 0$, this model demonstrates nonet symmetry. If the C_i 's remain equal but $A_8 \neq 0$, the $SU(3)$ symmetry is broken by one λ_8 . This is a special case of the strong nonet symmetry model which is compatible with VMD (compare (2.15) with $f_0 = A_0$, $f_3 = f_5 = A_8/2$ and the remaining $f_i = 0$). If the PCAC coupling constants are not equal, a broader symmetry breaking structure than those outlined in Chapter II is found. This model is the result of symmetry breaking by more than one λ_8 matrix.

4.4 The Predictions of the Model

In this section, various choices of the PCAC coupling constants are made. In each case, A_0 and A_8 are determined by fitting (4.17) to available decay widths. Notice that C_π affects only the $\phi \rightarrow \pi\gamma$, $\rho \rightarrow \pi\gamma$ and $\omega \rightarrow \pi\gamma$ rates, C_K affects only the $K^{*0} \rightarrow K^0\gamma$ and $K^{*+} \rightarrow K^+\gamma$ rates and C_8 and C_0 only enter those rates which involve η and η' .

It is first assumed that $C_\pi = C_K = C_8 = C_0$. Solution 1, Table 6 ($A_0 = 0.650 \text{ GeV}^{-1}$, $A_8 = 0.152 \text{ GeV}^{-1}$) gives the predictions based on the best fit of (4.17) to all five available rates. Solution 2 ($A_0 = 0.560 \text{ GeV}^{-1}$, $A_8 = 0.313 \text{ GeV}^{-1}$) uses a fit which omits the $\phi \rightarrow \eta\gamma$ rate. The symmetry breaking structure of (4.17) with $C_\pi = C_K = C_8 = C_0$ shows only one improvement over the nonet model--it is possible for either $\Gamma(K^{*0} \rightarrow K^0\gamma)$ or $\Gamma(\phi \rightarrow \eta\gamma)$ to be consistent with $\Gamma(\omega \rightarrow \pi\gamma)$. For ideal vector mixing, $\phi \rightarrow \pi\gamma$ does not proceed. The $\rho \rightarrow \pi\gamma$ rate remains high, near its nonet value.

TABLE 6

Predictions[†] of the Current Algebra Model

Decay Mode	Soln 1	Soln 2	Soln 3	Soln 4	Experiment
$\omega \rightarrow \pi\gamma$	(790)	(800)	(800)	(800)	880 ± 60 [1]
$K^{*0} \rightarrow K^0\gamma$	(130)	(75)	(75)	(75)	75 ± 35 [1]
$\rho \rightarrow \pi\gamma$	(83)	(84)	(84)	(84)	35 ± 10 [1]
$\phi \rightarrow \pi\gamma$	(0.04)	(0.04)	(0.04)	(0.04)	5.7 ± 2.1 [1]
$\phi \rightarrow \eta\gamma$	(62)	11	28	64	64 ± 10 [1,7]
$\omega \rightarrow \eta\gamma$	6.5	6.5	6.5	11	$3.0^{+2.5}_{-1.8}$ or 29 ± 7 [7]
$K^{*+} \rightarrow K^+\gamma$	31	19	19	19	<80 [3]
$\rho \rightarrow \eta\gamma$	50	50	50	87	50 ± 13 or 76 ± 15 [7]
$\eta' \rightarrow \omega\gamma$	9.4	9.6	9.6	6.2	<50 [1]
$\eta' \rightarrow \rho\gamma$	100	100	100	68	<300 [1]
$\phi \rightarrow \eta'\gamma$	0.30	0.05	0.14	0.13	--
$\Gamma(\eta' \rightarrow \rho\gamma) / \Gamma(\eta' \rightarrow \omega\gamma)$	11	11	11	11	9.9 ± 2.0 [8]

[†] All rates in KeV.

The possibility that the PCAC coupling constants are unequal is now investigated. Several current algebra and sum rule calculations [33,34,35] provide possible values for the C_i 's. Under least dispute is the C_K/C_π ratio--from $K \rightarrow \mu \nu$ decay experiments $C_K/C_\pi = 1.13 \pm 0.03$ [33]. This ratio is used in solution 3 ($A_0 = 0.601 \text{ GeV}^{-1}$, $A_8 = 0.242 \text{ GeV}^{-1}$). The fit to A_0 and A_8 is based on all the decay data except $\Gamma(\phi \rightarrow \eta \gamma)$; the predictions use $C_8 = C_0 = C_\pi$. Here also, the symmetry breaking structure does not destroy the nonet ratios of $\Gamma(\rho \rightarrow \pi \gamma) : \Gamma(\omega \rightarrow \pi \gamma) : \Gamma(\phi \rightarrow \pi \gamma)$. The $K^{*0} \rightarrow K^0 \gamma$ width may be fixed at the experimental value; the $\phi \rightarrow \eta \gamma$ rate remains low.

Adjustment of C_8 and C_0 is now attempted. Many discussions of C_8 and C_0 have appeared [34,35], the suggested C_8/C_π and C_0/C_π ratios varying widely. Solution 4 ($A_0 = 0.601 \text{ GeV}^{-1}$, $A_8 = 0.242 \text{ GeV}^{-1}$; $C_8/C_\pi = 0.702$ and $C_0/C_\pi = 1.133$) uses the values of A_0 and A_8 from solution 3 and Chanowitz's [35] ratio $C_8/C_0 = 0.62$. While both $\Gamma(K^{*0} \rightarrow K^0 \gamma)$ and $\Gamma(\phi \rightarrow \eta \gamma)$ are predicted to agree with experiment, $\Gamma(\rho \rightarrow \pi \gamma)$ and $\Gamma(\phi \rightarrow \pi \gamma)$ remain near their nonet values. Since C_8 and C_0 don't enter these last rates, nothing can be done about this problem. Other values of C_8 and C_0 also give $\Gamma(\phi \rightarrow \eta \gamma) \sim 64 \text{ KeV}$ but only a small range of values is consistent with $\Gamma(\eta' \rightarrow \rho \gamma) < 300 \text{ KeV}$.

The symmetry breaking structure induced in the VP_γ amplitude by this current algebra technique is not quite that which is required to explain the observed radiative decay widths. Small adjustments in θ_V could probably cure the

$\phi \rightarrow \pi\gamma$ width. The latitude in C_8 and C_0 which is consistent with $\Gamma(\phi \rightarrow \pi\gamma) \sim 64$ KeV and $\Gamma(\eta' \rightarrow \rho\gamma) < 300$ KeV could be used to adjust the other η and η' widths. The real problem lies with $\Gamma(\rho \rightarrow \pi\gamma)$ which is predicted near its nonet value. A more general symmetry breaking structure is needed to destroy the nonet relationship among $\Gamma(\omega \rightarrow \pi\gamma)$, $\Gamma(\rho \rightarrow \pi\gamma)$ and $\Gamma(\phi \rightarrow \pi\gamma)$.

CHAPTER V

THE SU(3) SYMMETRY BREAKING MODELS
WITH NONET SYMMETRY5.1 The Models

The four general λ_8 symmetry breaking models which demonstrate nonet symmetry are discussed in this chapter. Of particular interest is the simplest of these models, the strong nonet symmetry model which demonstrates Boson symmetry.

First, a $V^{(8)}V^{(8)}P^{(8)}$ model with λ_8 symmetry breaking is studied. This model is extended to include the vector and pseudoscalar singlet sectors and then, with VMD, is turned into a radiative decay model. It is seen that this model is essentially equivalent to the most general strong nonet symmetry model with Boson symmetry and λ_8 symmetry breaking.

The strong nonet symmetry and Boson symmetry constraints are then loosened in an attempt to account for those rates that are not well predicted by the first model.

5.2 A VVP Model With SU(3)
Symmetry Breaking

Muraskin and Glashow [36] write down the most general Lagrangian for the $V^{(8)}V^{(8)}P^{(8)}$ vertex where the SU(3) symmetry is broken by a λ_8 scalar spurion. This Lagrangian may be modified to include vector and pseudoscalar singlets by simply replacing octets with nonets. The Muraskin and Glashow [36] Lagrangian so extended is:

$$\begin{aligned}
\mathcal{L} = & \epsilon^{\mu\nu\rho\sigma} [g_0 \text{Tr} (\partial_\mu V_\nu P \partial_\rho V_\sigma) \\
& + g_1 \text{Tr} (\partial_\mu V_\nu \partial_\rho V_\sigma) \text{Tr} (P \lambda_8) \\
& + g_2 \text{Tr} (\partial_\mu V_\nu P) \text{Tr} (\partial_\rho V_\sigma \lambda_8) \\
& + g_3 \text{Tr} (\partial_\mu V_\nu \lambda_8 \partial_\rho V_\sigma P)], \tag{5.1}
\end{aligned}$$

where

$$\begin{aligned}
V_\mu &= \frac{1}{\sqrt{2}} \sum_{i=0}^8 \lambda_i V_\mu^i, \\
P &= \frac{1}{\sqrt{2}} \sum_{i=0}^8 \lambda_i P^i.
\end{aligned}$$

The term in (5.1) which describes the interaction of V^m (momentum p_m , polarization ϵ_m), V^n (momentum p_n , polarization ϵ_n) and P^i (momentum p_i) is:

$$\mathcal{L}_{VVP}^{mni} = \frac{1}{\sqrt{2}} \tilde{g}_{\min} \epsilon_{\mu\nu\rho\sigma} (p_m)^\mu (\epsilon_m)^\nu (p_n)^\rho (\epsilon_n)^\sigma, \tag{5.2}$$

where

$$\begin{aligned}
\tilde{g}_{\min} = & g_0 d_{\min} + 2g_1 \delta_{mn} \delta_{i8} + g_2 (\delta_{im} \delta_{n8} + \delta_{in} \delta_{m8}) \\
& + g_3 (d_{8mk} d_{kin} + d_{8nk} d_{kim} - d_{8ik} d_{kmn}) \\
& (m, i, n, k=0, \dots, 8). \tag{5.3}
\end{aligned}$$

As expected, this amplitude exhibits Boson symmetry.

This VVP model leads to the following radiative decay model. Using VMD and (5.2),

$$\mathcal{L}_{VP\gamma}^{mni} = \sqrt{2} \frac{e}{g_\rho} \tilde{g}_{\min} \epsilon_{\mu\nu\rho\sigma} (p_m)^\mu (\epsilon_m)^\nu (p_n)^\rho (\epsilon_n)^\sigma, \tag{5.4}$$

where n is now the photon index. The corresponding $V \rightarrow P\gamma$ decay rate is

$$\Gamma(V^m \rightarrow P^i \gamma) = \frac{1}{48\pi} \left(\frac{e}{g_\rho} \tilde{g}_{\min} \right)^2 \left(\frac{M_m^2 - M_i^2}{M_m} \right)^3. \quad (5.5)$$

From chapter II, the most general λ_8 symmetry breaking model with strong nonet symmetry and Boson symmetry predicts

$$\Gamma(V^m \rightarrow P^i \gamma) = \frac{1}{96\pi} (g_{\min})^2 \left(\frac{M_m^2 - M_i^2}{M_m} \right)^3. \quad (5.6)$$

where

$$\begin{aligned} g_{\min} = & f_0 d_{\min} + (2f_3 - f_4) d_{8ik} d_{kmn} \\ & + f_4 (d_{8nk} d_{kim} + d_{8mk} d_{kin}) \\ & + f_6 \delta_{8i} \delta_{mn} \\ & + f_7 (\delta_{8n} \delta_{im} + \delta_{8m} \delta_{in}). \quad (m, i, k=0, \dots, 8) \end{aligned} \quad (5.7)$$

Comparison of (5.5) and (5.6) suggests

$$\begin{aligned} f_0 &= \frac{\sqrt{2}e}{g_\rho} g_0, \\ f_3 &= 0, \\ f_4 &= \frac{\sqrt{2}e}{g_\rho} g_3, \\ f_6 &= \frac{\sqrt{2}e}{g_\rho} (2g_1), \\ f_7 &= \frac{\sqrt{2}e}{g_\rho} g_2. \end{aligned} \quad (5.8)$$

Since in the most general case it is not necessary that $f_3 = 0$, this Muraskin and Glashow derived model lacks one degree of

freedom. This stems from the form of the VVP Lagrangian (5.1)--while this has the most general λ_8 symmetry breaking structure for octets, it lacks one degree of freedom when singlets are also considered.

For most of the radiative decays, this lack of generality is transparent. With the exception of $K^{*+} \rightarrow K^+ \gamma$, all the decays of interest (see Table 7) involve SU(3) indices which satisfy:

$$d_{8nk} d_{kim} + d_{8mk} d_{kin} - 2 d_{8ik} d_{kmn} = 0. \quad (5.9)$$

Rearrangement of (5.7) gives

$$\begin{aligned} g_{\min} = & f_0 d_{\min} \\ & + (2f_3 + f_4) (d_{8nk} d_{kim} + d_{8mk} d_{kin} - d_{8ik} d_{kmn}) \\ & + (-2f_3) (d_{8nk} d_{kim} + d_{8mk} d_{kin} - 2 d_{8ik} d_{kmn}) \\ & + f_6 \delta_{8i} \delta_{mn} + f_7 (\delta_{8n} \delta_{im} + \delta_{8m} \delta_{in}). \end{aligned} \quad (5.10)$$

Use of (5.9) now indicates that for all decays, except $K^{*0} \rightarrow K^0 \gamma$, the restricted model (5.3)-(5.5) is equivalent to the most general model (5.6)-(5.7). The restricted model bases its predictions of $\Gamma(K^{*0} \rightarrow K^0 \gamma)$ on the assumption that $f_3 = 0$; if $f_3 \neq 0$, then $\Gamma(K^{*0} \rightarrow K^0 \gamma)$ should be computed using (5.7) or (5.10).

For clarification, it is worth mentioning that in the published version of this model [37] the following set of coupling constants is used:

$$\begin{aligned}
A &= \frac{e}{\sqrt{48\pi} g_\rho} g_0, \\
B &= -2 \frac{e}{\sqrt{48\pi} g_\rho} g_3, \\
C &= \frac{e}{\sqrt{48\pi} g_\rho} (g_2 + g_3), \\
D &= \frac{e}{\sqrt{48\pi} g_\rho} (2g_1 - \frac{1}{3} g_3). \tag{5.11}
\end{aligned}$$

These constants yield a particularly simple form for the $V^{(8)}_P{}^{(8)}_\gamma$ amplitude.

5.3 The Strong Nonet Model With Boson Symmetry

The predictions of the general strong nonet model with Boson symmetry and SU(3) symmetry breaking are now compared with experiment. From the available data f_3 can not be obtained; as a result, the $K^{*+} \rightarrow K^+ \gamma$ rate is ambiguous and is quoted using $f_3 = 0$. All other rates are totally specified by the model.

The predictions of this model are presented in Table 7. The constants f_0 , f_4 , f_6 and f_7 are used; equivalently, g_0 , g_1 , g_2 and g_3 or A , B , C and D could be used. Solution 1 ($f_0 = 0.539 \text{ GeV}^{-1}$, $f_4 = 0.420 \text{ GeV}^{-1}$, $f_6 = -0.320 \text{ GeV}^{-1}$ and $f_7 = -0.059 \text{ GeV}^{-1}$) fits the five measured rates. In solution 2 ($f_0 = 0.472 \text{ GeV}^{-1}$, $f_4 = 0.174 \text{ GeV}^{-1}$, $f_6 = -0.110 \text{ GeV}^{-1}$ and $f_7 = -0.054 \text{ GeV}^{-1}$), $\Gamma(\omega \rightarrow \pi \gamma)$ is omitted from the fit. In solution 3 ($f_0 = 0.551 \text{ GeV}^{-1}$, $f_4 = 0.448 \text{ GeV}^{-1}$, $f_6 = -0.349 \text{ GeV}^{-1}$ and $f_7 = -0.055 \text{ GeV}^{-1}$), $\Gamma(\rho \rightarrow \pi \gamma)$ is omitted from the

TABLE 7

Predictions[†] of the Strong Nonet Symmetry Model with
Boson Symmetry and SU(3) Symmetry Breaking

Decay Mode	Soln 1	Soln 2	Soln 3	Soln 4	Experiment
$\omega \rightarrow \pi\gamma$	(810)	430	(880)	(810)	880 ± 60 [1]
$K^{*0} \rightarrow K^0\gamma$	(75)	(75)	(175)	(120)	75 ± 35 [1]
$\rho \rightarrow \pi\gamma$	(70)	(35)	78	(71)	35 ± 10 [1]
$\phi \rightarrow \pi\gamma$	(6.7)	(5.7)	(5.7)	(6.1)	5.7 ± 2.1 [1]
$\phi \rightarrow \eta\gamma$	(64)	(64)	(64)	(62)	64 ± 10 [1,7]
$\omega \rightarrow \eta\gamma$	0.30	0.78	0.30	(3.3)	$3.0^{+2.5}_{-1.8}$ or 29 ± 7 [7]
$K^{*+} \rightarrow K^+\gamma$	170*	51*	190*	110*	<80 [3]
$\rho \rightarrow \eta\gamma$	10	16	9.7	(45)	50 ± 13 or 76 ± 15 [7]
$\eta' \rightarrow \omega\gamma$	10	4.7	12	8.8	<50 [1]
$\eta' \rightarrow \rho\gamma$	140	69	150	120	<300 [1]
$\phi \rightarrow \eta'\gamma$	0.04	0.16	0.03	0.19	--
$\Gamma(\eta' \rightarrow \rho\gamma) / \Gamma(\eta' \rightarrow \omega\gamma)$	13	15	13	(14)	9.9 ± 2.0 [8]

[†]All rates in KeV.

* May be adjusted by appropriate choice of f_3 .

fit. In all cases, most of the symmetry breaking enters through the f_4 term and is found to be substantial¹ ($\sim 80\%$).

Many of the inconsistencies of the nonet model are resolved in this symmetry breaking scheme: $\phi \rightarrow \pi\gamma$ proceeds through the symmetry breaking terms; both $\Gamma(K^{*0} \rightarrow K^0\gamma)$ and $\Gamma(\phi \rightarrow \eta\gamma)$ are independent of $\Gamma(\omega \rightarrow \pi\gamma)$ and may take their measured values. The inconsistency of the $\rho \rightarrow \pi\gamma$ and $\omega \rightarrow \pi\gamma$ rates does, however, remain--if $\Gamma(\omega \rightarrow \pi\gamma)$ takes its measured value, $\Gamma(\rho \rightarrow \pi\gamma)$ is predicted too large by a factor of 2.2. This problem is discussed further in the next section.

The amount of symmetry breaking required in these fits causes some problem for rates which are reasonable in the nonet model. In particular, $\Gamma(\rho \rightarrow \eta\gamma)$ and $\Gamma(\omega \rightarrow \eta\gamma)$ are predicted too low and $\Gamma(\eta' \rightarrow \rho\gamma)/\Gamma(\eta' \rightarrow \omega\gamma)$ too high. Solution 4 ($f_0 = 0.623 \text{ GeV}^{-1}$, $f_4 = 0.269 \text{ GeV}^{-1}$, $f_6 = -0.057 \text{ GeV}^{-1}$ and $f_7 = -0.056 \text{ GeV}^{-1}$) fits to the five established rates, $\Gamma(\rho \rightarrow \eta\gamma) = 50 \pm 13 \text{ KeV}$, $\Gamma(\omega \rightarrow \eta\gamma) = 3 \pm 2 \text{ KeV}$ and $\Gamma(\eta' \rightarrow \rho\gamma)/\Gamma(\eta' \rightarrow \omega\gamma) = 9.9$. The $\rho \rightarrow \eta\gamma$ and $\omega \rightarrow \eta\gamma$ rates may be obtained at the expense of a slightly wide $K^{*0} \rightarrow K^0\gamma$ width, but $\Gamma(\eta' \rightarrow \rho\gamma)/\Gamma(\eta' \rightarrow \omega\gamma)$ remains about 14. These rates are examined again as the strong nonet and Boson symmetry assumptions are lifted.

That the predicted values of $\Gamma(K^{*+} \rightarrow K^+\gamma)$ sometimes exceed the experimental upper bound is of little concern. This width may be brought within bounds by adjustment of f_3 .

5.4 The $\rho \rightarrow \pi\gamma$ Width

The failure of this model to predict the measured $\rho \rightarrow \pi\gamma$ rate is a serious shortcoming. In this section, three

remedial suggestions are explored. Working within the context of the present model, the measured $\rho \rightarrow \pi\gamma$ width may be accommodated by changing the vector mixing angle. This solution is considered inadequate because the narrowness of many of the ϕ decay widths could no longer be attributed to the OZI rule. A second solution is to discard VMD--a strong nonet model with no Boson symmetry provides a consistent description of the five established decays. A third possibility, which is not entirely fatuous, is that the measured $\rho \rightarrow \pi\gamma$ width may be wrong.

To understand why the present model predicts $\Gamma(\rho \rightarrow \pi\gamma) \sim 80$ KeV when $\Gamma(\omega \rightarrow \pi\gamma) \sim 880$ KeV, it is convenient to examine the unitary symmetry structure of the corresponding decay amplitudes. From (5.7),

$$g_{\rho\pi\gamma} = \frac{1}{3} f_0 + \frac{1}{3} (4f_3 - f_4) + \frac{1}{\sqrt{3}} f_7,$$

$$g_{V^8\pi\gamma} = \frac{1}{\sqrt{3}} f_0 + \frac{1}{\sqrt{3}} (4f_3 - f_4) + f_7, \quad (5.12)$$

so that,

$$g_{\rho\pi\gamma} = \frac{1}{\sqrt{3}} g_{V^8\pi\gamma}. \quad (5.13)$$

From (1.2),

$$|8\rangle = \sin \theta_V |\omega\rangle + \cos \theta_V |\phi\rangle. \quad (5.14)$$

Hence,

$$g_{\rho\pi\gamma} = \frac{1}{\sqrt{3}} (\sin \theta_V g_{\omega\pi\gamma} + \cos \theta_V g_{\phi\pi\gamma}). \quad (5.15)$$

With θ_V ideal and $g_{\phi\pi\gamma} = 0$,

$$g_{\rho\pi\gamma} = \frac{1}{3} g_{\omega\pi\gamma},$$

and the nonet ratio $\Gamma(\omega \rightarrow \pi\gamma)/\Gamma(\rho \rightarrow \pi\gamma) \sim 9$ is obtained. This is not altered much by a small value for $g_{\phi\pi\gamma}$.

That adjustment of θ_V may lead to a consistent solution for the $\rho \rightarrow \pi\gamma$, $\omega \rightarrow \pi\gamma$ and $\phi \rightarrow \pi\gamma$ rates is seen from (5.15). From the experimental rates, experimental values of $g_{\rho\pi\gamma}$, $g_{\omega\pi\gamma}$ and $g_{\phi\pi\gamma}$ are obtained:

$$\begin{aligned} g_{\rho\pi\gamma} &= \pm 0.15(98) \text{ GeV}^{-1}, \\ g_{\omega\pi\gamma} &= \pm 0.77(81) \text{ GeV}^{-1}, \\ g_{\phi\pi\gamma} &= \pm 0.04(13) \text{ GeV}^{-1}. \end{aligned} \tag{5.16}$$

These values are consistent with (5.15) if $\theta_V = \pm 24^\circ$ or $\pm 18^\circ$. Solution 1 Table 8 ($f_0 = 0.473 \text{ GeV}^{-1}$, $f_4 = 0.723 \text{ GeV}^{-1}$, $f_6 = -0.616 \text{ GeV}^{-1}$ and $f_7 = -0.236 \text{ GeV}^{-1}$) fits the five established rates to the strong nonet model with Boson symmetry and $\theta_V = 24^\circ$. Notice the very large¹ SU(3) symmetry breaking necessary to account for the narrow $\phi \rightarrow \pi\gamma$ width. This is similar to the case of the SU(3) model of Boal, Graham and Moffat--here too, large deviation from ideal vector mixing is accompanied by large symmetry breaking, nonet symmetry breaking in this instance. The strong nonet model with Boson symmetry and $\theta_V = 24^\circ$ has trouble with the newly measured η and η' rates. $\Gamma(\rho \rightarrow \eta\gamma)$ and $\Gamma(\omega \rightarrow \eta\gamma)$ may be raised to near their observed values, but then $\Gamma(K^{*0} \rightarrow K^0\gamma) \sim 180 \text{ KeV}$ and

TABLE 8

Predictions[†] of other Nonet Symmetry Models
with SU(3) Symmetry Breaking

Decay Mode	Soln 1	Soln 2	Soln 3	Soln 4	Soln 5	Experiment
$\omega \rightarrow \pi\gamma$	(880)	(880)	(860)	(810)	(880)	880 ± 60 [1]
$K^{*0} \rightarrow K^0\gamma$	(74)	(74)	(150)	(75)	(75)	75 ± 35 [1]
$\rho \rightarrow \pi\gamma$	(35)	(35)	(41)	(71)	(35)	35 ± 10 [1]
$\phi \rightarrow \pi\gamma$	(5.7)	(5.7)	(5.6)	(6.7)	(5.7)	5.7 ± 2.1 [1]
$\phi \rightarrow \eta\gamma$	(64)	(64)	(61)	(64)	(64)	64 ± 10 [1,7]
$\omega \rightarrow \eta\gamma$	0.43	0.68	(1.7)	(3.0)	(3.0)	$3.0^{+2.5}_{-1.8}$ or 29 ± 7 [7]
$K^{*+} \rightarrow K^+\gamma$	1.7*	0.04*	4.6*	2.2*	0.07*	<80 [3]
$\rho \rightarrow \eta\gamma$	0.12	2.2	(49)	(50)	(50)	50 ± 13 or 76 ± 15 [7]
$\eta' \rightarrow \omega\gamma$	7.2	6.5	5.2	25	44	<50 [1]
$\eta' \rightarrow \rho\gamma$	210	160	130	520	830	<300 [1]
$\phi \rightarrow \eta'\gamma$	0.0001	0.004	0.19	1.0	3.6	--
$\Gamma(\eta' \rightarrow \rho\gamma) / \Gamma(\eta' \rightarrow \omega\gamma)$	29	25	24	21	19	9.9 ± 2.0 [8]

[†]All rates in KeV.

* May be adjusted by appropriate choice of f_2 .

$\Gamma(\eta' \rightarrow \rho\gamma)/\Gamma(\eta' \rightarrow \omega\gamma) \sim 70$. Nonideal vector mixing might be justified on the basis of overwhelming success but here only partial success has been found--another cure for the $\rho \rightarrow \pi\gamma$ rate is sought.

If θ_V is to be ideal, a model must be found in which (5.15) is not valid. The nonet symmetry structure is not the source of the problems for only octet relations are needed to deduce (5.13) and hence (5.15). To explain $\Gamma(\rho \rightarrow \pi\gamma) \sim 35$ KeV, it is necessary to abandon VMD. That the measured $\rho \rightarrow \pi\gamma$ rate is inconsistent with VMD is seen again in the next chapter. In the next section, it is demonstrated how removing the Boson symmetry can explain the $\rho \rightarrow \pi\gamma$ rate.

Before giving up ideal vector mixing or VMD, it is reasonable to consider the reliability of the measured $\rho \rightarrow \pi\gamma$ width. This rate has been measured only once [4] in a difficult Primakoff effect experiment. The data analysis is quite complicated since the relative phase of the coulomb and strong production amplitudes is unknown. While suggestions [14] that the analysis might admit the further solution $\Gamma(\rho \rightarrow \pi\gamma) \sim 80$ KeV have been effectively rebuffed by the experimenters [4] doubt still hangs over the published rate. Another measurement of the $\rho \rightarrow \pi\gamma$ width, especially in an e^+e^- experiment, would be desirable.

5.5 Loosening the Symmetry Assumptions

In this section, the Boson symmetry restriction is lifted in an attempt to explain $\Gamma(\rho \rightarrow \pi\gamma) \sim 35$ KeV. The strong

nonet symmetry assumption is also loosened to one of weak nonet symmetry--this may offer an explanation of the recently measured η and η' radiative decay processes.

The strong nonet symmetry model with no Boson symmetry uses (5.6) where now

$$\begin{aligned}
 g_{\min} = & f_0 d_{\min} + (f_3 - f_4 + f_5) d_{8ik} d_{kmn} \\
 & + (-f_3 + f_4 + f_5) d_{8nk} d_{kim} + (f_3 + f_4 - f_5) d_{8mk} d_{kin} \\
 & + f_6 \delta_{8i} \delta_{mn} + f_7 \delta_{8n} \delta_{im} + f_8 \delta_{8m} \delta_{in}. \quad (5.17)
 \end{aligned}$$

Two redundancies occur in (5.17)--one is due to the general identity (2.16) and the other, which holds for all processes except $K^{*+} \rightarrow K^+ \gamma$, follows from (5.9). As a result five coupling constants characterize this model when $K^{*+} \rightarrow K^+ \gamma$ is not considered: f_0 , f_4 , f_6 , f_7 and f_8 . To obtain $\Gamma(K^{*+} \rightarrow K^+ \gamma)$, f_3 must also be specified. Solution 2 Table 8 ($f_0 = 0.472 \text{ GeV}^{-1}$, $f_4 = 0.580 \text{ GeV}^{-1}$, $f_6 = -0.469 \text{ GeV}^{-1}$, $f_7 = -0.189 \text{ GeV}^{-1}$ and $f_8 = -0.051 \text{ GeV}^{-1}$) fits the five established rates. If $\Gamma(\omega \rightarrow \eta \gamma) = 3 \pm 2 \text{ KeV}$ and $\Gamma(\rho \rightarrow \eta \gamma) = 50 \pm 13 \text{ KeV}$ are also included in the fit solution 3 ($f_0 = 0.610 \text{ GeV}^{-1}$, $f_4 = 0.329 \text{ GeV}^{-1}$, $f_6 = -0.051 \text{ GeV}^{-1}$, $f_7 = -0.162 \text{ GeV}^{-1}$ and $f_8 = -0.050 \text{ GeV}^{-1}$) is obtained. As expected, $\Gamma(\rho \rightarrow \pi \gamma) \sim 35 \text{ KeV}$ may be obtained if Boson symmetry is not in force. The η and η' rates pose a problem similar to that of the strong nonet symmetry model with Boson symmetry. The five established rates require so much symmetry breaking that $\rho \rightarrow \eta \gamma$ and $\omega \rightarrow \eta \gamma$ become suppressed; if these last processes take their observed values, the $K^{*0} \rightarrow K^0 \gamma$ width must

increase. Furthermore, the $\Gamma(\eta' \rightarrow \rho\gamma)/\Gamma(\eta' \rightarrow \omega\gamma)$ ratio is predicted too high.

The weak nonet symmetry model with Boson symmetry uses the following g_{\min} :

$$\begin{aligned}
 g_{\min} = & f_0 d_{\min} + (2f_3 - f_4) d_{8ik} d_{kmn} \\
 & + f_4 (d_{8nk} d_{kim} + d_{8mk} d_{kin}) \\
 & + f_6 \delta_{8i} \delta_{mn} + f_7 (\delta_{8n} \delta_{im} + \delta_{8m} \delta_{in}) \\
 & + f_9 d_{mn8} \delta_{io} + f_{10} d_{ni8} \delta_{mo} \\
 & + f_{11} \delta_{mo} \delta_{io} \delta_{n8}.
 \end{aligned} \tag{5.18}$$

From (2.17) and (5.9), it is seen that two redundancies are present for all decays except $K^{*+} \rightarrow K^+ \gamma$. The constants f_0, f_4, f_6, f_7, f_9 and f_{10} characterize the model for most decays; only for $K^{*+} \rightarrow K^+ \gamma$ must f_3 also be specified. Since this model satisfies Boson symmetry it is expected to predict $\Gamma(\rho \rightarrow \pi\gamma)$ too high. Solution 4 Table 8 ($f_0 = 0.541 \text{ GeV}^{-1}$, $f_4 = 0.602 \text{ GeV}^{-1}$, $f_6 = -0.196 \text{ GeV}^{-1}$, $f_7 = -0.118 \text{ GeV}^{-1}$, $f_9 = 0.877 \text{ GeV}^{-1}$ and $f_{10} = -0.154 \text{ GeV}^{-1}$) fits to the five established rates, $\Gamma(\omega \rightarrow \eta\gamma) = 3 \pm 2 \text{ KeV}$ and $\Gamma(\rho \rightarrow \eta\gamma) = 50 \pm 13 \text{ KeV}$.

For processes not involving η and η' , these predictions are similar to the strong symmetry model with Boson symmetry. In this model, $\Gamma(\omega \rightarrow \eta\gamma)$ and $\Gamma(\rho \rightarrow \eta\gamma)$ may be accommodated without a large $K^{*0} \rightarrow K^0 \gamma$ width. Problems however occur for $\Gamma(\eta' \rightarrow \rho\gamma)$ which violates its upper bound. The ratio $\Gamma(\eta' \rightarrow \rho\gamma)/\Gamma(\eta' \rightarrow \omega\gamma) = 9.9$ may be obtained, unfortunately this

must be accomplished by raising $\Gamma(\eta' \rightarrow \omega\gamma)$ above its bound, rather than by lowering $\Gamma(\eta' \rightarrow \rho\gamma)$.

The most general SU(3) symmetry breaking model with nonet symmetry is the weak nonet model with no Boson symmetry. For this scheme,

$$\begin{aligned}
 g_{\min} = & f_0 d_{\min} + (f_3 - f_4 + f_5) d_{8ik} d_{kmn} \\
 & + (-f_3 + f_4 + f_5) d_{8nk} d_{kim} + (f_3 + f_4 - f_5) d_{8mk} d_{kin} \\
 & + f_6 \delta_{8i} \delta_{mn} + f_7 \delta_{8n} \delta_{im} + f_8 \delta_{8m} \delta_{in} \\
 & + f_9 d_{mn8} \delta_{io} + f_9 d_{mn8} \delta_{io} + f_{10} d_{mi8} \delta_{mo} \\
 & + f_{11} \delta_{mo} \delta_{io} \delta_{n8}.
 \end{aligned} \tag{5.19}$$

From (2.16), (2.17) and (5.9), three redundancies are observed for all processes except $K^{*+} \rightarrow K^+ \gamma$. The constants $f_0, f_4, f_6, f_7, f_8, f_9$ and f_{10} characterize the model; f_3 is needed in addition to predict $\Gamma(K^{*+} \rightarrow K^+ \gamma)$. Solution 5 Table 8 ($f_0 = 0.472 \text{ GeV}^{-1}$, $f_4 = 0.586 \text{ GeV}^{-1}$, $f_6 = -0.205 \text{ GeV}^{-1}$, $f_7 = -0.191 \text{ GeV}^{-1}$, $f_8 = 0.015 \text{ GeV}^{-1}$, $f_9 = 1.515 \text{ GeV}^{-1}$ and $f_{10} = -0.087 \text{ GeV}^{-1}$) fits to the five established data, $\Gamma(\omega \rightarrow \eta\gamma) = 3 \pm 2 \text{ KeV}$ and $\Gamma(\rho \rightarrow \eta\gamma) = 50 \pm 13 \text{ KeV}$. The only problem is with the η' rates: $\Gamma(\eta' \rightarrow \rho\gamma)$ violates its upper bound and $\Gamma(\eta' \rightarrow \rho\gamma)/\Gamma(\eta' \rightarrow \omega\gamma) \sim 19$. The last ratio may be reduced to the observed value but, as a result, $\Gamma(\eta' \rightarrow \omega\gamma)$ also violates its upper bound--this is similar to the other weak nonet symmetry model.

5.6 Conclusions

The symmetry breaking structure of the λ_8 symmetry models with nonet symmetry is able to account for the observed $\omega \rightarrow \pi\gamma$, $K^{*0} \rightarrow K^0\gamma$, $\phi \rightarrow \pi\gamma$ and $\phi \rightarrow \eta\gamma$ rates. It is especially interesting that $\Gamma(\phi \rightarrow \pi\gamma) \sim 6$ KeV may be obtained even when ideal vector mixing is assumed.

Using ideal vector mixing, the observed $\rho \rightarrow \pi\gamma$ rate can only be explained by abandoning the Boson symmetry which a $VP\gamma$ model should have if it were compatible with a VVP model through VMD. Imposition of Boson symmetry would require that $\Gamma(\rho \rightarrow \pi\gamma) \sim 70-80$ KeV.

In the strong nonet models, the symmetry breaking needed to explain $\Gamma(\omega \rightarrow \pi\gamma)$, $\Gamma(K^{*0} \rightarrow K^0\gamma)$, $\Gamma(\phi \rightarrow \pi\gamma)$ and $\Gamma(\phi \rightarrow \eta\gamma)$ results in a suppression of $\Gamma(\omega \rightarrow \eta\gamma)$ and $\Gamma(\rho \rightarrow \eta\gamma)$. Only in a weak nonet symmetry model can these last two rates attain the lower of their possible observed values while maintaining the proper rates for the first four rates.

The ratio $\Gamma(\eta' \rightarrow \rho\gamma)/\Gamma(\eta' \rightarrow \omega\gamma)$ is found to be about 15-25 in most of the models. In the weak nonet models it is possible to get $\Gamma(\eta' \rightarrow \rho\gamma)/\Gamma(\eta' \rightarrow \omega\gamma) \sim 10$ by a slight adjustment of $\Gamma(\omega \rightarrow \eta\gamma)$ and $\Gamma(\rho \rightarrow \eta\gamma)$ about their observed values. Unfortunately both $\Gamma(\eta' \rightarrow \omega\gamma)$ and $\Gamma(\eta' \rightarrow \rho\gamma)$ then violate quite severely their experimental upper bounds.

It is clear that none of the nonet models gives a completely satisfactory explanation of the observed radiative decay rates. What successes that are seen seem hardly remarkable given that the number of explained data usually

equals the number of available coupling constants.

On the other hand, all the nonet models with λ_8 symmetry breaking can explain the four well measured nondisputed rates. The remaining data which seem difficult to explain are not on such firm ground experimentally. A measurement of $\rho^0 \rightarrow \pi^0 \gamma$ is needed, the phase problem with $\omega \rightarrow \eta \gamma$ and $\rho \rightarrow \eta \gamma$ must be resolved, absolute rates for $\eta' \rightarrow \omega \gamma$ and $\eta' \rightarrow \rho \gamma$ should be obtained and, in addition, the remaining rates, $\Gamma(K^{*+} \rightarrow K^+ \gamma)$ and $\Gamma(\phi \rightarrow \eta' \gamma)$, should be measured. Until some of these rates have been better established, it would be premature to eliminate any of the nonet symmetry models as possible explanations for the radiative decays of mesons.

CHAPTER VI

OTHER RADIATIVE AND HADRONIC DECAYS

6.1 The Basic Interactions

As described in section 1.7 and illustrated in Figure 1, many different hadronic and radiative decay rates may be predicted once the VVP and VPP hadronic vertices and the VMD $V\gamma$ vertex are known. In this chapter, three different VVP models are used along with standard versions of VMD and the VPP interaction to predict rates for such processes as $V \rightarrow P\gamma$, $P \rightarrow \gamma\gamma$, $P \rightarrow PP\gamma$ and $V \rightarrow PPP$.

The Lagrangians of interest are

$$\mathcal{L}_{VVP}^{mnp} = g_{VVP}^{mnp} \epsilon_{\mu\nu\rho\sigma} (p_m)^\mu (\epsilon_m)^\nu (p_n)^\rho (\epsilon_n)^\sigma, \quad (6.1)$$

$$\mathcal{L}_{VP}^{mjk} = \frac{1}{2} g_\rho f_{mjk} (\epsilon_m)^\mu (p_k - p_j)_\mu, \quad (6.2)$$

$$\mathcal{L}_{V\gamma}^m = \frac{e}{g_\rho} M_m^2 (\delta_{m3} + \frac{1}{\sqrt{3}} \delta_{m8}). \quad (6.3)$$

Both (6.2) and (6.3) are the standard SU(3) Lagrangians.

Depending on the form of g_{VVP}^{mnp} in (6.1), the VVP Lagrangian may or may not demonstrate SU(3) symmetry breaking.

Each VVP model to be examined stems from a $VP\gamma$ model with the required Boson symmetry. If

$$\mathcal{L}_{VP\gamma}^{mi} = g_{\min} \delta_{n\gamma} \epsilon_{\mu\nu\rho\sigma} (p_m)^\mu (\epsilon_m)^\nu (p_n)^\rho (\epsilon_m)^\sigma,$$

then

$$g_{VVP}^{mnp} = \frac{g_\rho}{2e} g_{\min}, \quad (6.4)$$

where n is now a general vector index. For a model with nonet symmetry and no $SU(3)$ symmetry breaking,

$$g_{VV^*P}^{mni} \propto d_{\min}.$$

In this chapter, the $SU(3)$ model with nonet symmetry breaking of Boal, Graham and Moffat [15] is used (g_{\min} from (1.16)). Also, the strong and weak nonet symmetry models with $SU(3)$ symmetry breaking are discussed (g_{\min} from (5.7) and (5.18) respectively).

6.2 The $P \rightarrow \gamma\gamma$ Width

Only the VVP vertex and VMD are needed to describe the $V \rightarrow PP$ decays (see Figure 1b). Using (6.1) and (6.3), the reduced T-matrix for $P \rightarrow \gamma\gamma$ is

$$T_o(P^i_{\gamma\gamma}) = g_{Pi\gamma\gamma} \epsilon_{\mu\nu\rho\sigma} (p_m)^\mu (\epsilon_m)^\nu (p_n)^\rho (\epsilon_n)^\sigma, \quad (6.5)$$

where

$$g_{Pi\gamma\gamma} = \frac{2e^2}{g_\rho} g_{VV^*P}^{mni} \delta_{n\gamma} \delta_{m\gamma}.$$

The decay width is

$$\Gamma(P^i \rightarrow \gamma\gamma) = \frac{1}{64\pi} (g_{Pi\gamma\gamma})^2 M_i^3. \quad (6.6)$$

By comparing the structures of the $V \rightarrow P\gamma$ and $P \rightarrow \gamma\gamma$ amplitudes, an interesting relation is obtained:

$$g_{Pi\gamma\gamma} = \frac{e}{g_\rho} (g_{V3Pi_\gamma} + \frac{1}{\sqrt{3}} g_{V8Pi_\gamma}),$$

so that

$$g_{\pi i \gamma \gamma} = \frac{e}{g_\rho} (g_{\rho \pi i \gamma} + \frac{\sin \theta_V}{\sqrt{3}} g_{\omega \pi i \gamma} + \frac{\cos \theta_V}{\sqrt{3}} g_{\phi \pi i \gamma}). \quad (6.7)$$

This is a restatement of VMD.

From (6.7), it is expected that the previously encountered inconsistency between the measured $\rho \rightarrow \pi \gamma$ width and VMD should be reflected in the $\pi \rightarrow \gamma \gamma$ width. The experimental amplitudes for the $\rho \rightarrow \pi \gamma$, $\omega \rightarrow \pi \gamma$ and $\phi \rightarrow \pi \gamma$ along with $\theta_V = 35^\circ$ may be used in (6.7) to predict that $\pi \rightarrow \gamma \gamma$ decay amplitude. It is found that

$$\Gamma(\pi \rightarrow \gamma \gamma) = 4.7 \text{ eV or } 5.7 \text{ eV}, \quad (6.8)$$

depending on the relative phase of the $\phi \rightarrow \pi \gamma$ amplitude.

Experimentally [1],

$$\Gamma(\pi \rightarrow \gamma \gamma) = 7.85 \pm 0.54 \text{ eV}. \quad (6.9)$$

Clearly the measured values of $\Gamma(\rho \rightarrow \pi \gamma)$, $\Gamma(\omega \rightarrow \pi \gamma)$, $\Gamma(\phi \rightarrow \pi \gamma)$ and $\Gamma(\pi \rightarrow \gamma \gamma)$ are not consistent with $\theta_V = 35^\circ$. Adjusting θ_V to bring about consistency, $\theta_V = \pm 48^\circ$ or $\pm 55^\circ$ is obtained. Notice that this is quite a different solution for θ_V than was found in chapter V to make $\Gamma(\rho \rightarrow \pi \gamma)$ and $\Gamma(\omega \rightarrow \pi \gamma)$ mutually consistent. There is no value of θ_V that reconciles the measured $\rho \rightarrow \pi \gamma$ rate with other measured rates and VMD.

The relation (6.7) holds if $\Gamma(\rho \rightarrow \pi \gamma) \sim 90 \text{ KeV}$ and if $\theta_V \sim 38^\circ$. For both the SU(3) scheme with nonet symmetry breaking and the nonet scheme with SU(3) symmetry breaking,

$$g_{V3\pi\gamma} = \frac{1}{\sqrt{3}} g_{V8\pi\gamma}.$$

Hence,

$$g_{\pi\gamma\gamma} = \frac{2e}{g_\rho} g_{\rho\pi\gamma} \quad (6.10)$$

and

$$g_{\pi\gamma\gamma} = \frac{2e}{g_\rho} \frac{1}{\sqrt{3}} (\sin \theta_V g_{\omega\pi\gamma} + \cos \theta_V g_{\phi\pi\gamma}). \quad (6.11)$$

Using the experimental $\pi \rightarrow \gamma\gamma$, $\omega \rightarrow \pi\gamma$ and $\phi \rightarrow \pi\gamma$ rates in (6.10) and (6.11), it is found that $\Gamma(\rho \rightarrow \pi\gamma) \sim 90$ KeV and that $\theta_V = \pm 32^\circ$ or $\pm 38^\circ$. These schemes are expected to be most successful if θ_V is near its ideal value; furthermore, they are not expected to account for the observed $\rho \rightarrow \pi\gamma$ rate.

6.3 The $V \rightarrow PPP$ Width

As seen in Figure 1c, the two strong vertices, VVP and VPP, are needed to describe the $V \rightarrow PPP$ decay. The process $V^m \rightarrow P^i P^j P^k$ is considered to occur in two stages: $V^m \rightarrow V^n P^k$, followed by $V^n \rightarrow P^i P^j$; other permutations of (ijk) also occur. The reduced T-matrix is:

$$\begin{aligned} T_o(V^m P^i P^j P^k) = & 4g_{V^m V^n P^i} g_\rho f_{njk} \epsilon_{\mu\nu\rho\sigma} \frac{(\epsilon_m)^\mu (p_m)^\nu (p_j)^\rho (p_k)^\sigma}{(p_j + p_k)^2 - M_n^2} \\ & + 4g_{V^m V^n P^j} g_\rho f_{nik} \epsilon_{\mu\nu\rho\sigma} \frac{(\epsilon_m)^\mu (p_m)^\nu (p_i)^\rho (p_k)^\sigma}{(p_i + p_k)^2 - M_n^2} \\ & + 4g_{V^m V^n P^k} g_\rho f_{nji} \epsilon_{\mu\nu\rho\sigma} \frac{(\epsilon_m)^\mu (p_m)^\nu (p_j)^\rho (p_i)^\sigma}{(p_j + p_i)^2 - M_n^2}, \end{aligned} \quad (6.12)$$

where n , the index of the intermediate vector meson, is

summed over all possibilities.

The two decays to be discussed here are $\omega \rightarrow \pi^0 \pi^+ \pi^-$ and $\phi \rightarrow \pi^0 \pi^+ \pi^-$. For these cases, the intermediate vector meson is always ρ and (6.12) simplifies:

$$T_0(V^m_{\pi^0 \pi^+ \pi^-}) = 4g_{V\rho\pi} g_\rho \varepsilon_{\mu\nu\rho\sigma} (\varepsilon_m)^\mu (p_m)^\nu (p_+)^\rho (p_-)^\sigma \times \left(\frac{1}{(p_+ + p_-)^2 - M_\rho^2} + \frac{1}{(p_+ + p_0)^2 - M_\rho^2} + \frac{1}{(p_- + p_0)^2 - M_\rho^2} \right). \quad (6.13)$$

The decay width is:

$$\Gamma(V^m_{\pi^0 \pi^+ \pi^-}) = \frac{1}{(2\pi)^5} \frac{1}{3} (4 g_{V\rho\pi} g_\rho)^2 M_m^2 \times \int d^3 p_+ d^3 p_- d^3 p_0 \frac{\delta^4(p_m - p_0 - p_+ - p_-)}{16 M_m E_0 E_+ E_-} \times F F^* (\vec{p}_+ \times \vec{p}_-) \cdot (\vec{p}_+ \times \vec{p}_-), \quad (6.14)$$

where

$$F = \frac{1}{(p_+ + p_-)^2 - M_\rho^2 - i\Gamma_\rho M_\rho} + \frac{1}{(p_+ + p_0)^2 - M_\rho^2 - i\Gamma_\rho M_\rho} + \frac{1}{(p_- + p_0)^2 - M_\rho^2 - i\Gamma_\rho M_\rho}.$$

This modified ρ propagator is used in order to incorporate the finite ρ lifetime. The decay width is abbreviated

$$\Gamma(V^m_{\pi^0 \pi^+ \pi^-}) = \frac{1}{(2\pi)^5} \frac{1}{3} (g_{V\rho\pi} g_\rho) M_m \times X(V^m), \quad (6.15)$$

where the phase space integral is hidden in $X(V^m)$. When needed, this is evaluated numerically using a programme due

to Torgerson[38].

VMD relates the $V \rightarrow 3P$ and $V \rightarrow P\gamma$ rates in a simple fashion. From (6.4),

$$\begin{aligned} g_{\omega\pi\gamma} &= \frac{2e}{g_\rho} (g_{\omega\rho\pi} + \frac{1}{\sqrt{3}} g_{\omega V 8\pi}), \\ g_{\phi\pi\gamma} &= \frac{2e}{g_\rho} (g_{\phi\rho\pi} + \frac{1}{\sqrt{3}} g_{\phi V 8\pi}). \end{aligned} \quad (6.16)$$

In all the VVP schemes of interest, both g_{883} and g_{083} vanish. As a result, for all the schemes of interest,

$$\Gamma(\omega \rightarrow 3\pi) / \Gamma(\omega \rightarrow \pi\gamma) = \frac{1}{2\pi^4} \frac{g_\rho^4}{e^2} \frac{M_\omega^4}{(M_\omega^2 - M_\pi^2)^3} X(\omega) = 9.2, \quad (6.17)$$

and

$$\Gamma(\phi \rightarrow 3\pi) / \Gamma(\phi \rightarrow \pi\gamma) = \frac{1}{2\pi^4} \frac{g_\rho^4}{e^2} \frac{M_\phi^4}{(M_\phi^2 - M_\pi^2)^3} X(\phi) = 115. \quad (6.18)$$

The experimental ratios [1] agree with these theoretical ones to within 10%.

The $K^* \rightarrow K\pi\pi$ process may also be discussed using this $V \rightarrow PPP$ formalism. In [39], several VVP and $VP\gamma$ models are used to predict the rate of this decay. Not only does this rate appear to be large enough to measure, but it also seems quite sensitive to the details of the VVP or $VP\gamma$ model used. A measurement of this rate should provide a good test of the popular VVP and $VP\gamma$ models.

6.4 The $P \rightarrow PP\gamma$ Width

The $P \rightarrow PP\gamma$ decay (Figure 1d) uses VMD as well as both the VVP and VPP vertices. The $P^i \rightarrow P^j P^k \gamma$ process occurs in three steps: $P^i \rightarrow V^m V^n$, followed by $V^m \rightarrow P^j P^k$ and $V^n \rightarrow \gamma$;

permutations of (ijk) and (mn) also occur. The appropriate reduced T-matrix is:

$$\begin{aligned}
 T_o(P^i P^j P^k \gamma) = & 4e g_{V^m V^n P^i} f_{mjk} \delta_{n\gamma} \epsilon_{\mu\nu\rho\sigma} \frac{(\epsilon_n)^\mu (p_n)^\nu (p_j)^\rho (p_k)^\sigma}{(p_j+p_k)^2 - M_m^2} \\
 & + 4e g_{V^m V^n P^j} f_{mik} \delta_{n\gamma} \epsilon_{\mu\nu\rho\sigma} \frac{(\epsilon_n)^\mu (p_n)^\nu (p_i)^\rho (p_k)^\sigma}{(p_i+p_k)^2 - M_m^2} \\
 & + 4e g_{V^m V^n P^k} f_{mji} \delta_{n\gamma} \epsilon_{\mu\nu\rho\sigma} \frac{(\epsilon_n)^\mu (p_n)^\nu (p_j)^\rho (p_i)^\sigma}{(p_j+p_i)^2 - M_m^2}
 \end{aligned} \tag{6.19}$$

The two decays of interest are $\eta \rightarrow \pi^+ \pi^- \gamma$ and $\eta' \rightarrow \pi^+ \pi^- \gamma$. For these decays only the first term of (6.19) is active; ρ is the intermediate vector meson. The η decay width is:

$$\begin{aligned}
 \Gamma(\eta \rightarrow \pi^+ \pi^- \gamma) = & \frac{1}{(2\pi)^5} (4e g_{\rho V n \eta} \delta_{n\gamma}) M_\eta^2 \\
 & \times \int d^3 p_n d^3 p_+ d^3 p_- \frac{\delta^4(p_\eta - p_n - p_+ - p_-)}{16 M_\eta E_n E_+ E_-} \\
 & \times \frac{(\vec{p}_+ \times \vec{p}_-) \cdot (\vec{p}_+ \times \vec{p}_-)}{((p_+ + p_-)^2 - M_\rho^2)^2 + \Gamma_\rho^2 M_\rho^2} .
 \end{aligned} \tag{6.20}$$

A corresponding expression holds for the η' decay. Notice that the finite ρ lifetime is again included in the ρ propagator. This decay width is abbreviated

$$\Gamma(\eta \rightarrow \pi^+ \pi^- \gamma) = \frac{1}{(2\pi)^5} (e g_{\rho V n \eta} \delta_{n\gamma})^2 M_\eta Y(\eta) \tag{6.21}$$

where $Y(\eta)$ incorporates the phase space integral. When needed, Y is evaluated numerically using a programme due to Torgerson[38].

Since, from (6.4)

$$\begin{aligned} g_{\rho\eta\gamma} &= \frac{2e}{g_\rho} g_{\rho V\eta} \delta_{\eta\gamma}, \\ g_{\rho\eta'\gamma} &= \frac{2e}{g_\rho} g_{\rho V\eta'} \delta_{\eta\gamma}, \end{aligned} \quad (6.22)$$

it follows that

$$\begin{aligned} \Gamma(\eta \rightarrow \pi\pi\gamma) / \Gamma(\rho \rightarrow \eta\gamma) &= \frac{3g_\rho^2 M_\eta M_\rho^3 Y(\eta)}{4\pi^4 (M_\rho^2 - M_\eta^2)^3} = 0.0025, \\ \Gamma(\eta' \rightarrow \pi\pi\gamma) / \Gamma(\eta' \rightarrow \rho\gamma) &= \frac{g_\rho^2 M_\eta^4 Y(\eta')}{4\pi^4 (M_\eta'^2 - M_\rho^2)^3} = 0.9612. \end{aligned} \quad (6.23)$$

These ratios are predicted by all the models of interest. Only the first of these ratios may be compared with experiment. Using $\Gamma(\eta \rightarrow \pi\pi\gamma) = 0.0416 \pm 0.006$ KeV [1], $\Gamma(\rho \rightarrow \eta\gamma) \sim 17$ KeV is predicted--this is much lower than the recent results of Andrews, et al. [7] suggest.

6.5 The Predictions of the Models

The SU(3) VP_γ model with nonet breaking [15] and the nonet VP_γ model with SU(3) breaking are now used to predict a variety of decay rates. Besides the $V \rightarrow P\gamma$ and $P \rightarrow V\gamma$ rates already discussed, the rates of the following processes have been measured [1]: $\pi \rightarrow \gamma\gamma$, $\eta \rightarrow \gamma\gamma$, $\omega \rightarrow 3\pi$, $\phi \rightarrow 3\pi$ and $\eta \rightarrow \pi\pi\gamma$; the $\eta' \rightarrow \pi\pi\gamma$ partial width is also available [1]. In the following, the model parameters are fit to the measured rates of these nine

decays: $\omega \rightarrow \pi\gamma$, $K^{*0} \rightarrow K^0\gamma$, $\phi \rightarrow \pi\gamma$, $\phi \rightarrow \eta\gamma$, $\pi \rightarrow \gamma\gamma$, $\eta \rightarrow \gamma\gamma$, $\omega \rightarrow 3\pi$, $\phi \rightarrow 3\pi$ and $\eta \rightarrow \pi\pi\gamma$. In the weak nonet model, the fit also includes the lower of the possible $\omega \rightarrow \eta\gamma$ and $\rho \rightarrow \eta\gamma$ rates [7]. Since $\Gamma(\rho \rightarrow \pi\gamma) \sim 35$ KeV is known to be incompatible with all these models, no attempt is made to fit it.

The first three solutions of Table 9 use the SU(3) symmetry nonet symmetry breaking model of Boal, Graham and Moffat [15]. Solution 1 ($g = 0.681 \text{ GeV}^{-1}$, $f = 0.461 \text{ GeV}^{-1}$, $f' = 0.778 \text{ GeV}^{-1}$) uses $\theta_V = 35^\circ$ and $\theta_P = -10^\circ$; this is for comparison with solutions 4 and 5. Solution 2 ($g = 0.523 \text{ GeV}^{-1}$, $f = 0.747 \text{ GeV}^{-1}$, $f' = 0.951 \text{ GeV}^{-1}$) uses $\theta_V = 24^\circ$ and $\theta_P = -10^\circ$. Solution 3 ($g = 0.719 \text{ GeV}^{-1}$, $f = 0.182 \text{ GeV}^{-1}$, $f' = 0.761 \text{ GeV}^{-1}$) uses $\theta_V = 37^\circ$ and $\theta_P = -24^\circ$. These last solutions should be compared with those of Table 2. Of the three mixing angle possibilities, the ones with θ_V almost ideal work marginally better than the one with $\theta_V = 24^\circ$ -- this follows from the discussions of section (6.2). Even so, none of these models works well. $\Gamma(K^{*0} \rightarrow K^0\gamma)$, $\Gamma(\rho \rightarrow \pi\gamma)$ and $\Gamma(\phi \rightarrow \eta\gamma)$ are all high approaching their nonet values; meanwhile, $\Gamma(\pi \rightarrow \gamma\gamma)$ and $\Gamma(\eta \rightarrow \gamma\gamma)$ are low and $\Gamma(\eta \rightarrow \pi\pi\gamma)$ is much too high. The SU(3) model with nonet symmetry breaking loses its ability to account for the $V \rightarrow P\gamma$ rates when faced with the other hadronic and radiative decays.

The last two solutions use nonet symmetry models with Boson symmetry and SU(3) symmetry breaking. Solution 4 ($f_0 = 0.592 \text{ GeV}^{-1}$, $f_4 = 0.438 \text{ GeV}^{-1}$, $f_6 = -0.311 \text{ GeV}^{-1}$, $f_7 = -0.055 \text{ GeV}^{-1}$) uses strong nonet symmetry; solution 5

TABLE 9
Predictions[†] of Meson Decay Rates in
Two Types of Symmetry Breaking Models

Decay Mode	Soln 1	Soln 2	Soln 3	Soln 4	Soln 5	Experiment
$\omega \rightarrow \pi\gamma$	(810)	(1000)	(810)	(960)	(960)	880 ± 60 [1]
$K^{*0} \rightarrow K^0\gamma$	(160)	(93)	(180)	(90)	(69)	75 ± 35 [1]
$\rho \rightarrow \pi\gamma$	71	42	79	85	86	35 ± 10 [1]
$\phi \rightarrow \pi\gamma$	(6.0)	(5.4)	(6.0)	(5.7)	(5.8)	5.7 ± 21 [1]
$\phi \rightarrow \eta\gamma$	(160)	(99)	(150)	(68)	(63)	64 ± 10 [1,7]
$\omega \rightarrow \eta\gamma$	7.5	27	4.8	0.71	(1.6)	$3.0^{+2.5}_{-1.8}$ or 29 ± 7 [7]
$K^{*+} \rightarrow K^+\gamma$	39	23	43	190*	130*	< 80 [3]
$\rho \rightarrow \eta\gamma$	37	29	35	16	(20)	50 ± 13 or 76 ± 15 [7]
$\eta' \rightarrow \omega\gamma$	2.8	2.2	0.035	12	45	< 50 [1]
$\eta' \rightarrow \rho\gamma$	35	120	0.41	160	290	< 300 [1]
$\phi \rightarrow \eta'\gamma$	0.35	0.83	0.30	0.053	0.35	--
$\pi \rightarrow \gamma\gamma$	(0.0061)	(0.0036)	(0.0069)	(0.0072)	(0.0073)	0.00785 ± 0.00054 [1]
$\eta \rightarrow \gamma\gamma$	(0.24)	(0.24)	(0.23)	(0.36)	(0.32)	0.323 ± 0.046 [1]
$\eta' \rightarrow \gamma\gamma$	2.2	6.3	0.050	6.2	8.3	< 20 [1]
$\omega \rightarrow 3\pi$	(7500)	(9300)	(7500)	(8900)	(8900)	9000 ± 400 [1]
$\phi \rightarrow 3\pi$	(690)	(620)	(690)	(660)	(660)	670 ± 70 [1]
$\eta \rightarrow \pi\pi\gamma$	(0.091)	(0.072)	(0.086)	(0.039)	(0.049)	0.0416 ± 0.006 [1]
$\eta' \rightarrow \pi\pi\gamma$	34	110	0.40	160	280	--
$\Gamma(\eta' \rightarrow \rho\gamma) / \Gamma(\eta' \rightarrow \omega\gamma)$	13	54	12	13	6.5	9.9 ± 2.0 [8]
$\Gamma(\eta' \rightarrow \gamma\gamma) / \Gamma(\eta' \rightarrow \rho\gamma)$	0.062	0.055	0.12	0.038	0.029	0.066 ± 0.011 [1]

[†] All rates in KeV.

* May be adjusted by appropriate choice of f_3 .

$(f_0 = 0.551 \text{ GeV}^{-1}, f_4 = 0.285 \text{ GeV}^{-1}, f_6 = -0.240 \text{ GeV}^{-1},$
 $f_7 = 0.021 \text{ GeV}^{-1}, f_9 = 0.567 \text{ GeV}^{-1}, f_{10} = 0.186 \text{ GeV}^{-1})$
 use weak nonet symmetry-- $\theta_V = 35^\circ$ and $\theta_P = -10^\circ$ are used
 in both cases. These solutions should be compared with
 those of Tables 7 and 8. Both models can account for the
 nine input rates. As expected, in both cases $\Gamma(\rho \rightarrow \pi\gamma) \sim 90$
 KeV. In the strong nonet model, $\Gamma(\omega \rightarrow \eta\gamma)$ and $\Gamma(\rho \rightarrow \eta\gamma)$ are
 predicted lower than measured [7]. This time when the strong
 nonet symmetry is loosened to weak nonet symmetry, good
 agreement is not achieved for $\Gamma(\rho \rightarrow \eta\gamma)$ --according to (6.23),
 $\Gamma(\rho \rightarrow \eta\gamma)$ can not be as high as measured if $\Gamma(\eta \rightarrow \pi\pi\gamma)$ is to
 remain at its measured value. Problems also occur among
 the η' partial widths.

Of the two principle explanations of the $V \rightarrow P\gamma$ decays,
 SU(3) symmetry with nonet symmetry breaking and nonet
 symmetry with SU(3) symmetry breaking, only the latter
 survives extension to other types of decays. While previously
 encountered problems with $\Gamma(\rho \rightarrow \pi\gamma)$ and the η and η' radiative
 decay rates persist, no new problems appear for the SU(3)
 symmetry breaking scheme in the treatment of the $P \rightarrow \gamma\gamma$,
 $V \rightarrow PPP$ and $P \rightarrow PP\gamma$ decay rates.

CHAPTER VII

RADIATIVE DECAYS IN AN SU(4) SCHEME

7.1 The Advent of SU(4)

The existence of a fourth quark, c , provides the simplest explanation for the narrow width of the $\psi(3100) 1^{--}$ particle. If ψ is a pure $c\bar{c}$ meson, the OZI rule, applied now to four quarks, requires that ψ should decay very slowly, if at all, into particles constructed from the u , d and s quarks. An SU(4) classification scheme is lent further credibility by the observation of particles with naked charm [40].

Several radiative decay modes of ψ have been observed. Rates are now known [19] for the decays $\psi \rightarrow \pi\gamma$, $\psi \rightarrow \eta\gamma$ and $\psi \rightarrow \eta'\gamma$. According to the OZI rule, all these processes should be totally suppressed. Assuming that the recently confirmed [41] spin zero charmonium state at around 2.8 GeV is the $T = 0$, $Y = 0$, $C = 0$ $c\bar{c} 0^{-+}$ meson η_c , the decay $\psi \rightarrow \eta_c \gamma$ is expected to proceed vigorously; instead, experiment [20] suggests that $\Gamma(\psi \rightarrow \eta_c \gamma) < 3.5 \text{ KeV}$. While the first three decay rates might be explained by a small admixture of $u\bar{u}/d\bar{d}/s\bar{s}$ quark content into ψ [42], the extreme suppression of $\psi \rightarrow \eta_c \gamma$ requires a more drastic solution. One suggestion has been the use of multiplet mixing [43]. Another possibility is that of symmetry breaking. In this chapter an SU(3) symmetry breaking scheme is

extended to SU(4) in the hope of explaining the radiative decays of ψ as well as the SU(3) radiative decays discussed earlier.

Other radiative decays of interest within the context of SU(4) include $D^{*0} \rightarrow D^0 \gamma$, $D^{*+} \rightarrow D^+ \gamma$ and $F^{*+} \rightarrow F^+ \gamma$. Because the charmed vector mesons have such low masses, π and γ emissions are the principle decay modes of these mesons.

7.2 The SU(4) Particle Classification

The vector and pseudoscalar mesons are assigned to the two $4 \otimes \bar{4}$ multiplets--a 15-plet and a singlet. Similar to the SU(3) case, the $T = 0$, $Y = 0$, $C = 0$ mesons are mixtures of the 15-plet and the singlet.

The vector mesons have the following SU(4) content:

$$\begin{aligned}
 |\rho^+ \rangle &= |\rho^- \rangle^\dagger = \frac{1}{\sqrt{2}} (|1\rangle - i|2\rangle) \\
 |\rho^0 \rangle &= |3\rangle \\
 |K^{*+} \rangle &= |K^{*-} \rangle^\dagger = \frac{1}{\sqrt{2}} (|4\rangle - i|5\rangle) \\
 |K^{*0} \rangle &= |\overline{K}^{*0} \rangle^\dagger = \frac{1}{\sqrt{2}} (|6\rangle - i|7\rangle) \\
 |D^{*0} \rangle &= |\overline{D}^{*0} \rangle^\dagger = \frac{1}{\sqrt{2}} (|9\rangle + i|10\rangle) \\
 |D^{*+} \rangle &= |D^{*-} \rangle^\dagger = \frac{1}{\sqrt{2}} (|11\rangle + i|12\rangle) \\
 |F^{*+} \rangle &= |F^{*-} \rangle^\dagger = \frac{1}{\sqrt{2}} (|13\rangle + i|14\rangle)
 \end{aligned} \tag{7.1}$$

The $T = 0$, $Y = 0$, $C = 0$ mesons are ω , ϕ and ψ and are assumed to be ideal mixtures of the singlet and the 8-th and 15-th

member of the 15-plet:

$$\begin{aligned}
 |\omega\rangle &= \frac{1}{\sqrt{3}} |8\rangle + \frac{1}{\sqrt{6}} |15\rangle + \frac{1}{\sqrt{2}} |0\rangle \\
 |\phi\rangle &= -\frac{\sqrt{2}}{3} |8\rangle + \frac{1}{\sqrt{12}} |15\rangle + \frac{1}{2} |0\rangle \\
 |\psi\rangle &= -\frac{\sqrt{3}}{2} |15\rangle + \frac{1}{2} |0\rangle.
 \end{aligned} \tag{7.2}$$

As a result of ideal mixing, these mesons have the following pure quark content:

$$\begin{aligned}
 |\omega\rangle &= \frac{1}{\sqrt{2}} (u\bar{u} + d\bar{d}) \\
 |\phi\rangle &= s\bar{s} \\
 |\psi\rangle &= c\bar{c}.
 \end{aligned}$$

Here ϕ is given the opposite phase from its SU(3) assignment; the SU(4) structure constants are, however, consistent with this choice of phase.

The pseudoscalar mesons are similarly assigned to the 15-plet and singlet:

$$\begin{aligned}
 |\pi^+\rangle &= |\pi^-\rangle^\dagger = \frac{1}{\sqrt{2}} (|1\rangle - i|2\rangle) \\
 |\pi^0\rangle &= |3\rangle \\
 |K^+\rangle &= |K^-\rangle^\dagger = \frac{1}{\sqrt{2}} (|4\rangle - i|5\rangle) \\
 |K^0\rangle &= |\bar{K}^0\rangle^\dagger = \frac{1}{\sqrt{2}} (|6\rangle - i|7\rangle) \\
 |D^0\rangle &= |\bar{D}^0\rangle^\dagger = \frac{1}{\sqrt{2}} (|9\rangle + i|10\rangle) \\
 |D^+\rangle &= |D^-\rangle^\dagger = \frac{1}{\sqrt{2}} (|11\rangle + i|12\rangle)
 \end{aligned}$$

$$|F^+\rangle = |F^-\rangle^\dagger = \frac{1}{\sqrt{2}} (|13\rangle + i|14\rangle). \quad (7.3)$$

The $T = 0$, $Y = 0$, $C = 0$ pseudoscalars with ideal mixing are

$$\begin{aligned} |\eta_\sigma\rangle &= \frac{1}{\sqrt{3}} |8\rangle + \frac{1}{\sqrt{6}} |15\rangle + \frac{1}{\sqrt{2}} |0\rangle \\ |\eta_s\rangle &= -\sqrt{\frac{2}{3}} |8\rangle + \frac{1}{\sqrt{12}} |15\rangle + \frac{1}{2} |0\rangle \\ |\eta_c\rangle &= -\frac{\sqrt{3}}{2} |15\rangle + \frac{1}{2} |0\rangle. \end{aligned} \quad (7.4)$$

Giving η and η' the same quark content as in $SU(3)$,

$$\begin{aligned} |\eta\rangle &= \sin(\theta_I - \theta_P) |\eta_\sigma\rangle - \cos(\theta_I - \theta_P) |\eta_s\rangle \\ |\eta'\rangle &= \cos(\theta_I - \theta_P) |\eta_\sigma\rangle + \sin(\theta_I - \theta_P) |\eta_s\rangle, \end{aligned} \quad (7.5)$$

where $\theta_I = \tan^{-1}(1/\sqrt{2}) \sim 35^\circ$. Using $\theta_P \sim -10^\circ$, η and η' are observed to have almost equal $u\bar{u}/d\bar{d}$ and $s\bar{s}$ quark content.

The electromagnetic current is assumed to be a specific mixture of a 15-plet and a singlet of vector currents:

$$J_\mu^{\text{em}} = J_\mu^3 + \frac{1}{\sqrt{3}} J_\mu^8 - \sqrt{\frac{2}{3}} J_\mu^{15} + \frac{\sqrt{2}}{3} J_\mu^0. \quad (7.6)$$

The $SU(4)$ content of the photon is

$$|\gamma\rangle = |3\rangle + \frac{1}{\sqrt{3}} |8\rangle - \sqrt{\frac{2}{3}} |15\rangle + \frac{\sqrt{2}}{3} |0\rangle. \quad (7.7)$$

Other proposed forms of J_μ^{em} are discussed in Appendix II.

7.3 The Radiative Decay Scheme

All the concepts introduced in the context of $SU(3)$ have their $SU(4)$ analogues. The formulation of symmetry

breaking, the OZI rule and VMD are now discussed. A symmetry breaking scheme for radiative decays is then developed--this scheme is a natural extension of the most general strong nonet and Boson symmetry SU(3) scheme with λ_8 symmetry breaking.

In SU(4) three $T = 0$, $Y = 0$, $C = 0$ scalar spurions exist: U_8 , U_{15} and U_0 . A symmetry breaking scheme in which charge, isospin, strangeness and charm are conserved must necessarily employ symmetry breaking by only λ_8 , λ_{15} and λ_0 . For reasons to become evident, λ_8 or λ_{15} breaking is called SU(4) breaking and λ_0 breaking is called 16-plet breaking.

The OZI rule is easily extended to include diagrams drawn with four quarks. As in SU(3), this rule forbids terms in the interaction Lagrangian which involve the trace over the internal symmetry index of an individual particle. The OZI rule thus requires that the 15-plet and the singlet be treated in the same way--this is 16-plet symmetry. A model with symmetry breaking may demonstrate either weak or strong 16-plet symmetry--the former if only the SU(4) invariant terms obey the OZI rule; the latter if all terms obey the OZI rule. As in SU(3), λ_0 symmetry breaking terms are equivalent to OZI violations. They are not allowed in an SU(4) scheme with 16-plet symmetry.

VMD is extended to SU(4) by allowing ψ as well as ρ , ω and ϕ to intermediate a radiative decay. The VMD Lagrangian is:

$$\lambda_{V^{\mathbf{n}}\gamma} = \frac{e}{g_\rho} M_m^2 (\delta_{\mathbf{n}3} + \frac{1}{\sqrt{3}} \delta_{\mathbf{n}8} - \sqrt{\frac{2}{3}} \delta_{\mathbf{n}15} + \frac{\sqrt{2}}{3} \delta_{\mathbf{n}0}). \quad (7.8)$$

An SU(4) VVP model and VMD may be used to derive a model for $V \rightarrow P\gamma$ radiative decays. As in SU(3), a $V \rightarrow P\gamma$ scheme so obtained has a decay amplitude which is symmetric in the vector and photon indices.

The most general strong 16-plet and Boson symmetric radiative decay model which uses λ_8 and λ_{15} symmetry breaking has nine SU(4) invariant coupling constants. These accompany one SU(4) invariant term, four terms which transform as λ_8 and four terms which transform as λ_{15} . The radiative decay widths are

$$\begin{aligned} \Gamma(V^{\mathbf{m}} \rightarrow P^{\mathbf{i}} \gamma) &= \frac{1}{96\pi} (g_{\min})^2 \left(\frac{M_m^2 - M_i^2}{M_m} \right)^3, \\ \Gamma(P^{\mathbf{i}} \rightarrow V^{\mathbf{m}} \gamma) &= \frac{1}{32\pi} (g_{\min})^2 \left(\frac{M_i^2 - M_m^2}{M_i} \right)^3, \end{aligned} \quad (7.9)$$

where

$$\begin{aligned} g_{\min} &= g_0 d_{\min} \\ &+ g_1 d_{8ik} d_{kmn} + g_2 (d_{8mk} d_{kin} + d_{8nk} d_{kim}) \\ &+ g_3 \delta_{8i} \delta_{mn} + g_4 (\delta_{8m} \delta_{in} + \delta_{8n} \delta_{im}) \\ &+ g_5 d_{15ik} d_{kmn} + g_6 (d_{15mk} d_{kin} + d_{15nk} d_{kim}) \\ &+ g_7 \delta_{15i} \delta_{mn} + g_8 (\delta_{15m} \delta_{in} + \delta_{15n} \delta_{im}), \end{aligned} \quad (7.10)$$

where n is the photon index; k is summed from 0 to 15.

In the next section this model is used to predict

rates of the type $V \rightarrow P\gamma$ and $P \rightarrow V\gamma$. In the following section VMD is used as well to discuss $V \rightarrow VP$ and $P \rightarrow 2\gamma$ rates.

7.4 The Predictions of the Model

The measured radiative decay widths are now used to fit the parameters of this SU(4) symmetry breaking model. Because all these rates are not independent, only seven of the nine parameters may be determined; as a result, some ambiguity remains in the predictions of the $K^{*+} \rightarrow K^+\gamma$, $D^{*+} \rightarrow D^+\gamma$ and $F^{*+} \rightarrow F^+\gamma$ rates.

The following identities hold for $\psi \rightarrow \pi\gamma$, $\psi \rightarrow \eta\gamma$, $\psi \rightarrow \eta'\gamma$ and all the SU(3) radiative decays except $K^{*+} \rightarrow K^+\gamma$:

$$2 d_{8ik} d_{kmn} = d_{8nk} d_{kim} + d_{8mk} d_{kin}, \quad (7.11)$$

$$2 d_{15ik} d_{kmn} = d_{15nk} d_{kim} + d_{15mk} d_{kin}, \quad (7.12)$$

and

$$d_{\min} = \sqrt{6} d_{15ik} d_{kmn}. \quad (7.13)$$

As a result, a fit to these rates yields values for these coupling constant combinations: $g_0 + \frac{1}{\sqrt{6}} (g_5 + 2g_6)$, $(g_1 + 2g_2)$, g_3 , g_4 , g_7 and g_8 . For $\psi \rightarrow \eta_c \gamma$ and $D^{*0} \rightarrow D^0 \gamma$, (7.11) and (7.12) hold but (7.13) does not. If either of these decays is considered, g_0 and $(g_5 + 2g_6)$ may be separately determined. In order to predict $\Gamma(K^{*+} \rightarrow K^+\gamma)$, separate knowledge of g_2 is needed; for $\Gamma(D^{*+} \rightarrow D^+\gamma)$ and $\Gamma(F^{*+} \rightarrow F^+\gamma)$, both g_2 and g_6 are needed.

In the fit presented in Table 10, the measured rates

TABLE 10

Predictions of Radiative Decay Widths in
the SU(4) Symmetry Breaking Model

Decay Mode	Model	Experiment
$\omega \rightarrow \pi\gamma$	(870)	880 ± 60 [1]
$K^{*0} \rightarrow K^0\gamma$	(100)	75 ± 35 [1]
$\rho \rightarrow \pi\gamma$	78	35 ± 10 [1]
$\phi \rightarrow \pi\gamma$	(5.9)	5.7 ± 2.1 [1]
$\phi \rightarrow \eta\gamma$	(63)	64 ± 10 [1,7]
$\omega \rightarrow \eta\gamma$	4.9	$3.0^{+2.5}_{-1.8}$ or 29 ± 7 [7]
$K^{*+} \rightarrow K^+\gamma$	21*	<80 [3]
$\rho \rightarrow \eta\gamma$	58	50 ± 13 or 76 ± 15 [7]
$\eta' \rightarrow \omega\gamma$	6.5	<50 [1]
$\eta' \rightarrow \rho\gamma$	130	<300 [1]
$\phi \rightarrow \eta'\gamma$	0.24	--
$\psi \rightarrow \pi\gamma$	(0.005)	0.005 ± 0.0032 [19]
$\phi \rightarrow \eta\gamma$	(0.055)	0.055 ± 0.012 [19]
$\psi \rightarrow \eta'\gamma$	(0.150)	0.152 ± 0.117 [19]
$\psi \rightarrow \eta_c\gamma$	0^{++}	<3.5 [20]
$D^{*0} \rightarrow D^0\gamma$	18^{++}	--
$D^{*+} \rightarrow D^+\gamma$	0.76^{++**}	--
$F^{*+} \rightarrow F^+\gamma$	0.09^{++**}	--
$\Gamma(\eta' \rightarrow \rho\gamma) / \Gamma(\eta' \rightarrow \omega\gamma)$	20	9.9 ± 2.0 [8]

† All rates in KeV.

†† $(g_5 + 2g_6)$ was chosen to suppress $\psi \rightarrow \eta_c\gamma$

* $g_2 = 0$

** $g_2 = g_6 = 0$

for $\omega \rightarrow \pi\gamma$, $K^{*0} \rightarrow K^0\gamma$, $\phi \rightarrow \pi\gamma$, $\phi \rightarrow \eta\gamma$, $\psi \rightarrow \pi\gamma$, $\psi \rightarrow \eta\gamma$ and $\psi \rightarrow \eta'\gamma$ are used to determine $g_0 + \frac{1}{\sqrt{6}}(g_5 + 2g_6)$, $(g_1 + 2g_2)$, g_3 , g_4 , g_7 and g_8 . Then $(g_5 + 2g_6)$ is chosen to completely suppress $\psi \rightarrow \eta_c\gamma$. The resulting coupling constants are $g_0 = 0.503 \text{ GeV}^{-1}$, $g_1 + 2g_2 = 0.248 \text{ GeV}^{-1}$, $g_3 = -0.001 \text{ GeV}^{-1}$, $g_4 = -0.052 \text{ GeV}^{-1}$, $g_5 + 2g_6 = 0.391 \text{ GeV}^{-1}$, $g_7 = 0.003 \text{ GeV}^{-1}$ and $g_8 = -0.0003 \text{ GeV}^{-1}$. The three ambiguous rates are predicted with $g_2 = g_6 = 0$.

This model gives reasonable predictions for all the input rates. The $K^{*0} \rightarrow K^0\gamma$ rate is a little high but still within experimental bounds. That all the three ψ rates are reproduced reflects the fact that they depend on independent combinations of g_3 , g_7 and g_8 ; in particular, $\Gamma(\psi \rightarrow \pi\gamma)$ depends on g_8 alone. That the model predicts $\Gamma(\rho \rightarrow \pi\gamma) \sim 80 \text{ KeV}$ is not suprising--the experimental rate is not compatible with the measured $\omega \rightarrow \pi\gamma$ rate and Boson symmetry. The predictions of $\Gamma(\omega \rightarrow \eta\gamma)$ and $\Gamma(\rho \rightarrow \eta\gamma)$ are in reasonable agreement with the recent measurements of Andrews, et al. [7]; the η' partial widths, however, are not in accord with the measurements of Zanfino, et al. [8]. The predicted $\eta_c \rightarrow \phi\gamma$ and $\eta_c \rightarrow \omega\gamma$ widths suggest that η_c is much broader than ψ . That substantial symmetry breaking is in effect is visible through the D^* radiative decay predictions--in a 16-plet scheme with no symmetry breaking, $\Gamma(\omega \rightarrow \pi\gamma) \sim 880 \text{ KeV}$ would require $\Gamma(D^{*0} \rightarrow D^0\gamma) \sim 70 \text{ KeV}$ and $\Gamma(D^{*+} \rightarrow D^+\gamma) \sim 4 \text{ KeV}$.

If instead of totally suppressing $\psi \rightarrow \eta_c\gamma$, $(g_5 + 2g_6)$ were chosen to satisfy the bound $\Gamma(\psi \rightarrow \eta_c\gamma) < 3.5 \text{ KeV}$ [20],

the charmed meson decay rates of Table 10 would change.

These bounds would be obtained:

$$15 \text{ KeV} < \Gamma(D^{*0} \rightarrow D^0 \gamma) < 21 \text{ KeV},$$

$$0.61 \text{ KeV} < \Gamma(D^{*+} \rightarrow D^+ \gamma) < 0.92 \text{ KeV},$$

$$0.04 \text{ KeV} < \Gamma(F^{*+} \rightarrow F^+ \gamma) < 0.15 \text{ KeV}.$$

Of course, the last two rates may still be adjusted using g_2 and g_6 .

7.5 Other Decays

In this section, $V \rightarrow VP$, $P \rightarrow \gamma\gamma$ and $V \rightarrow e^+e^-$ decays are discussed within the context of the SU(4) version of VMD.

The VVP Lagrangian which, with the help of VMD, leads to the $VP\gamma$ decay width (7.9) is:

$$\mathcal{L}_{VVP}^{m,n,p,i} = \frac{g_\rho}{2e} g_{\min} \varepsilon_{\mu\nu\rho\sigma} (p_m)^\mu (\varepsilon_m)^\nu (p_n)^\rho (\varepsilon_n)^\sigma, \quad (7.14)$$

where g_{\min} is given in (7.10). The $V^m \rightarrow V^n P^i$ decay width is

$$\Gamma(V^m \rightarrow V^n P^i) = \frac{1}{96\pi} \left(\frac{g_\rho}{e} g_{\min} \right)^2 \frac{[(M_m^2 - M_i^2)^2 + M_n^4 - 2M_n^2(M_m^2 + M_i^2)]^{3/2}}{M_m^3}. \quad (7.15)$$

Several decays of the type $\psi \rightarrow VP$ have been measured [20]; these include $\psi \rightarrow \rho\pi$, $\psi \rightarrow K^* \bar{K}$, $\psi \rightarrow \phi\eta$ and $\psi \rightarrow \phi\eta'$. While all these processes are OZI forbidden, they may proceed through the g_8 symmetry breaking term. In Table 11 are listed the predictions of (7.15) for several ratios of these rates; the experimental ratios are also presented. Notice that $\Gamma(\psi \rightarrow \rho\pi)$

TABLE 11

Ratios of $\psi \rightarrow VP$ Widths

Ratio	Model	Experiment [20]
$\Gamma(\psi \rightarrow K^* \bar{K}, \text{ all})$	1.1	1.1 ± 0.2
$\Gamma(\psi \rightarrow \rho \pi, \text{ all})$		
$\frac{\Gamma(\psi \rightarrow \phi \eta)}{\Gamma(\psi \rightarrow \rho \pi, \text{ all})}$	0.13	0.064 ± 0.038
$\frac{\Gamma(\psi \rightarrow \phi \eta')}{\Gamma(\psi \rightarrow \rho \pi, \text{ all})}$	0.093	0.045 ± 0.037

and $\Gamma(\psi \rightarrow K^* \bar{K})$ are mutually consistent, as are $\Gamma(\psi \rightarrow \phi \eta)$ and $\Gamma(\psi \rightarrow \phi \eta')$; however $\Gamma(\psi \rightarrow \phi \eta) / \Gamma(\psi \rightarrow \rho \pi)$ appears off by a factor of about two.

The absolute scale of the $V \rightarrow VP$ widths is also set by (7.15). From (7.9) and (7.15):

$$\Gamma(\psi \rightarrow \pi \gamma) = \frac{e^2}{g_\rho^2} \frac{(M_\psi^2 - M_\pi^2)^3}{(M_\psi^2 - M_\pi^2)^2 + M_\rho^4 - 2M_\rho^2 (M_\psi^2 + M_\pi^2)}^{3/2} \Gamma(\psi \rightarrow \rho^0 \pi^0). \quad (7.13)$$

Using the experimental value [20], $\Gamma(\psi \rightarrow \rho \pi, \text{all}) = 0.76 \pm 0.19$ KeV, VMD predicts that

$$\Gamma(\psi \rightarrow \pi \gamma) = 0.78 \text{ eV}. \quad (7.16)$$

This is considerably lower than the measured rate [19]:

$$\Gamma(\psi \rightarrow \pi \gamma) = 5.0 \pm 3.2 \text{ eV}. \quad (7.17)$$

The $P \rightarrow \gamma \gamma$ decays may also be studied using (7.8) - (7.10). The $P \rightarrow \gamma \gamma$ decay width is

$$\Gamma(P^i \rightarrow \gamma \gamma) = \frac{1}{64\pi} \left(\frac{e}{g_\rho} g_{\min} \right)^2 M_i^3. \quad (7.18)$$

Using the coupling constants of Table 10, the following predictions are made: $\Gamma(\pi \rightarrow 2\gamma) = 7.04 \text{ eV}$, $\Gamma(\eta \rightarrow 2\gamma) = 0.56 \text{ KeV}$, $\Gamma(\eta' \rightarrow 2\gamma) = 5.72 \text{ KeV}$ and $\Gamma(\eta_c \rightarrow \gamma \gamma) = 280 \text{ eV}$. The last rate is quoted for $\Gamma(\psi \rightarrow \eta_c \gamma) = 0$; the bound $\Gamma(\psi \rightarrow \eta_c \gamma) < 3.5 \text{ KeV}$ implies $\Gamma(\eta_c \rightarrow \gamma \gamma) < 3.7 \text{ KeV}$. That the $\eta \rightarrow 2\gamma$ width is a little wide is not alarming--a fit to all $V \rightarrow P\gamma$ and $P \rightarrow 2\gamma$ data would improve this rate without substantially altering the $V \rightarrow P\gamma$ predictions.

The VMD vertex alone is needed to describe $V^m \rightarrow e^+ e^-$.

Since this process occurs via an intermediate photon, $V^m \rightarrow \gamma \rightarrow e^+ e^-$, the amplitude of this process is proportional to $\delta_{m\gamma}$. It is expected that

$$\Gamma(\rho \rightarrow e^+ e^-) : \Gamma(\omega \rightarrow e^+ e^-) : \Gamma(\phi \rightarrow e^+ e^-) : \Gamma(\psi \rightarrow e^+ e^-) \sim 9:1:2:8, \quad (7.19)$$

While experimentally the ratio is seen to be $\sim 9:1:2:2$. Unless the electromagnetic current has a strong q^2 dependence not indicated in (7.6)-(7.7), VMD seems to fail.

The predictions of the $VP\gamma$ model and VMD seem to be only moderately consistent with experiment. The ratio of $V \rightarrow VP$ rates are very sensitive to the $VP\gamma$ symmetry breaking structure so the problem in this quarter may not be simply a result of VMD. At such energies as are needed to produce ψ , higher vector multiplets, whose membership includes $\rho'(1600)$, are also available to intermediate a radiative decay--perhaps (7.8) is a naive expression of VMD. In the context of $SU(4)$ it is not clear whether VMD works poorly, as the $\Gamma(\psi \rightarrow e^+ e^-)$ prediction suggests, or whether other complications arise to cloud the issues.

7.6 Conclusions

The strong 16-plet and Boson symmetric $SU(4)$ $V \rightarrow P\gamma$ model with λ_8 and λ_{15} symmetry breaking seems to work as well as the $SU(3)$ counterpart. The rate predictions for the $SU(3)$ processes are quite comparable to those of Table 7, solutions 3 and 4. As before, the measured $\rho \rightarrow \pi\gamma$ rate is incompatible with VMD. The model is also able to account

for the measured $\psi \rightarrow \pi\gamma$, $\psi \rightarrow \eta\gamma$ and $\psi \rightarrow \eta'\gamma$ rates. Large¹ symmetry breaking is needed to suppress the OZI allowed $\psi \rightarrow \eta_c\gamma$ decay. Some ambiguity is still present in the $K^{*+} \rightarrow K^+\gamma$, $D^{*+} \rightarrow D^+\gamma$ and $F^{*+} \rightarrow F^+\gamma$ rates, for both g_2 and g_6 remain to be specified.

The success of this $V \rightarrow P\gamma$ model used together with VMD is more difficult to judge. Some ratios among the $\psi \rightarrow VP$ rates agree with measurements, some are off by a factor of two. The $\Gamma(\psi \rightarrow \pi\gamma) : \Gamma(\psi \rightarrow \rho\pi)$ ratio is low and the $P \rightarrow \gamma\gamma$ widths are just in moderate agreement with experiment. The real problem with VMD appears in the prediction of $\Gamma(\psi \rightarrow e^+e^-)$.

While this SU(4) symmetry breaking scheme provides a good description for the observed $V \rightarrow P\gamma$ decays, the use of this model with VMD requires more investigation. In fact, the use of VMD itself in the context of SU(4) must be studied further.

CHAPTER VIII

CONCLUSIONS

8.1 The SU(3) $V \rightarrow P\gamma$ and $P \rightarrow V\gamma$ Decays

A wide variety of radiative decay models has been presented in this thesis. For the most part it was the SU(3) symmetry structure that was the topic of concern; however, the mixing angle choice and the Boson symmetry structure of the model were also discussed on occasion. While no model was able to explain all the experimental data, some did prove to be remarkably successful and physically reasonable.

Four models were presented that accounted for all five of the more-or-less established rates, $\Gamma(\omega \rightarrow \pi\gamma)$, $\Gamma(K^{*\circ} \rightarrow K^0\gamma)$, $\Gamma(\rho \rightarrow \pi\gamma)$, $\Gamma(\phi \rightarrow \pi\gamma)$ and $\Gamma(\phi \rightarrow \eta\gamma)$. The first was the SU(3) symmetry model with nonet symmetry breaking [15], solution 1 Table 2; nonideal vector mixing was used, $\theta_V = 24^\circ$. The other models were models with nonet symmetry and SU(3) symmetry breaking. The strong nonet symmetry model with Boson symmetry and $\theta_V = 24^\circ$, solution 1 Table 8, accounted for all five rates. So did the strong and weak nonet symmetry models with no Boson symmetry and standard mixing angles, solutions 2 and 5 Table 8.

Two models could account for all the established rates except $\Gamma(\rho \rightarrow \pi\gamma) \sim 35$ KeV. Given the dispute [14,4] over this rate, models which predict $\Gamma(\rho \rightarrow \pi\gamma) \sim 80$ KeV should

not be rejected yet. The strong and weak nonet symmetry models with SU(3) symmetry breaking, Boson symmetry and standard mixing, solution 3 Table 7 and solution 4 Table 8 respectively, reproduced all the five established rates except for $\Gamma(\rho \rightarrow \pi\gamma)$ which was predicted near its VMD value. The current algebra model, solution 4 Table 6, with its multiple SU(3) breaking was able to account for $\Gamma(\omega \rightarrow \pi\gamma)$, $\Gamma(K^{*0} \rightarrow K^0\gamma)$ and $\Gamma(\phi \rightarrow \eta\gamma)$. As mentioned at the time, a slight adjustment of θ_V could produce the desired $\phi \rightarrow \pi\gamma$ rate and not appreciably alter the other rates.

At this point, two facts have become apparent. First, substantial¹ symmetry breaking, either SU(3) or nonet symmetry breaking, is needed to explain the observed $V \rightarrow P\gamma$ decay rates. Second, only two of $\Gamma(\rho \rightarrow \pi\gamma) \sim 35$ KeV, $\theta_V = 35^\circ$ and Boson symmetry are possible. If the $VP\gamma$ model demonstrates Boson symmetry and, thereby, may be related to some VVP model through VMD, then either $\theta_V = 24^\circ$ and $\Gamma(\rho \rightarrow \pi\gamma) \sim 35$ KeV or $\theta_V = 35^\circ$ and $\Gamma(\rho \rightarrow \pi\gamma) \sim 80$ KeV. If no Boson symmetry is present, then both $\theta_V = 35^\circ$ and $\Gamma(\rho \rightarrow \pi\gamma) \sim 35$ KeV are possible.

None of the models predicted all of $\Gamma(\omega \rightarrow \eta\gamma)$, $\Gamma(\rho \rightarrow \eta\gamma)$ and $\Gamma(\eta' \rightarrow \rho\gamma)/\Gamma(\eta' \rightarrow \omega\gamma)$ in agreement with experiment [7,8]. The SU(3) model with nonet symmetry breaking predicted $\omega \rightarrow \eta\gamma$ and $\rho \rightarrow \eta\gamma$ amplitudes of opposite phase but $\Gamma(\rho \rightarrow \eta\gamma)$ was too low; all the strong nonet models with SU(3) symmetry breaking suggested that $\omega \rightarrow \eta\gamma$ and $\rho \rightarrow \eta\gamma$ were quite suppressed; in the weak nonet models, enough coupling constants were available to produce either of the two $\Gamma(\omega \rightarrow \eta\gamma)$ and $\Gamma(\rho \rightarrow \eta\gamma)$ experimental

solutions. The $\Gamma(\eta' \rightarrow \rho\gamma)/\Gamma(\eta' \rightarrow \omega\gamma)$ ratio was even more problematic. In the nonet symmetry scheme with no SU(3) symmetry breaking, it was high (~ 11) and grew even larger with the introduction of symmetry breaking. This ratio was highest (30 - 50) in the schemes with $\theta_V = 24^\circ$ and somewhat lower (15 - 25) in the schemes with $\theta_V = 35^\circ$. The weak nonet symmetry schemes demonstrated the additional problem that $\Gamma(\eta' \rightarrow \rho\gamma) > 300 \text{ KeV}$; when attempt was made to fit the measured $\Gamma(\eta' \rightarrow \rho\gamma)/\Gamma(\eta' \rightarrow \omega\gamma)$ ratio, $\Gamma(\eta' \rightarrow \omega\gamma)$ also went above experimental bounds. None of these models is obviously superior to the others on the basis of the η and η' predictions.

Some of these reasonably successful models are more justifiable than others when the phenomenological implications of their symmetry structure is examined. The success of the OZI rule in explaining the decays of strange particles suggests that both nonet symmetry and $\theta_V \sim 35^\circ$ are important --the former forces singlets to couple with the same strength as octets, the latter insures that $\phi \sim s\bar{s}$. That θ_V should be near 40° is obtained from the quadratic mass formula. Faced with the necessity of symmetry breaking, SU(3) symmetry breaking is a natural choice because of its previous successes in explaining mass spectra; also, the alternative of nonet symmetry breaking is undesirable because of its connection with OZI violations. The successes of VMD in other radiative processes suggest that the $VP\gamma$ model sought here should be related to a VVP model through VMD, the $VP\gamma$ model thus requiring Boson symmetry. Perhaps, given some of

the interpretive problems with VMD, this is one of the least important requirements for the desired VP_γ model. All of these considerations point to a VP_γ model with nonet symmetry, $SU(3)$ symmetry breaking, standard mixing angles and, perhaps, Boson symmetry. The strong and weak nonet symmetry models with $SU(3)$ symmetry breaking satisfy these criteria.

8.2 The VMD Related Decays

A VP_γ model with Boson symmetry may be further judged by its ability to predict decays of the type $P \rightarrow \gamma\gamma$, $V \rightarrow PPP$ and $P \rightarrow PP_\gamma$. While a success in making such predictions is certainly significant, a failure should not necessarily be blamed on the VP_γ model--it may be VMD which is at fault. With this word of caution, some of the successful VP_γ models are compared with respect to their ability to predict the VMD related rates.

The models which used $\theta_V = 24^\circ$ could not explain the measured $\pi \rightarrow \gamma\gamma$ rate. While attempting to accomodate some of the VMD related rates, these models lost their previous ability to fit the $V \rightarrow P_\gamma$ rates. The nonet symmetry models with $SU(3)$ symmetry breaking, Boson symmetry and standard mixing angles faired much better--all the VMD related rates could be explained without substantially altering the $V \rightarrow P_\gamma$ and $P \rightarrow V_\gamma$ rate predictions. If VMD is correct, the nonet symmetry models with $SU(3)$ symmetry breaking and standard mixing angles are the most successful of the VP_γ models.

It is worthwhile noting that, by assuming VMD, the VP_γ models with artificial θ_V and the VP_γ models which lack

nonet symmetry are eliminated. These are precisely the models that would be eliminated on phenomenological arguments based on the OZI rule and mass formulae.

8.3 Extensions to SU(4)

Another realm into which an SU(3) $VP\gamma$ model may be extended is the world of SU(4). A model would be successful indeed if it could explain the radiative decays of ψ as well as all the previously discussed SU(3) decays.

The strong nonet symmetry model with SU(3) symmetry breaking and Boson symmetry was extended, in a natural way, to an SU(4) model. The model accounted for all the ψ radiative decays without substantially altering the SU(3) $V \rightarrow P\gamma$ and $P \rightarrow V\gamma$ rate predictions. In fact, with a slight widening of the $K^{*0} \rightarrow K^0\gamma$ width, $\Gamma(\omega \rightarrow \eta\gamma)$ and $\Gamma(\rho \rightarrow \eta\gamma)$ were predicted close to one of the measured solutions [7]; the $\Gamma(\eta' \rightarrow \rho\gamma)/\Gamma(\eta' \rightarrow \omega\gamma)$ ratio did, however, remain in disagreement with experiment [8].

A further extension to include SU(4) VMD related rates was not particularly successful but VMD, itself, was considered to be highly suspect in the SU(4) context.

8.4 Experiments

In the last few years much attention has been devoted to the measurement of radiative decay rates of vector and pseudoscalar mesons. Hopefully this interest will continue long enough to resolve some of the theoretical ambiguities. While, of course, all new measurements are important, some

particular experiments are especially so.

Among the SU(3) rates, the $\rho^0 \rightarrow \pi^0 \gamma$ rate is the most crucial. If $\theta_V \sim 35^\circ$ is accepted, then VMD lives or dies depending on the value of $\Gamma(\rho \rightarrow \pi \gamma)$. Given the difficulties of a Primakoff effect experiment, it would be desirable if this process could be studied in an e^+e^- setup.

Other SU(3) processes of interest include the η and η' decays: $\rho \rightarrow \eta \gamma$, $\omega \rightarrow \eta \gamma$, $\phi \rightarrow \eta \gamma$, $\eta' \rightarrow \rho \gamma$, $\eta' \rightarrow \omega \gamma$ and $\phi \rightarrow \eta' \gamma$. Of these, only the third has been measured more than once. Since partial widths are available for $\eta' \rightarrow \rho \gamma$ and $\eta' \rightarrow \omega \gamma$, the measurement of $\Gamma(\eta')$ would be sufficient to determine these rates absolutely. These η and η' rates would help settle pseudoscalar mixing angle ambiguities and would help choose among the more-or-less successful $VP\gamma$ models listed above.

Since $\Gamma(K^{*+} \rightarrow K^+ \gamma) / \Gamma(K^{*0} \rightarrow K^0 \gamma)$ is very sensitive to the symmetry breaking structure of the $VP\gamma$ model used, a measurement of the $K^{*+} \rightarrow K^+ \gamma$ rate would be useful.

Of the SU(4) processes, those involving η_c are of the most interest: $\eta_c \rightarrow \rho \gamma$, $\eta_c \rightarrow \omega \gamma$, $\eta_c \rightarrow \phi \gamma$ and $\psi \rightarrow \eta_c \gamma$. While it now appears that there exists a spinless $c\bar{c}$ state at around 2.8 GeV, it still must be substantiated that it really is η_c . Only when the η_c rates are known can such alternatives as slightly nonideal mixing angles [42], multiplet mixing [43] and symmetry breaking be evaluated.

The charmed meson radiative decays are of interest for two reasons. First of all, radiative decay is an important decay mode for these mesons because, except for π emission,

their only alternative is to decay weakly. Secondly, these rates provide a measure of symmetry breaking in a way similar to the $K^{*+} \rightarrow K^+ \gamma$ rate mentioned above.

8.5 Conclusions

After the examination of a wide variety of $VP\gamma$ models and a large selection of radiative decay data, several conclusions may be drawn. Substantial¹ symmetry breaking, either of the nonet or $SU(3)$ variety, is needed in a $VP\gamma$ model to account for the observed $V \rightarrow P\gamma$ and $P \rightarrow V\gamma$ rates. An inconsistency is seen to exist between VMD and the measured rate for $\rho \rightarrow \pi\gamma$ --if this rate does not change, VMD will be in serious trouble. Except for this problem, several $VP\gamma$ schemes can account for all the reasonably established experimental rates. Among these schemes are some that are quite justifiable on phenomenological grounds; in particular, the nonet symmetry schemes which demonstrate $SU(3)$ symmetry breaking and which use standard mixing angles are quite successful and extend well to describe other $SU(3)$ VMD related decays and, to $SU(4)$, to describe the radiative decays of ψ . While the ultimate judgement of the success of these radiative decay models must await further experimental data, it is clear that the use of symmetry breaking has greatly advanced the understanding of the radiative decays of vector and pseudoscalar mesons.

FOOTNOTES

¹The amount of symmetry breaking for a given model may be judged by comparing the coupling constants of the symmetry breaking terms to the coupling constant of the SU(3) invariant nonet symmetric term. In this way, it is seen that the baryon loop models have about 25% symmetry breaking. The current algebra models display about 40% symmetry breaking through the quark mass differences and another 30% through the pseudoscalar leptonic decay constants. The most successful models (the nonet symmetry breaking model of chapter I and the nonet symmetry SU(3) symmetry breaking models of chapter V) all have more than 80% symmetry breaking. In an absolute sense, the amount of symmetry breaking needed to explain the observed $V \rightarrow P\gamma$ widths is large--the decay amplitudes do not arise principally from the SU(3) invariant nonet symmetric term but instead have symmetry breaking contributions which are as important as the symmetric one.

This amount of symmetry breaking should be compared with that previously encountered in hadron physics [49]. The application of mass formulae to many meson and baryon multiplets suggests that, with the possible exception of the pseudoscalar mesons, mass symmetry breaking is less than about 15%. Examination of several hadronic interactions, including $V \rightarrow PP$, $B(8) \rightarrow B(8)P$, $B(10) \rightarrow B(8)P$, indicates no need for SU(3) symmetry breaking in the hadronic coupling constants. Against this background of reasonably good SU(3) symmetry, the amount of symmetry breaking needed for the $V \rightarrow P\gamma$ decays is indeed anomalously large.

REFERENCES

1. T. G. Trippe et al., Rev. Mod. Phys. 48, S51 (1976).
2. W. C. Carithers et al., Phys. Rev. Lett. 35, 349 (1975).
3. C. Bemporad et al., Nucl. Phys. B51, 1 (1973).
4. B. Gobbi et al., Phys. Rev. Lett. 33, 1450(1974), and 37, 1439(1976).
5. G. Cosme et al., preprint LAL 1279 (1975).
6. M. Basile et al., Nucl. Phys. B44, 605 (1972); D. Benarksas, Phys. Lett. 42B, 511 (1972).
7. D. E. Andrews et al., Phys. Rev. Lett. 38, 198 (1977).
8. C. J. Zangino et al., Phys. Rev. Lett. 38, 930 (1977).
9. Y. Anisovitch et al., Phys. Lett. 16, 194 (1965); C. Becchi and G. Morpurgo, Phys. Rev. 140, B687 (1965); A. Dar and V. F. Weisskopf, Phys. Lett. 26B, 670 (1968); C. Soloviev, Phys. Lett. 16, 345 (1965); W. Thirring, Phys. Lett. 16, 335 (1965); For reviews see: B. T. Field, Models of Elementary Particles, (Blaisdell Publishing Co., Waltham, Mass., 1965); J. J. J. Kokkedee, The Quark Model, (Q. A. Benjamin, Inc., New York, 1969); G. Morpurgo, in Theory and Phenomenology in Particle Physics, edited by A. Zichichi (Academic Press, New York, 1969).
10. R. Torgerson, Phys. Rev. D10, 2951 (1974).
11. M. Gell-Mann, D. H. Sharp and W. D. Wagner, Phys. Rev. Lett. 8, 261 (1962); R. F. Daschen and D. H. Sharp, Phys. Rev. 133, B1585 (1964).
12. S. Okubo, Phys. Lett. 5, 165 (1963); G. Zweig, CERN Report No. 8419/TH412, (1964) unpublished; I. Iizuka, K. Okada and O. Shito, Progr. Theor. Phys. 35, 1061 (1966); G. Zweig, in Symmetries in Elementary Particle Physics, edited by A. Zichichi (Academic Press, New York, 1965).
13. A. Bohm and R. B. Teese, Phys. Rev. Lett. 38, 629 (1977).
14. P. J. O'Donnell, Phys. Rev. Lett. 36, 177 (1976).
15. D. H. Boal, R. H. Graham and J. W. Moffat, Phys. Rev. Lett. 36, 714 (1976).

16. L. M. Brown, H. Munczek and Paul Singer, Phys. Rev. Lett. 10, 707 (1968); Paul Singer, Phys. Rev. D1, 86 (1970); A. Kotlewski, W. Lee, M. Suzuki and J. Thaler, Phys. Rev. D8, 348 (1973).
17. L. H. Chan, L. Clavelli, and R. Torgerson, Phys. Rev. 185, 1754 (1969).
18. M. Roos, Helsinki University Report No. ISBN 951-45-06-3-0, (1975) unpublished.
19. W. Braunschweig et al., Phys. Lett. 67B, 243 (1977).
20. B. H. Wiik and G. Wolf, DESY Report No. DESY 77/01 (to be published).
21. G. Wentzel, Phys. Rev. 101, 1214 (1956).
22. J. Steinberger, Phys. Rev. 76, 1180 (1949).
23. R. Rockmore and T. F. Wong, Phys. Rev. Lett. 28, 1736 (1972); R. Rockmore and T. F. Wong, Phys. Rev. D7, 3425 (1973); A. N. Kamal and R. Rockmore, Phys. Rev. D9, 752 (1974); R. Rockmore and A. N. Kamal, Phys. Rev. D10, 2091 (1974).
24. R. Rockmore, Phys. Rev. D11, 620 (1975).
25. M. Gronau, Phys. Rev. D5, 118 (1972).
26. V. Barger and M. Olsson, Phys. Rev. 146, 1080 (1966).
27. G. J. Aubrecht II and M. S. K. Razmi, Phys. Rev. D12, 2120 (1975).
28. M. Gell-Mann, Phys. Rev. 125, 1067 (1962).
29. H. Lehmann, K. Symanzik and W. Zimmerman, Nuovo Cim. 1, 205 (1955).
30. M. Gell-Mann and M. Iévy, Nuovo Cim. 16, 705 (1960); Y. Nambu, Phys. Rev. Lett. 4, 380 (1960).
31. Y. Nambu and E. Shrauner, Phys. Rev. 128, 862 (1962).
32. J. J. Sakurai, Currents and Mesons, (The University of Chicago Press, Chicago and London, 1969).
33. H. Ebenhöh et al., Z. Phys. 24, 473 (1971).

34. V. S. Mathur et al., Phys. Rev. D1, 2058 (1970); S. L. Glashow and S. Weinberg, Phys. Rev. Lett. 20, 224 (1968); L. M. Chounet et al., Phys. Rep. 4, 199 (1972); K. Kawarabayashi and W. W. Wada, Phys. Rev. Lett. 19, 1193 (1967); A. N. Kamal, Nucl. Phys. B12, 123 (1969); A. N. Kamal, Nucl. Phys. B15, 637 (1970).
35. M. S. Chanowitz, Phys. Rev. Lett. 35, 977 (1975).
36. M. Muraskin and S. L. Glashow, Phys. Rev. 132, 482 (1963).
37. B. J. Edwards and A. N. Kamal, Phys. Rev. Lett. 36, 241 (1976); B. J. Edwards and A. N. Kamal, Ann. Phys. 102, 252 (1976).
38. R. Torgerson, three body phase space programme (private communication).
39. D. H. Boal et al., Phys. Lett. 66B, 165 (1977).
40. G. Goldhaber et al., in Proceedings of the Stanford Linear Accelerator Center Summer Institute, (1976) unpublished.
41. CERN Courier, No. 1/2 Vol. 18, 17 (1978).
42. A. Kazi, G. Kramer and D. H. Schiller, Acta Phys. Austriaca 45, 65 and 195 (1976).
43. D. H. Boal, Phys. Rev. Lett. 37, 1333 (1976); H. Fritzsch and J. D. Jackson, Phys. Lett. 66B, 365 (1977); D. H. Boal and R. Torgerson, Phys. Rev. D15, 327 (1977).
44. J. J. J. Kokkedee, The Quark Model, (W. A. Benjamin, Inc., New York, 1969).
45. C. Becchi and G. Morpurgo, Phys. Rev. 140, B687 (1965).
46. A. Bohm, M. Hossain and R. B. Teese, C.P.T. preprint ORO 274, to be published in Phys. Rev. D; A. Bohm and R. B. Teese, Arguments Concerning an $SU(3)$ Scalar Term in the Electromagnetic Current Operator and the Value for $\Gamma(\rho \rightarrow \pi\gamma)$, to be published in Phys. Rev. D.
47. B. J. Edwards and A. N. Kamal, Phys. Rev. Lett. 39, 66 (1977).
48. A. N. Kamal, Quark Anomalous Moments and Meson Radiative Decays, to be published in Phys. Rev. D.
49. N. P. Samios et al., Rev. Mod. Phys. 46, 49 (1978).

APPENDIX I

RADIATIVE DECAYS IN THE QUARK MODEL

The Nonrelativistic Quark Model

The M1 transition amplitude between the 3S_1 and 1S_0 $q_i \bar{q}_j$ bound states is to be calculated. The 3S_1 state is the vector meson and is assigned the nonrelativistic wavefunction [44],

$$\Psi_V = f_V(\{\underline{r}\}) \phi_V, \quad (A.1)$$

where f_V contains all the spatial dependence and ϕ_V contains all the spin-unitary spin dependence; each is separately normalized to unity. For the different possible spin projections of V, ϕ_V takes these forms:

$$\begin{aligned} \phi_V(s_z = +1) &= q_i^\uparrow \bar{q}_j^\uparrow, \\ \phi_V(s_z = 0) &= \frac{1}{\sqrt{2}} (q_i^\uparrow \bar{q}_j^\downarrow + q_i^\downarrow \bar{q}_j^\uparrow), \\ \phi_V(s_z = -1) &= q_i^\downarrow \bar{q}_j^\downarrow. \end{aligned} \quad (A.2)$$

The 1S_0 state is the pseudoscalar meson and is similarly assigned a nonrelativistic wavefunction,

$$\Psi_P = f_P(\{\underline{r}\}) \phi_P.$$

The spin-unitary spin part takes this form:

$$\phi_P = \frac{1}{\sqrt{2}} (q_i^\dagger \bar{q}_j^\dagger - q_i^\dagger \bar{q}_j^\dagger). \quad (\text{A.3})$$

The interaction operator which induces an M1 transition of the i -th quark is [45]:

$$H_i = \left[\frac{e\hbar}{2Mc} \underline{L}_i \cdot (\underline{k} \times \underline{\varepsilon}) + \frac{e_i}{e} \underline{\sigma}_i \cdot (\underline{k} \times \underline{\varepsilon}) \right] e^{i\underline{k} \cdot \underline{r}_i} \quad (\text{A.4})$$

where e_i and \underline{r}_i are the charge and position, respectively, of the i -th quark; \underline{L}_i and $\underline{\sigma}_i$ are the orbital and intrinsic spin angular momentum operators of the i -th quark; \underline{k} and $\underline{\varepsilon}$ are the 3-momentum and polarization of the emitted photon; M is the quark mass. Because $L = 0$ for both the 3S_1 and 1S_0 states, the first term of (A.4) is impotent. The quark model matrix element for $V \rightarrow P\gamma$ is then:

$$\langle P | H | V \rangle = \langle \Psi_P | \sum_i \frac{e_i}{e} \underline{\sigma}_i \cdot (\underline{k} \times \underline{\varepsilon}) e^{i\underline{k} \cdot \underline{r}_i} | \Psi_V \rangle. \quad (\text{A.5})$$

When this has been computed, it should be compared with the meson matrix elements derived earlier, for example (1.9).

The first step is to separate out the space dependent parts of (A.5) and to perform the spatial integrations. For the i -th term in the sum in (A.5), the spatial part is

$$\int d\tau f_P^* (\{\underline{r}\}) e^{i\underline{k} \cdot \underline{r}_i} f_V (\{\underline{r}\}),$$

where

$$d\tau = \prod_j d^3 r_j \delta\left(\frac{1}{N} \sum_j \underline{r}_j\right).$$

In the usual long wavelength approximation $e^{i\underline{k} \cdot \underline{r}_i}$ is

approximated by 1 and then the P and V wavefunctions are assumed to overlap completely. These two assumptions reduce all the spatial integrations to unity. It is at this stage that momentum dependence and meson form factors might have entered the VP_γ amplitude but in the usual approximations these features are not present.

The spin-unitary spin part of the matrix element is now calculated. Depending on the spin projection of V different parts of H contribute, for $s_z = +1, 0, -1$ respectively, only σ_- , σ_z , σ_+ are effective:

$$\begin{aligned}
 \langle \phi_P | H | \phi_V (s_z = +1) \rangle &= \frac{-\mu}{\sqrt{2}} \left(\frac{e_i + e_j}{e} \right) (\underline{k} \times \underline{\varepsilon})_+, \\
 \langle \phi_P | H | \phi_V (s_z = 0) \rangle &= \mu \left(\frac{e_i + e_j}{e} \right) (\underline{k} \times \underline{\varepsilon})_z, \\
 \langle \phi_P | H | \phi_V (s_z = -1) \rangle &= \frac{\mu}{\sqrt{2}} \left(\frac{e_i + e_j}{e} \right) (\underline{k} \times \underline{\varepsilon})_-.
 \end{aligned} \tag{A.6}$$

Using $\underline{\varepsilon}_V$ as the polarization of V,

$$\langle \phi_P | H | \phi_V \rangle = \mu \left(\frac{e_i + e_j}{e} \right) \underline{\varepsilon}_V \cdot (\underline{k} \times \underline{\varepsilon}). \tag{A.7}$$

The fraction $(e_i + e_j)/e$ may be simplified using some properties of SU(3). Each $q_i \bar{q}_j$ pair corresponds to a superposition of mesons, each of which has a prescribed SU(3) index and may be represented by a superposition of λ matrices. For example,

$$u\bar{d} \sim \rho^+ \sim \frac{1}{\sqrt{2}} (|1\rangle - i|2\rangle) \sim \frac{1}{\sqrt{2}} (\lambda_1 - i\lambda_2) \sim \sqrt{2} \begin{pmatrix} 0 & 0 & 0 \\ 1 & 0 & 0 \\ 0 & 0 & 0 \end{pmatrix}.$$

In fact the state $q_i \bar{q}_j$ may always be represented by a 3×3 matrix whose only nonvanishing element is the ji -th; this $q_i \bar{q}_j$ state is the meson with SU(3) index m and

$$(\lambda_m)_{\alpha\beta} = \sqrt{2} \delta_{j\alpha} \delta_{i\beta}. \quad (\text{A.8})$$

Using this representation,

$$\left\{ \frac{1}{2} \lambda_m, \frac{1}{2} \lambda_{\bar{m}} \right\} = \frac{1}{2} (\delta_{i\alpha} \delta_{i\beta} + \delta_{j\alpha} \delta_{j\beta}), \quad (\text{A.9})$$

so that,

$$\begin{aligned} \left\{ \frac{1}{2} \lambda_m, \frac{1}{2} \lambda_{\bar{m}} \right\} = \frac{1}{2\sqrt{2}} & \left[\lambda_3 \left(\frac{1}{\sqrt{2}} (\delta_{i1} + \delta_{j1}) - \frac{1}{\sqrt{2}} (\delta_{i2} + \delta_{j2}) \right) \right. \\ & + \lambda_8 \left(\frac{1}{\sqrt{6}} (\delta_{i1} + \delta_{j1}) + \frac{1}{\sqrt{6}} (\delta_{i2} + \delta_{j2}) - \sqrt{\frac{2}{3}} (\delta_{i3} + \delta_{j3}) \right) \\ & \left. + \lambda_0 \left(\frac{1}{\sqrt{3}} (\delta_{i1} + \delta_{j1}) + \frac{1}{\sqrt{3}} (\delta_{i2} + \delta_{j2}) + \frac{1}{\sqrt{3}} (\delta_{i3} + \delta_{j3}) \right) \right]. \end{aligned} \quad (\text{A.10})$$

From the definition of the SU(3) structure constants it follows that

$$\begin{aligned} d_{m\bar{m}3} &= \frac{1}{2} ((\delta_{i1} + \delta_{j1}) - (\delta_{i2} + \delta_{j2})), \\ d_{m\bar{m}8} &= \frac{1}{2\sqrt{3}} ((\delta_{i1} + \delta_{j1}) + (\delta_{i2} + \delta_{j2}) - 2(\delta_{i3} + \delta_{j3})), \end{aligned} \quad (\text{A.11})$$

and that

$$d_{m\bar{m}\gamma} = \frac{2}{3} (\delta_{i1} + \delta_{j1}) - \frac{1}{3} (\delta_{i2} + \delta_{j2}) - \frac{1}{3} (\delta_{i3} + \delta_{j3}). \quad (\text{A.12})$$

Using $e_1 = \frac{2}{3} e$ and $e_2 = e_3 = -\frac{1}{3} e$,

$$d_{m\bar{m}\gamma} = \frac{e_i + e_j}{e}. \quad (\text{A.13})$$

This expression for $(e_i + e_j)/e$ is easier to work with when the mesons of concern are constructed from a superposition of $q\bar{q}$ states.

Combining the spatial integrations and the spin-unitary spin sums and using mesons built from a combination of $q\bar{q}$ states, the full M1 matrix element for the $V^m \rightarrow P^i_\gamma$ decay is

$$\langle P^i | H | V^m \rangle = \mu d_{mi\gamma} \underline{\epsilon}_m \cdot (\underline{k} \times \underline{\epsilon}). \quad (\text{A.14})$$

Up to factors of E_m/M_m which are unity in the nonrelativistic limit, (A.14) is the nonrelativistic reduction of a matrix element of the form,

$$T_{V^m P^i_\gamma} \sim \frac{\mu}{M_m} d_{mi\gamma} \epsilon_{\mu\nu\rho\sigma} (k_m)^\mu (\epsilon_m)^\nu (k)^\rho (\epsilon)^\sigma. \quad (\text{A.15})$$

If M_m is assigned the vector multiplet mass, this is exactly the same as the nonet matrix element (1.9). If M_m is the actual mass of V^m , some symmetry breaking through masses is present; compare [10]. Most quark model authors [44,45] start with (A.14), use nonrelativistic phase space techniques to calculate $\Gamma(V^m \rightarrow P^i_\gamma)$ and then adjust the kinematical factors to give $\Gamma(V^m \rightarrow P^i_\gamma)$ the proper relativistic form (1.10). The essential point is that the quark model yields the same SU(3) structure and the same basic Lorentz structure for the VP_γ amplitude as do calculations on the meson level. The only possible point of divergence involves the spatial

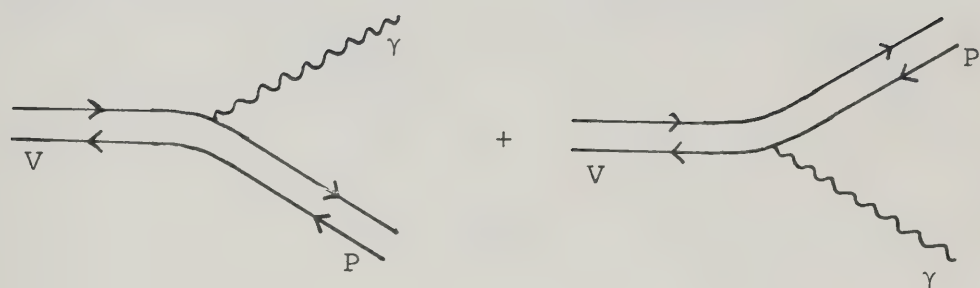
overlap of the $q\bar{q}$ wavefunctions--if this overlap weren't approximated by unity, the quark model would suggest some extra momentum or mass dependence of the matrix element over that proposed in the standard meson calculations.

Quark Line Diagrams

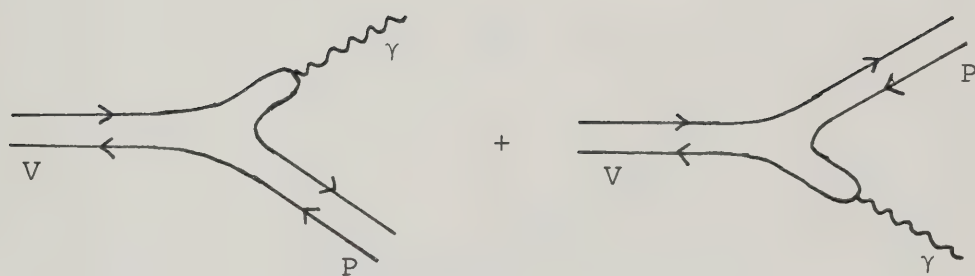
The $VP\gamma$ Lagrangians of Chapter II may be easily visualized in terms of quark line diagrams. Particles whose internal symmetry indices are summed under a single trace in the Lagrangian are all connected in the corresponding quark line diagram.

In Figure 4a are illustrated the two contributions to $\text{Tr}(\{V,A\}P)$. Picturing V as $q_i\bar{q}_j$, the first diagram has strength e_i and the second strength e_j thus accounting for the total strength $(e_i + e_j)$ found above. The quark lines of Figure 4a may be distorted somewhat, as in Figure 4b, thereby preparing the stage for the application of VMD. Erasing the photons in Figure 4b, a VVP vertex results. The two contributions are identical except for the interchange of the two vector mesons and, as a result, the sum of the two contributions demonstrates the required Boson symmetry.

In Figures 5-8, all the terms of the most general $SU(3)$ $VP\gamma$ Lagrangian with λ_8 symmetry breaking, (2.13), are illustrated. The diagrams are drawn in such a manner that VMD may later be applied. In the most general scheme, each of these twelve diagrams has a strength which is independent of that of the other diagrams.

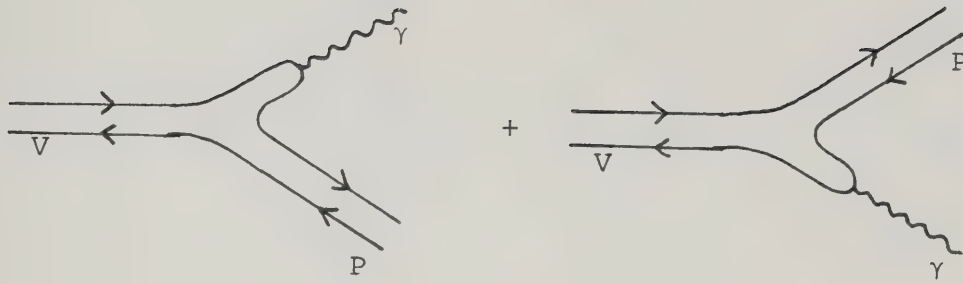


(a)

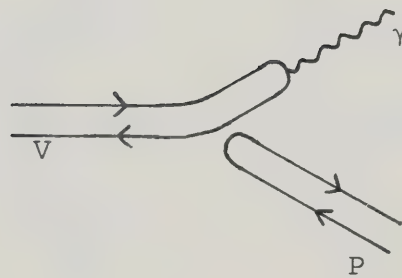


(b)

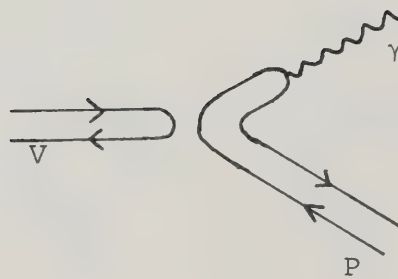
Figure 4. Quark Line Diagram for $V \rightarrow P \gamma$. (a) $\text{Tr} (\{V, A\} P)$,
 (b) VMD version of $\text{Tr} (\{V, A\} P)$.



(a)

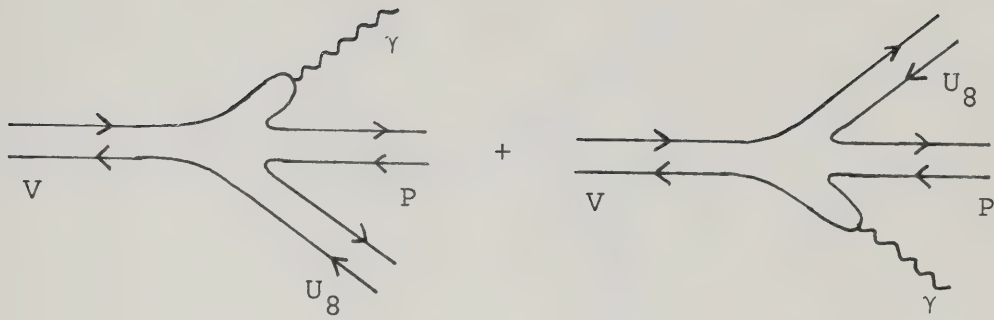


(b)

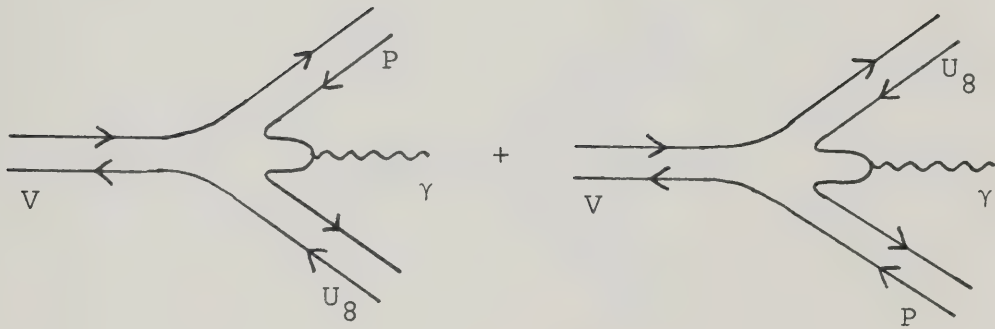


(c)

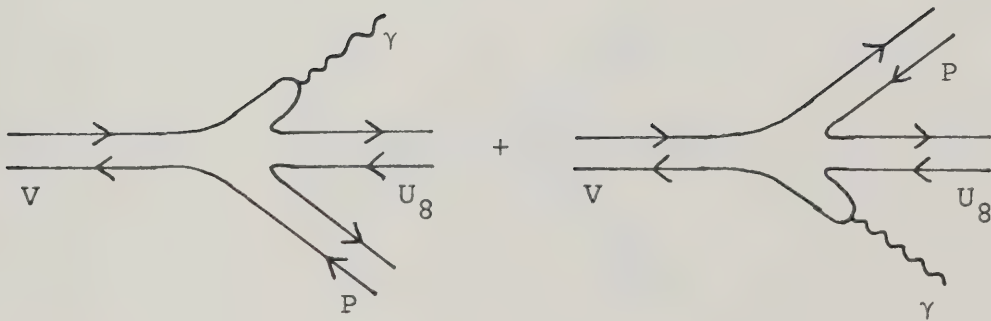
Figure 5. $SU(3)$ Invariant Contributions to \mathcal{L} . (a) $\text{Tr}(\{V, A\}P)$, (b) $\text{Tr}(VA) \text{Tr}(P)$, (c) $\text{Tr}(V) \text{Tr}(AP)$.



(a)

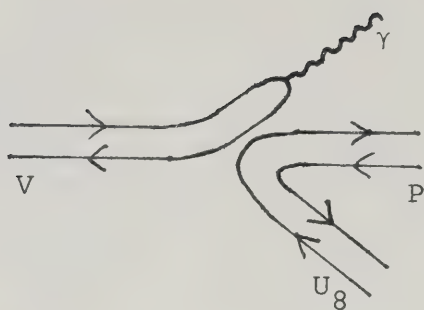


(b)

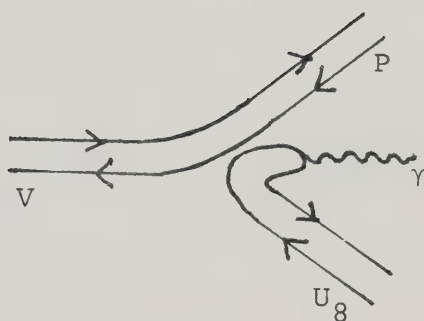


(c)

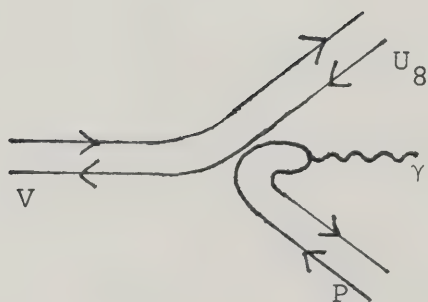
Figure 6. Totally Connected SU(3) Symmetry Breaking contributions to \mathcal{L} . (a) $\text{Tr} (VAPU_8) + \text{Tr} (VU_8PA)$, (b) $\text{Tr} (VPAU_8) + \text{Tr} (VU_8AP)$, (c) $\text{Tr} (VAU_8P) + \text{Tr} (VP U_8A)$.



(a)

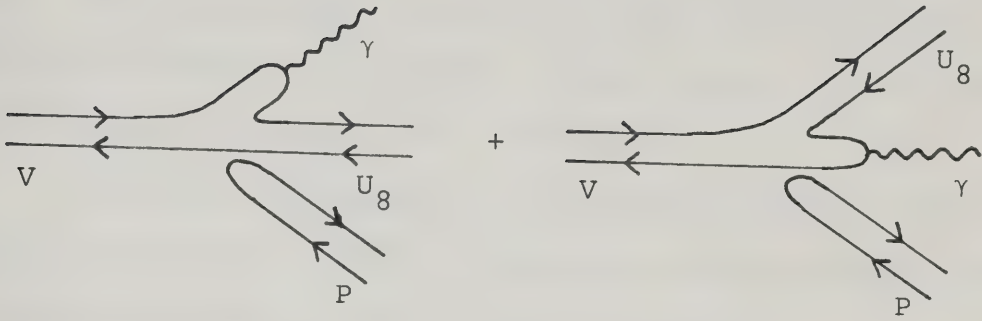


(b)

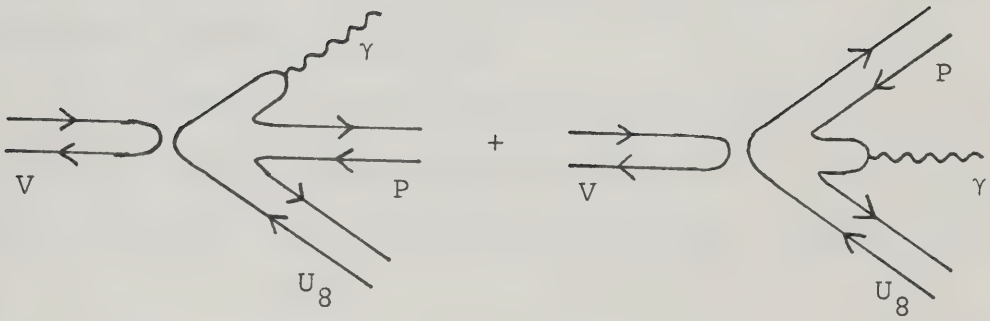


(c)

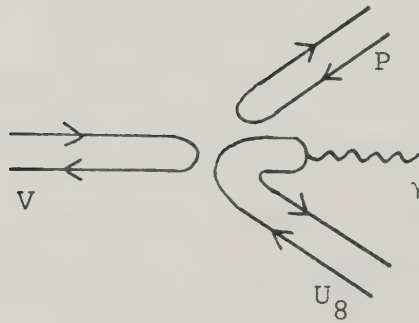
Figure 7. Pairwise Connected $SU(3)$ Symmetry Breaking Contributions to \mathcal{L} . (a) $\text{Tr}(VA) \text{Tr}(PU_8)$, (b) $\text{Tr}(VP) \text{Tr}(AU_8)$, (c) $\text{Tr}(VU_8) \text{Tr}(AP)$.



(a)



(b)



(c)

Figure 8. Disconnected $SU(3)$ Symmetry Breaking Contributions to \mathcal{L} . (a) $\text{Tr} (\{V, A\} U_8) \text{Tr} (P)$, (b) $\text{Tr} (V) \text{Tr} (\{A, P\} U_8)$, (c) $\text{Tr} (V) \text{Tr} (P) \text{Tr} (A U_8)$.

In Figure 5, the SU(3) invariant contributions are shown. Notice that the diagrams in Figure 5b and c have individual disconnected initial or final state particles--these diagrams represent OZI violations.

In Figure 6, the totally connected diagrams with one U_8 scalar spurion are given. These diagrams represent three of the OZI allowed λ_8 symmetry breaking terms.

The other three OZI allowed λ_8 symmetry breaking terms are represented by the diagrams of Figure 7. These diagrams are pairwise connected.

In Figure 8 are the remaining contributions. Each diagram has one U_8 and a disconnected V or P. These diagrams represent symmetry breaking terms which also violate the OZI rule.

The two types of nonet symmetry are imposed as follows. For weak nonet symmetry, SU(3) invariant OZI violating terms are forbidden--Figure 5b and c are not permitted. For strong nonet symmetry, no OZI violating terms are allowed--Figure 8a, b and c are also forbidden. The remaining symmetry breaking terms may simulate OZI violations but when the U_8 scalar spurion is remembered, are seen to be properly connected.

If VMD is to be compatible with the $VP\gamma$ model, removal of the photon from all these diagrams must result in a legitimate VVP vertex. Erasing the photon from all these diagrams, it is seen that Figure 6a and c are identical except for the interchange of the two vectors; likewise, Figure 7a

and c are similar. Since a VVP model must demonstrate Boson symmetry, Figure 6a and c and also Figure 7a and c must have the same strength. This is the Boson symmetry condition derived in Chapter II.

While all the possible symmetry breaking structures may be enumerated without the help of quarks, it all becomes clearer when quark line diagrams are used.

APPENDIX II

ALTERNATE FORMS OF THE ELECTROMAGNETIC CURRENT

The electromagnetic current in SU(3) is usually taken to be the following superposition of the third and eighth members of an SU(3) octet of currents:

$$J_{\mu}^{\text{em}} = J_{\mu}^3 + \frac{1}{\sqrt{3}} J_{\mu}^8. \quad (\text{B.1})$$

As a result, J^{em} couples to the quarks according to their charges:

$$J_{\mu}^{\text{em}} \sim \frac{2}{3} \bar{u} \gamma_{\mu} u - \frac{1}{3} \bar{d} \gamma_{\mu} d - \frac{1}{3} \bar{s} \gamma_{\mu} s. \quad (\text{B.2})$$

The $\mu = 0$ component of J^{em} , integrated over all space, is a quark charge operator:

$$Q = \sum_i e_i n_i \quad (\text{B.3})$$

and, after a nonrelativeistic reduction, the spatial part of J^{em} gives rise to a quark Dirac magnetic moment operator:

$$\vec{M} = \sum_i \frac{e_i}{2m_i} \vec{\sigma}_i \quad (\text{B.4})$$

where e_i and m_i are the charge and mass of the i -th quark and n_i and σ_i are the number and spin operators in the space of the i -th quark. In Appendix I, (B.4) was used with degenerate quark masses. From the charge operator (B.3), the Gell-Mann--Nishijima formula may be deduced:

$$Q = T_3 + \frac{1}{2} Y. \quad (B.5)$$

Singlet Contributions to J^{em}

Bohm and Teese [13,46] suggest the possibility of a singlet contribution to the electromagnetic current. With

$$J_{\mu}^{\text{em}} = J_{\mu}^3 + \frac{1}{\sqrt{3}} J_{\mu}^8 + \alpha J_{\mu}^0, \quad (B.6)$$

interesting consequences are found for meson radiative decays.

Assuming the usual particle assignments and nonet symmetry, this current gives the following $V_{P^i\gamma}^{m1}$ vertex:

$$g_{mi\gamma} = g_0 d_{\min} (\delta_{n3} + \frac{1}{\sqrt{3}} \delta_{n8} + \alpha \delta_{n0}). \quad (B.7)$$

As a result,

$$\begin{aligned} g_{\omega\pi\gamma} &= g_0 \\ g_{\rho\pi\gamma} &= g_0 \left(\frac{1}{3} + \sqrt{\frac{2}{3}} \alpha \right) \end{aligned} \quad (B.8)$$

and the $\omega \rightarrow \pi\gamma$ and $\rho \rightarrow \pi\gamma$ rates are independent.

This model is equivalent to a λ_8 symmetry breaking model in which the standard current is used. The vertex (B.7) is the same as

$$g_{mi\gamma} = g_0 (d_{\min} + \sqrt{2} \alpha \delta_{8n} \delta_{mi}) (\delta_{n3} + \frac{1}{\sqrt{3}} \delta_{n8}). \quad (B.9)$$

Introducing a singlet part to the electromagnetic current is equivalent to using a specific type of λ_8 symmetry breaking-- (B.9) is the amplitude for a λ_8 symmetry breaking model with strong nonet symmetry and no Boson symmetry; compare (2.15) with all the coupling constants except f_0 and f_7 equal to

zero. It is the lack of Boson symmetry which allows $\Gamma(\omega \rightarrow \pi\gamma)$ and $\Gamma(\rho \rightarrow \pi\gamma)$ to be consistent. The experience of Chapter V suggests that the $\omega \rightarrow \eta\gamma$, $\rho \rightarrow \eta\gamma$, $\eta' \rightarrow \omega\gamma$ and $\eta' \rightarrow \rho\gamma$ rates can not be explained in this scheme--this is also found by Bohm and Teese [13,46].

It is not clear a priori how such a singlet current is constructed. One possibility, the interpretation taken in [47], is that J° is a singlet current constructed from the three quarks already used:

$$J_\mu^\circ \sim \bar{u} \gamma_\mu u + \bar{d} \gamma_\mu d + \bar{s} \gamma_\mu s. \quad (B.10)$$

Such a current couples to all quarks with the same strength and, when taken between baryon states, is seen to be proportional to baryon number. This appears to be the type of singlet Bohm and Teese use in [13]. The problem with such a singlet is that it results in a modification of the Gell-Mann --Nishijima formula:

$$Q = T_3 + \frac{1}{2} Y + \frac{\alpha}{\sqrt{6}} B \quad (B.11)$$

and assigns incorrect charges to the observed baryons.

The other possibility is that J° is constructed from new quarks; perhaps,

$$J_\mu^\circ = \frac{2}{3} \bar{c} \gamma_\mu c + \frac{2}{3} \bar{t} \gamma_\mu t - \frac{1}{3} \bar{b} \gamma_\mu b. \quad (B.12)$$

In this case, the singlet current makes no contribution to the "old" baryon charges but may possibly affect the baryon

magnetic moments. This is the type of current Bohm and Teese use in [46]. Unless the singlet current is explicitly given, no connection can be made between the baryon sector and meson radiative decays.

Quark Anomalous Magnetic Moments

Another way to alter J^{em} is to introduce anomalous magnetic moments for the quarks:

$$\vec{M} = \sum_i \mu_i \vec{\sigma}_i, \quad (\text{B.13})$$

where

$$\mu_i = \frac{e_i}{2m_i} + K_i \mu.$$

Assuming that the u and d quarks have the same mass and letting $m_3/m_1 = \xi$,

$$\begin{aligned} \mu_1 &= \mu \left(\frac{2}{3} + K_1 \right), \\ \mu_2 &= \mu \left(-\frac{1}{3} + K_2 \right), \\ \mu_3 &= \mu \left(-\frac{1}{3}\xi + K_3 \right), \end{aligned} \quad (\text{B.14})$$

where

$$\mu = \frac{e}{2m_1} = 2.79 \mu_B.$$

These magnetic moments result in a $VP\gamma$ vertex of the form:

$$\begin{aligned} g_{mi\gamma} &= \frac{g_0}{\mu} ((\mu_1 - \mu_2) d_{mi3} \\ &+ \frac{1}{\sqrt{3}} (\mu_1 + \mu_2 - 2\mu_3) d_{mi8} \\ &+ \sqrt{\frac{2}{3}} (\mu_1 + \mu_2 + \mu_3) d_{m10}). \end{aligned} \quad (\text{B.15})$$

For processes which use only the spatial components of J^{em} , it appears as if

$$J_{\mu}^{\text{em}} \sim \sum_i \frac{\mu_i}{\mu} \bar{q}_i \gamma_{\mu} q_i \quad (\text{B.16})$$

or equivalently that

$$\begin{aligned} J_{\mu}^{\text{em}} = & \frac{1}{\mu} ((\mu_1 - \mu_2) J_{\mu}^3 \\ & + \frac{1}{\sqrt{3}} (\mu_1 + \mu_2 - 2\mu_3) J_{\mu}^8 \\ & + \sqrt{\frac{2}{3}} (\mu_1 + \mu_2 + \mu_3) J_{\mu}^0). \end{aligned} \quad (\text{B.17})$$

Because (B.3) and the standard Gell-Mann--Nishijima formula still hold, (B.17) must not be used to calculate charge.

For arbitrary values of the quark magnetic moments, this J^{em} is seen to have J^3 and J^8 in non standard proportions; also, some singlet contribution is present. The standard relative amounts of J^3 and J^8 are restored if

$$\mu_2 = \mu_3, \quad (\text{B.18})$$

and the singlet vanishes if,

$$\mu_1 + \mu_2 + \mu_3 = 0. \quad (\text{B.19})$$

Quark anomalous magnetic moments may be generated through strong interaction corrections using the standard electromagnetic current. If degenerate quark masses are used in such a calculation, (B.18) and (B.19) automatically hold [48]. It is clear from (B.15) to (B.17) that nondegenerate

quark masses, even without anomalous magnetic moments, are sufficient to produce an unusual apparent J^{em} .

The vertex (B.15) may be rewritten:

$$g_{mi\gamma} = \frac{g_o}{\mu} ((\mu_1 - \mu_3) d_{min} + \sqrt{3} (\mu_3 - \mu_2) d_{8nk} d_{kim} \\ + \frac{2}{\sqrt{3}} (\mu_1 + 2\mu_2) \delta_{8n} \delta_{im}) (\delta_{n3} + \frac{1}{\sqrt{3}} \delta_{n8}).$$

$$k = 0, \dots, 8 \quad (B.20)$$

This model too is a special case of a λ_8 symmetry breaking model with strong nonet symmetry and no Boson symmetry; compare (2.15) with all coupling constants except f_o , f_4 ($=f_5$), and f_7 equal to zero. Again, it is possible to reconcile $\Gamma(\omega \rightarrow \pi\gamma)$ and $\Gamma(\rho \rightarrow \pi\gamma)$ but problems occur among the η and η' rates.

Because this model may be used in both the baryon and meson sectors it is instructive to examine some of its predictions. The following symmetry breaking parametrization is used:

$$r = \frac{g_{\omega\pi\gamma}}{g_{\rho\pi\gamma}} = \frac{\mu_1 - \mu_2}{\mu_1 + \mu_2},$$

$$t = \frac{g_{K^{*0}K^0\gamma}}{g_{\rho\pi\gamma}} = \frac{\mu_2 + \mu_3}{\mu_1 + \mu_2}. \quad (B.21)$$

In the quark model with no anomalous magnetic moments and degenerate quark masses, $r = 3$ and $t = -2$; the same predictions hold in the nonet symmetry model of Chapter I. In terms of these parameters, the baryon magnetic moments should occur

in these ratios:

$$\frac{\mu_p}{\mu_n} = \frac{3 + 5r}{3 - 5r},$$

$$\frac{\mu_\Lambda}{\mu_n} = 3 \left[\frac{2t + r - 1}{3 + 5r} \right]. \quad (\text{B.22})$$

Ideally, r and t should be chosen to satisfy (B.21) and (B.22) simultaneously. Unfortunately, the experimental measurement [1] suggest that these sets of equations are not consistent and only one of (B.21) and (B.22) can hold.

Choosing $r = 3.21$ and $t = -1.8$, the experimental values for μ_p/μ_n and μ_Λ/μ_p are obtained. Fixing g_0 in (B.15) so that $\Gamma(\omega \rightarrow \pi\gamma) = 880$ KeV, predictions very similar to the nonet predictions of Solution 1 Table 1 result. The only significant improvement is $\Gamma(\phi \rightarrow \eta\gamma) = 71$ KeV; one mild improvement also occurs, $\Gamma(K^{*0} \rightarrow K^0\gamma) = 150$ KeV. $\Gamma(\rho \rightarrow \pi\gamma)$ remains near its nonet value and $\phi \rightarrow \pi\gamma$ is completely forbidden with ideal vector mixing.

Choosing $r = 4.9$ and $t = -1.9$, the experimental rates for $\omega \rightarrow \pi\gamma$, $\rho \rightarrow \pi\gamma$ and $K^{*0} \rightarrow K^0\gamma$ are obtained. $\Gamma(\phi \rightarrow \eta\gamma)$ is predicted very low, 0.2 KeV, and $\Gamma(\eta' \rightarrow \rho\gamma)/\Gamma(\eta' \rightarrow \omega\gamma) = 25$. $\Gamma(\phi \rightarrow \pi\gamma)$ remains zero. Meanwhile, the baryon magnetic moments are quite distorted, $\mu_p/\mu_n = -1.28$ and $\mu_\Lambda/\mu_p = +0.01$.

Quark anomalous magnetic moments, while loosening the $V\bar{P}\gamma$ vertex structure somewhat, do not provide consistent predictions for the meson radiative decay rates and the baryon magnetic moments.

B30224